UNIVERSITÀ DEGLI STUDI DI MILANO

SCUOLA DI DOTTORATO IN MEDICINA MOLECOLARE

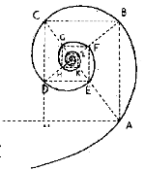

CICLO XXVIII

Anno Accademico 2014/2015

TESI DI DOTTORATO DI RICERCA

MED/07

INTERACTION BETWEEN THE HYPOXIA INDUCIBLE FACTOR 1 ALPHA AND THE HUMAN POLYOMAVIRUS BK: A RISK FACTOR FOR THE DEVELOPMENT OF POLYOMAVIRUS ASSOCIATED NEPHROPATHY

Dottorando: Lucia **SIGNORINI**

Matricola N°: **R10322**

TUTORE: Prof. Pasquale **FERRANTE**

CO-TUTORE: Dott.ssa Serena **DELBUE**

DIRETTORE DEL DOTTORATO: Ch.mo Prof. Mario **CLERICI**

ABSTRACT

Polyomaviruses are nonenveloped viruses with an icosahedral capsid of about 40-45 nm in diameter. The human polyomavirus BK (BKV) is a member of the Polyomaviridae family detected in 1971 in the urine of an immunosuppressed renal transplant recipient who developed ureteric stenosis. BKV has a worldwide seroprevalence of about 90%. After the primary infection, BKV establishes a life-long latency within the urogenital tract. The severe immunological impairment occurring in transplant kidney recipients leads to BKV reactivation that may result in the polyomavirus associated nephropathy (PVAN). During transplantation, kidney is subjected to hypoxic conditions, driven by the action of Hypoxia Inducible Factor (HIF). It has been proved that HIF isoform-1α (HIF-1α) may interact with several viruses, but till now there are no evidences regarding the interaction between BKV and HIF-1α. In the present study, we aimed to achieve a better understanding about the relation between BKV infection and hypoxia conditions in kidney cells in case of transplantation. Firstly, 17 kidney paraffin-embedded tissue samples were collected from kidney transplant patients, who developed or not PVAN (PVAN and NOT PVAN group) and from a control group in order to evaluate HIF-1α expression levels in vivo. Total RNA was extracted from paraffin embedded tissues, reverse transcripted into cDNA and HIF-1α expression was measured by means of a qualitative Real Time PCR. Then, in vitro experiments were conducted using the VERO cell line to evaluate the possible interaction between the BKV promoter and HIF-1α. Luciferase and Chromatin Immunoprecipitation (ChIP) assays were performed on BKV transfected VERO cells, to verify the interaction between the viral promoter and HIF-1α. In parallel, to clarify the nature of the interaction between HIF-1α and the BKV promoter, the sequences were in silico analyzed using BLASTN 2.2.32+ software to find whether one or more hypoxia response elements (HRE) core sequences were present in the BKV promoters. Finally, the effect of hypoxia on BKV replication was assessed by evaluating BKV replication in BKV infected VERO cells, treated and not treated with the hypoxia mimic Cobalt Chloride ($CoCl_2$). The HIF-1α expression level resulted 13.6 folds higher in PVAN tissues than in the control group while no differences were observed between the NOT PVAN tissues and the control group. Luciferase assay showed that the presence of HIF-1α stabilized the BKV promoter, increasing its activity from 2-folds to 6-folds ($p<0.05$) in transfected cells. ChIP assay showed a physical interaction between HIF-1α and the BKV promoter. BLASTN analysis showed no match between HRE sequence and the BKV promoter sequences, confirming that no binding sites for HIF-1α are present in the viral promoter. Finally, data obtained from BKV infected VERO cells revealed that BKV viral load was 5-fold increased in $CoCl_2$ treated cells compared to not treated infected cells. These data, taken together, are significant to define the role of hypoxic stress in BKV replication after renal transplantation. In particular, it can be concluded that the replication of this opportunistic virus, mainly due to immunosuppressive therapy, is furthermore stimulated and favorite by HIF-1α activation, driven by hypoxic conditions during transplantation. The experimental results suggested a hypothetical molecular mechanism underling this thesis, which can be outlined as follows: cellular response to hypoxic environment prevents HIF-1α proteasomal degradation, allowing the creation of a HIF-1 active complex. This complex translocates to the nucleus where it binds to the BKV promoter,

stimulating the transcription of viral genes and promoting the BKV replication. If confirmed by further experiments, this scenario may have important clinical implications: exposition to hypoxia during renal transplantation process should be considered as a crucial risk factor for the development of PVAN. These findings could be translated into clinical practice, replacing modulation of HIF system with ex-vivo organ preservation technologies, such as extra-corporeal membrane oxygenation, or considering HIF-1α as a target to be inhibited, perhaps using RNA interference technology.

SOMMARIO

I Polyomavirus sono virus privi di envelope con un capside icosaedrico di 40-45 nm di diametro. Il Polyomavirus umano BK (BKV) è un membro della famiglia dei Polyomaviridae ed è stato isolato per la prima volta nel 1971 dalle urine di un paziente sottoposto a trapianto di rene, il quale aveva sviluppato stenosi dell'uretere. BKV è ubiquitario nella popolazione mondiale e presenta una sieroprevalenza del 90% circa. In seguito alla prima infezione, generalmente asintomatica, BKV instaura latenza nel tratto uro-genitale. Uno stato di profonda immunocompromissione, tipico nei soggetti sottoposti a trapianto di rene, provoca una riattivazione di BKV che può portare allo sviluppo della nefropatia associata ai polyomavirus (PolyomaVirus Associated Nephropaty, PVAN). Durante il processo di trapianto, il rene è soggetto ad una condizione di ipossia, modulata dall'azione dei fattori inducibili dell'ipossia (Hypoxia Inducible Factors, HIF). Differenti studi hanno dimostrato che l'isoforma 1 alpha di HIF (HIF-1α) può interagire con diversi virus ma, ad oggi, non esistono informazioni riguardo l'interazione tra HIF-1α e BKV. Lo scopo del presente studio è quello di chiarire la relazione tra le infezioni da parte di BKV e la condizione di ipossia nelle cellule renali in caso di trapianto. In primo luogo, per valutare i livelli di espressione di HIF-1α in vivo, sono stati reclutati un totale di 17 pazienti sottoposti a trapianto di rene, comprendenti pazienti che hanno sviluppato o meno PVAN (PVAN e NOT PVAN) e pazienti controllo. L'RNA totale è stato estratto dalle biopsie paraffinate di ciascun paziente, retrotrascritto in cDNA e l'espressione di HIF-1α è stata valutata mediante un saggio di real time PCR qualitativo. Successivamente, per valutare una possibile interazione tra il promotore di BKV e HIF-1α, sono stati condotti esperimenti in vitro sulla linea cellulare VERO. Per verificare l'interazione tra il promotore virale e HIF-1α sono stati condotti un saggio luciferasico e un saggio di immunoprecipitazione della cromatina (ChIP) su cellule VERO trasfettate con BKV. In parallelo, per chiarire la natura dell'interazione tra HIF-1α e il promotore di BKV, è stata eseguita un'analisi in silico usando il software BLASTN 2.2.32+ per evidenziare l'eventuale presenza nel promotore virale di una o più sequenze responsive all'ipossia (Hypoxia Responsive Element, HRE). Infine, è stato valutato l'effetto dell'ipossia sulla replicazione virale, monitorando la replicazione di BKV in cellule VERO infettate con BKV e trattate o meno con l'ipossia-mimetico cloruro di cobalto ($CoCl_2$). L'espressione di HIF-1α è risultata essere 13.6 volte aumentata in tessuti PVAN rispetto al gruppo di controllo mentre nessuna differenza è stata osservata tra il gruppo NOT PVAN e il gruppo controllo. Il saggio luciferasico ha mostrato che la presenza di HIF-1α nelle cellule trasfettate stabilizza il promotore di BKV, incrementando la sua attività in un range compreso tra le 2 e le 6 volte ($p<0.05$). Il saggio di ChIP ha mostrato l'esistenza di un'interazione fisica tra HIF-1α e il promotore di BKV. L'analisi effettuata con BLASTN ha mostrato l'assenza di HRE nella sequenza del promotore di BKV confermando l'assenza di siti di attacco per HIF-1α nel promotore virale. Infine, i dati ottenuti dalle cellule VERO infettate con BKV, hanno mostrato che la carica virale è 5 volte aumentata nelle cellule trattate con $CoCl_2$ rispetto alle cellule non trattate. Tutti questi dati, risultano importanti per definire un ruolo dello stress ipossico nella replicazione di BKV in seguito al trapianto renale. In particolare, è possibile concludere che la replicazione di questo virus opportunista, dovuta principalmente alla terapia immunosoppressiva, è oltretutto stimolata e favorita dall'attivazione di HIF-1α,

guidata dalle condizioni di ipossia durante il processo di trapianto. I risultati sperimentali suggeriscono un ipotetico meccanismo molecolare alla base di questa tesi, che può essere spiegato come segue: la risposta cellulare all'ambiente ipossico previene la degradazione proteasomale di HIF-1α permettendo la creazione di un complesso HIF-1 attivo. Questo complesso trasloca quindi nel nucleo dove si lega al promotore di BKV promuovendo la trascrizione dei geni virali e stimolando la replicazione di BKV. Se confermato da esperimenti futuri, questo scenario potrebbe avere importanti implicazioni cliniche: l'esposizione a stati di ipossia durante il processo di trapianto dovrebbe essere considerato un fattore di rischio cruciale per lo sviluppo di PVAN. Queste informazioni potrebbero essere traslate nella pratica clinica, sostituendo la modulazione del sistema degli HIF con tecnologie di preservazione dell'organo ex-vivo, come per esempio l'ossigenazione extra corporea, oppure considerando HIF-1α come un target da inibire usando, per esempio, la tecnologia dell'RNA interference.

INDEX

LIST OF SYMBOLS

17-AAG	17-allylaminogeldanamycin
ARNT	Aryl hydrocarbon receptor nuclear translocator
ATN	Acute tubular necrosis
ATP	Adenosine triphosphate
BBB	Blood-Brain Barrier
bHLH	Basic helix-loop-helix
BKV	BK virus
CAD	C-terminal activation domain
CBP	CREB binding protein
CHIP	Carboxyl terminus of Hsc70-interacting protein
ChIP	Chromatin Immunoprecipitation
CMV	Cytomegalovirus
$CoCl_2$	Cobalt Chloride
CTRL	Control group
DMEM	Dulbecco's Modified Eagle Medium
DMSO	Dimethyl Sulfoxide
E box	Enhancer box
EBV	Epstein Barr virus
Elk-1	Ets family transcription factor 1
EPO	Erythropoietin
ERK-MAPK	ERC/microtubule-associated proteins
FBS	Fetal Bovine Serum
FIH1	Factor Inhibiting HIF-1α
FOXA2	Forkhead box protein A2
GAPDH	Glyceraldehyde-3-phosphate dehydrogenase
GLUT1	Glucose Transporter-1
H_2O_2	Hydrogen peroxide
HAF	Hypoxia-associated factor
HBV	Hepatitis B virus
HBx X	Protein of hepatitis B virus
HCC	Hepatocellular carcinoma
HCV	Hepatitis C virus
HEK	Human embrionic kidney
HHV8	Human herpesvirus 8
HIF	Hypoxia Inducible Factor
HIF-1-α	Hypoxia Inducible Factor isoform 1-α
HIFs	Hypoxia inducible factors

HNF-4	Hepatocyte nuclear factor 4
HPV-16	Human papillomavirus-16
HREs	Hypoxia response elements
Hsc70	Heat shock cognate 70
Hsp90	Heat shock protein 90
HTLV-1	Human T-cell leukemia virus type 1
HUV-EC-C	Human umbilical vein-vascular endothelium cells
IGFBP3	Insulin-like growth factor- binding protein-3
IRI	Ischemia reperfusion injury
IVIG	Intravenous Ig
JCV	JC virus
LANA	Latency-associated nuclear antigen
LDHA	Lactate Dehydrogenase
LMP1	Latent membrane protein 1
MAP	Mitogen activated protein
MAPK	Mitogen-activated protein kinase
MDR1	Multi-drug resistance 1
MetLuc	Metridia Luciferase
MTT	3-[4,5-dimethylthiazol-2-yl]-2,5-diphenyltetrazolium bromide
NAD	N-terminal activation domain
NCCR	Non Coding Control Region
NEMO	NF-KB essential modulator
NLS	Nuclear Localization Signal
NPV	Negative predictive value
ODD	Oxygen-dependent degradation domain
PAS	PER-ARNT-SIM
PAU-1	Plasminogen activator inhibitor-1
PBS	Phosphate Buffer Saline
PEG	Polyethylene glycol
PHD	Prolyl hydroxylase domain
PML	Progressive Multifocal Leukoencephalopathy
PP2A	Protein phosphates 2A
PPV	Positive predictive value
pRb	Retinoblastoma protein
PVAN	Polyomavirus associated nephropathy
pVHL	Von-Hippel Lindau protein
qPCR	Quantitative Real Time PCR
RACK1	Receptor of activated protein kinase C

Real Time PCR	Real time polymerase chain reaction
Ref-1	Redox effector factor 1
ROS	Reactive oxygen species
RPA	Replication protein A
RSV	Respiratory syncytial virus
RT	Quantiscript Reverse Transcriptase
SNPs	Single nucleotide polymorphisms
SRC-1	Steroid receptor coactivator
SUMO	Small ubiquitin-like modifier protein
SV40	Simian virus 40
TAD	Transactivation and stability domain
TAg	Large tumor antigen
tAg	Small tumor antigen
TGF-β	Transforming Growth Factor-beta
TIF-2	Transcription intermediary factor-2
truncTAg	Truncated tumour antigen
VEGF	Vascular endothelial growth factor
VERO	African green monkey kidney cell line
VP1	Viral protein 1
VSV	Vesicular stomatitis virus
WW	Polyomavirus BK archetypal strain

LIST OF FIGURES

LIST OF TABLES

1. INTRODUCTION

1.1 HUMAN POLYOMAVIRUS BK

The human polyomavirus BK (BKV) is a member of the *Polyomaviridae* family detected in 1971 in the urine of an immunosuppressed renal transplant recipient who developed ureteric stenosis; the new virus was named as the initials of the patient BK [Gardner et al., 1971]. Polyomavirus are nonenveloped virus with an icosahedral capsid of about 40-45 nm in diameter. BK virions consist of 88% proteins and 12% DNA. BKV and the strictly related JC polyomavirus (JCV) were the first human viruses isolated that strongly resembled the morphology and genomic organization of the previously described oncogenic polyomaviruses simian virus 40 (SV40) and mouse polyomavirus. The viral genome is composed by a single copy of a circular double-stranded DNA [Khalili and Stoner, 2001]. Primary infection occurs predominantly during childhood and after the primary infection, often asymptomatic, it establishes a life-long subclinical latency mostly within the kidney, the urogenital tract and probably also in B lymphocytes and other locations in immunocompetent individuals [Dörries et al.,1997; Shah 1996; Dolei et al., 2000; Dörries et al.,1994]. Intermittent or chronic BKV reactivation can occur in individuals with perturbed immune conditions leading to different symptomatology with different degrees of severity. For these reasons, during the recent years, BKV has drawn the attention of the scientific and medical communities because of its potential to cause human diseases.

1.1.1 GENOME

BKV genome consists of a single copy of circular double-stranded DNA molecule of about 5 kilobase pairs. BKV genome can be divided into three functional regions: the genetically conserved early and late regions and a hypervariable regulatory region called Non Coding Control Region (NCCR) that contains the bidirectional promoter for both the early and late regions

[Cole et al., 2001; Moens et al., 2001]. The early region encodes for the three viral regulatory proteins: the large tumor antigen (TAg), the small tumor antigen (tAg). The late coding region, expressed only after the initiation of DNA replication, contains the genetic information for the major capsid viral protein 1 (VP1) and the two minor viral capsid proteins 2 and 3 (VP2 and VP3) and for a small protein called agnoprotein (figure 1).

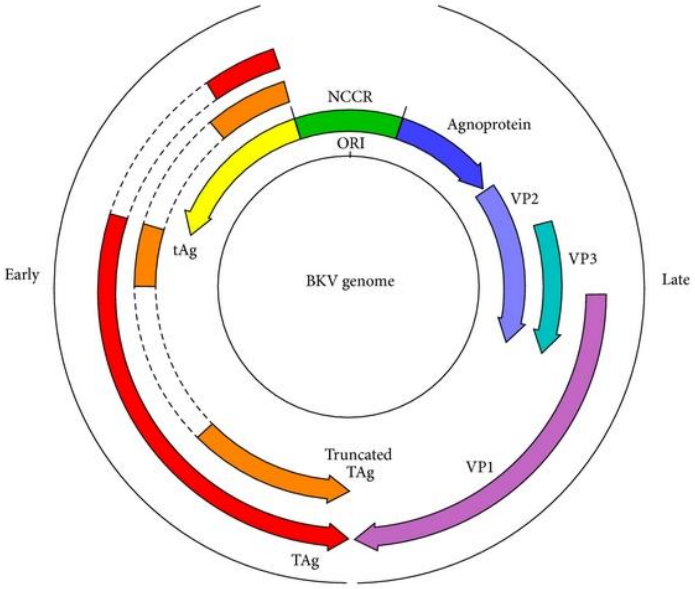

Figure 1. Schematic representation of the functional organization of BKV genome [http://www.hindawi.com/journals/jir/2013/373579/fig2/]

1.1.2 NON CODING CONTROL REGION

The NCCR is the genome sequence that contains the origin of replication and the sequences involved in the transcriptional regulation of both early and late genes. The NCCR sequence has been arbitrarily divided into four transcription factor binding sequence blocks, called O (142bp), P (68bp), Q (39bp), R (63bp) and S (63bp). The liner configuration is defined as the archetypal strain (WW) (figure 2).

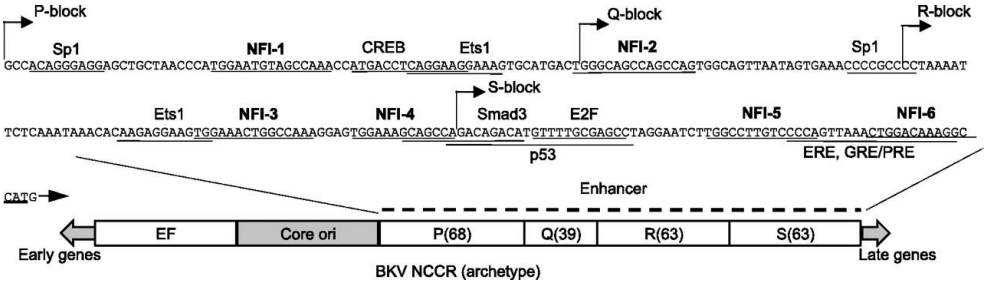

Figure 2. BKV sequence blocks [Liang et al.,2012]

The NCCR displays an higher degree of variability than that displayed in the other regions of the genome. This variations are due to deletions, duplications and other rearrangements and were determined after several cell culture passages. In particular, duplication of P-block sequence, and Q and R blocks completely deletion (O_{142}-P_{68}-$P_{1\text{-}7;26\text{-}68}$-$P_{64}$-$S_{63}$), are typical of the Dunlop strain, widely used for *in vitro* experiments. It has been shown that the BKV Dunlop strain grows well in human embryonic kidney (HEK), Vero and human umbilical vein-vascular endothelium cells (HUV-EC-C) [Seif et al., 1979]. Also naturally occurring NCCRs variants show duplication or triplication of the P region including portion of the neighbouring Q region. Likewise, deletions are found to occur anywhere within the P, Q, R and S regions. Several *in vivo* evidences demonstrate that even if the archetypal conformation is the most prevalent in patients and healthy subjects, BKV with rearranged NCCR is present in cerebrospinal fluid from patients with neurological complications [Bárcena-Panero et al., 2012], in the plasma of renal transplant patients [Gosert et al., 2008], in subjects affected by polyomavirus-associated nephropathy (PVAN) [Azzi et al., 2006; Randhawa et al., 2003] and AIDS patients (table 1) [Jorgensen et al., 2003]. Correlations between NCCR rearrangements with transcriptional activity and transformation efficiency have been well studied. Rearrangements in the NCCR can remove, create or increase the

number of transcription factor binding sites creating variation in the replication and the transcription of the virus genome [Moens et al., 1995a].

ISOLATE	REFERENCE	SOURCE
Gardner	Gardner et al., 1971	renal transplant patient
Dunlop	Seif et al., 1979	renal transplant patient
MG	Lecatsas et al.,1976	renal transplant patient
SB	Gibson and Gardner, 1983	patient with lymphoma, England
AS	Coleman, 1980	pregnant woman
DB	Tavis et al., 1990	bone marrow transplant patient
BO	Borgatti et al., 1981	immunosuppressed children, Italy
WW	Rubinstein et al., 1987	immunocompetent patient

Table 1. list of some BKV strains and sources from which the strains have been isolated

1.1.3 EARLY REGION

The early region is a functional region of the genome that encodes for the regulatory proteins TAg and tAg, which are products of two alternatively spliced mRNAs. In 1989 Bollag and colleagues reported the existence of a third form of BKV tumour antigen, called truncated tumour antigen (truncTAg), that was presumed to be a proteolytic degradation product of the TAg [Bollag et al., 1989]. In 2009 Abend and colleagues presented evidences about the expression of the truncTAg, encoded from an alternatively spliced mRNA derived from the excision of a second intron from the mRNA encoding TAg [Abend et al., 2009]. The early region is expressed during the early stages of the viral life cycle and can be expressed later during infection, after the onset of viral DNA replication.

TAg is a multifunctional protein of 695 amino acids involved in DNA replication and transcription. The ability of BKV to transform cells is due to its capability to deregulate the cell growth control as a means to drive resting cells into S phase, in which DNA replication is maximized. The

major transformation domains have been well defined in the N-terminal and C-terminal of the TAg sequence [Ahuja et al., 2005]. These are: the N-terminal J domain that interacts with the heat shock cognate 70 (Hsc70) co-chaperone protein [Campbell et al., 1997; Kelley and Georgopoulos C, 1997], the N-terminal retinoblastoma protein (pRb) binding domain contains a conserved LXCXE motif throught which TAg associates with pRb and its family members, p107 and p130 [DeCaprio et al., 1988, Harris et al., 1996] and the C-terminal bipartite p53 binding region [Cavender et al., 1995; Kierstead and Tevethia 1993; Li et al., 2003]. Through its N terminus, TAg also interacts with two other proteins that are involved in cell growth control, the E3 ubiquitin ligase, CUL7 and the mitotic spindle checkpoint protein, Bub1 [Ali et al., 2004; Cotsiki et al., 2004; Kohrman and Imperiale, 1992].

tAg is generated by an alternative splicing of the early transcript that generates a Cys-rich protein composed of 172 residues, located both in the nucleus and the cytoplasm. TAg and tAg share the amino-terminal 82 amino acids and contain different carboxy-terminal regions. tAg is composed by a N-terminal J domain and a C-terminal unique domain. The protein shares its N-terminal 78 residues with the N-terminal sequence of TAg, including the region of the J domain [3,31,32 Cho]. Study about tAg of SV40 showed that it exhibits an α-helix structure with two zinc-binding sites. The J domain contains three helices and has a structure similar to the J domain of SV40 TAg. The unique domain is composed of four helices and three of these helices are directly involved in the interaction with two zinc ions. The J and unique domain have an interface that is mostly hydrophobic. Considerably fewer studies have been aimed at characterizing the role of tAg in virus multiplication compared to TAg [Moens et al., 2007]. The major recognized role is to provides a helper function for TAg by augmenting the viral replication and trans-activation of the viral promoter, resulting in increased virus yeld in permissive cells

[Moens et al., 2001; Rundell at al., 2001]. Indeed, tAg seems to exert its effect by inhibition of the heterodimeric holoenzyme protein phosphates 2A (PP2A), a family of abundantly expressed serine-threonine phosphatases implicated in the regulation of many cellular processes, including regulation of different signal transduction pathways and cell cycle progression [Arroyo et al., 2005; Sontag et al., 2006].

1.1.4 LATE REGION

The late region encodes for three structural capsid proteins VP1, VP2 and VP3, generated from a common precursor mRNA by alternative splicing, and for a small protein called agnoprotein.

VP1, *VP2* and *VP3* consist of 351, 232 and 362 residues respectively and each protein contains three functional domains that facilitate the packaging of the complete virus particle:

The Nuclear Localization Signal (NLS), important to mediate the transport of the capsid proteins to the nucleus after their expression in the cytoplasm. It has been shown that BKV VP1 contains the same amino terminal motif that has been demonstrated to be sufficient for SV40 VP1 targeting to the nucleus [Wychowski et al., 1986].

The DNA-binding domain. It has been shown that VP1, VP2 and VP3 bind viral and non-viral DNA [Clever et al., 1993]. The DNA binding domain in SV40 VP1 has not been mapped yet, but SV40 VP1, in its carboxyl-terminal extremity, contains a domain of 40 amino acids that are sufficient to bind double stranded as well as single stranded DNA. It has been demonstrated that 31 of these amino acid residues are conserved in BKV VP2 and VP3, suggesting that these two proteins can also associate with DNA [Chang et al., 1993]

Protein-protein interaction domain: residues 222-234 of SV40 VP3 represent a VP1 interaction domain [Gharakhanian et al., 1988]. This region is 80% conserved in BVK VP3.

The *Agnoprotein* is a 70 amino acids long polypeptide that predominantly resides in the cytosol and in the perinuclear region in association with the outer nuclear membrane, but a minor fraction of the protein can also be detected in the nucleus [Nomura et al., 1983; Okada et al., 2001; Khalili et al., 2005]. It is know that a particular BKV strain (strain AS) encoding a N-terminal modified agnoprotein that can be successfully propagated in cell culture while, BKV variants with deleted agnogene, were detected in the urine of renal transplant patients [Tavis et al., 1989; Olsen et al., 2006]. From studies about the JCV genome is known that the agnoprotein can bind the TAg but the biological relevance of this interaction is poorly understood. The hypothesis is that agnoprotein repressed both basal and TAg-mediated late transcription and viral DNA replication [Safak et al., 2001]. Whether agnoprotein influences the transforming ability of TAg is not known.

1.1.5 CAPSID

The tertiary structure of the major capsid protein VP1 can be divided into three modules: a N-terminal arm, an anti-parallel β-sandwich with jelly-roll topology and a long C-terminal extension [Liddington et al., 1991; Stehle et al., 1996] (figure 3). The first 15 residues of the N-terminal arm are probably involved in the interaction with the virus genome. The different β-strands are connected by elaborate loops protruding outward the structure of the β-sandwich itself. The loops, that also contain α-helix structures, have been named BC, DE, EF, GH and HI. The BC, DE and HI closely interact at the outward end of the β-sandwich. The BC loop can be divided into two smaller loops: BC1 and BC2. The long EF loop forms a small jelly-roll structure on the side of the β-sandwich. The C-terminal arm can be

divided into three segments: the “C helix” residues, the “C insert” and the “C loop”. The C-terminal arm mediates the binding between the VP1 pentamers.

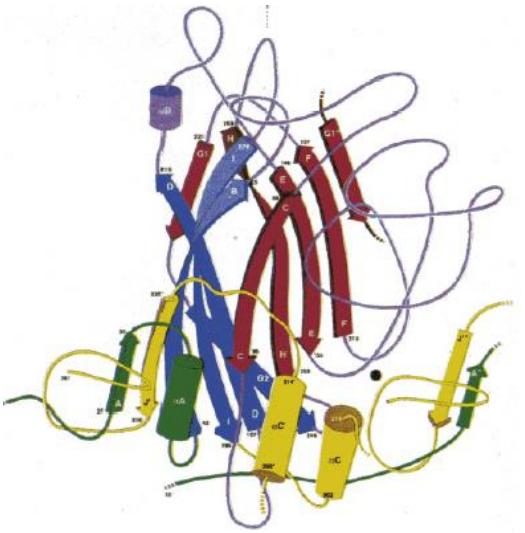

Figure 3. Richardson diagram of the SV40 VP1 subunit [Liddington et al., 1991]

The complete amino acid sequence of the BKV VP1 is reported (figure 4). The loops are shown, as well as the different β-strands, β-helices, the N-terminal and the C-terminal arms. Based on amino acid comparison, it has been shown that the VP1 sequence of BKV is divergent from the sequence of other polyomaviruses primarily in the region forming the extracellular loops and is relatively conserved in the β-sheet framework.

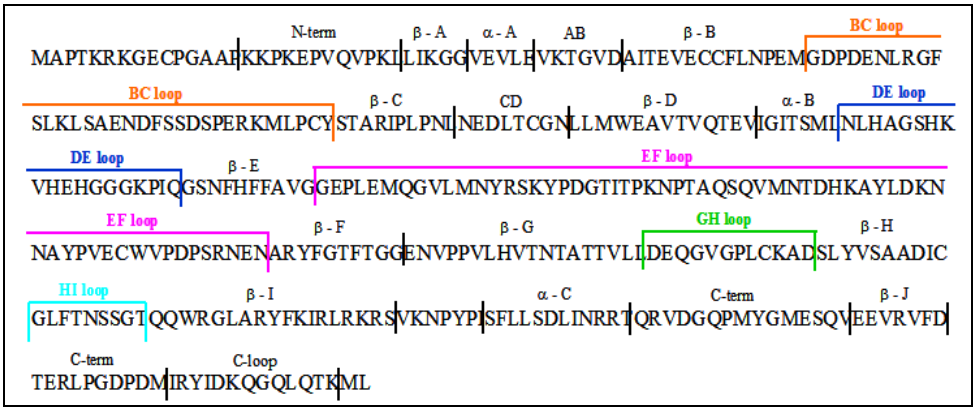

Figure 4. Amino acid sequence of the BKV major capsid protein VP1

The three-dimensional structure of both SV40 and murine polyomavirus has been determined [Liddington et al., 1991; Griffith et al., 1992]. Based on the similarity of their gene organizations as well as their high sequence homology, the solved crystal structure of SV40 VP1 has been used as a template to create a model of the BKV capsid structure. In 2003 a three-dimensional model of the BKV capsid has been created by analysing through electron microscopy the structure of BKV virus-like particles generated using recombinant baculoviruses [Li TC et al., 2003; Nilsson et al., 2005]. The results basically confirm the high similarity between the SV40 and the BKV capsid structure. The predicted structure of the BKV capsid consists of 72 capsomers of VP1 centred on the vertices of a T=7 icosahedral surface lattice. A single copy of either VP2 or VP3 is associated with each capsomer. The VP1 capsomer is built as a ring of five VP1 monomers, tightly linked by interacting loops between the framework of β-strands. The connection between the pentamers within the virion is allowed by the C-terminal domain of each VP1 monomer that forms an extended arm, which interacts extensively with subunits of the neighbouring pentamers, thereby tying the pentamers together in the virion shell. Each pentamer receives five invading arms, one from each of five other pentamers, and donates five arms to surrounding pentamers (figure 5 a,b).

Twelve of the 72 pentamers that form the capsid structure are surrounded by five other pentamers, while the remaining 60 are surrounded by six pentamers. There are three different kinds of pentamer-pentamer interaction: a three-fold cluster and two different two-fold clusters. Therefore, according to the different interpentamer bounding environments, the monomers that build up the pentamer can be divided into subunits α, α',α'', β, β' and γ. α, α', and α'' form a a three-fold interaction, β and β' form one kind of two-fold interaction, while γ forms another kind of two-fold interaction, while γ forms another kind of two-fold interaction (figure 5 c). Calcium ions seem to play an important role in viral assembly [Brady et al., 1977], while disulfide bonds are thought to be involved in maintaining the stability of polyomavirus capsid [Chen et al., 2001].

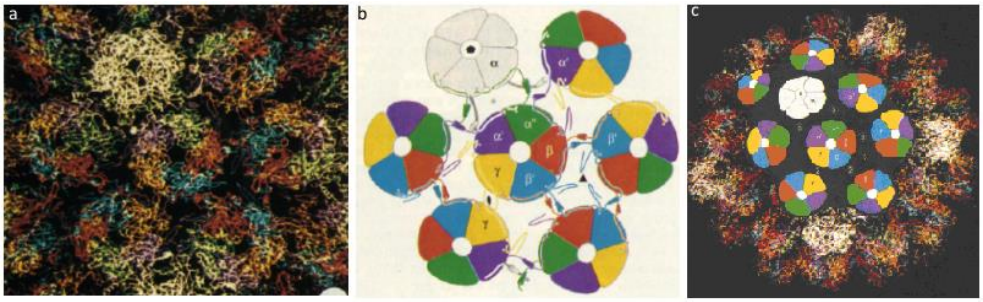

Figure 5. Schematic representation showing the way the C-terminal arm of each monomer ties the pentamers together *(a,b).* Overall view of SV40 virion. The six unique monomers are indicated and the icosahedral symmetry axis 5, 3 and 2 are indicated *(c)* [Liddington et al., 1991]

1.1.6 LIFECYCLE

The lifecycle of polyomaviruses can be arbitrarily divided into early and late stages. The early stage begins with the attachment of the virus to the surface of the host cell and continues until the onset of viral DNA replication. The late stage of infection extends from the onset of viral DNA replication to the end of the lytic lifecycle (figure 6).

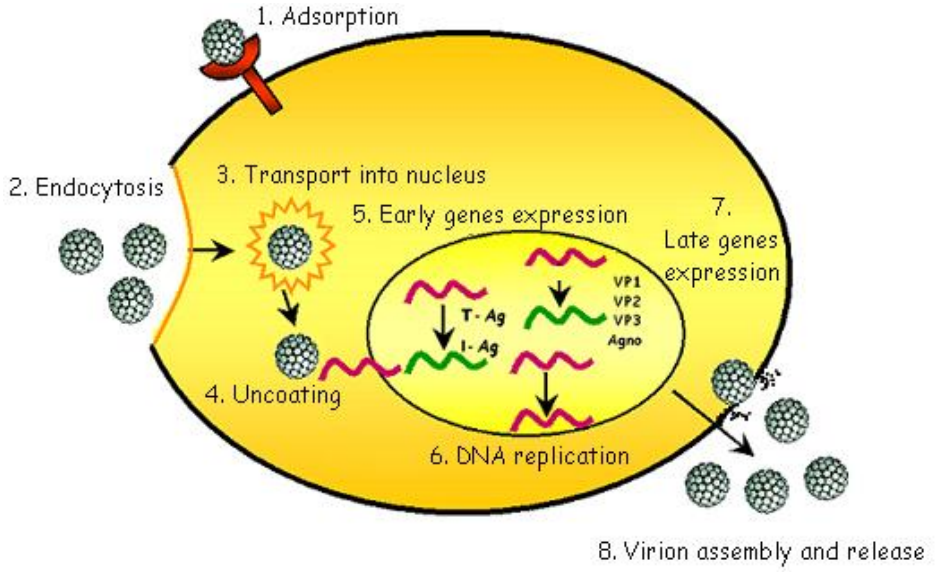

Figure 6. Polyomavirus lifecycle

Adsorption: infection of permissive cells is initiated by binding of the virion to specific cell surface receptors. The efficient entry of BKV requires the interaction between virus and cell surface sialic acids. A study conducted by Dugan and colleagues demonstrated that a N-linked glycoprotein with α(2,3)-linked sialic acid mediates productive BKV attachment and entry into host cells [Dugan et al., 2005]. *In vitro* experiments have demonstrated that JCV requires N-linked glycoprotein containing terminal α(2,6)-linked sialic acid to successfully infect the human glial cells [Liu et al., 1998].

Entry, intracellular trafficking and uncoating: after the initial binding to their host cell, viral capsids are internalized by caveolae-mediated endocytosis [Eash et al., 2004; Anderson et al., 1996] and are transported to the nucleus, where the DNA is uncoated. After the entry into the cell, BKV is transported through the cytosol to the nucleus. The active cytoskeletal transport machinery plays an important role in this intracellular migration [Dohner and Sodeik, 2005]. Most studies indicated that the uncoating of

polyomaviruses occurs within the nucleus [Drachenberg et al., 2003; Nakanishi et al., 1996] and that virion particles enter the nucleus through the nuclear pore complex [Clever et al., 1991].

Early mRNA transcription, processing and translation: once virions have been uncoated, the viral minichromosome is used by RNA polymerase II as a template for transcription to produce early viral mRNAs**.** The T antigens are generated by alternative splicing of the same precursor mRNA.

DNA replication: subsequent to early transcription and synthesis of the viral regulatory proteins there is the switch to DNA replication. A major role for initiation of DNA replication is played by T-Ag, which binds to specific sequences within the origin of replication and promotes the unwinding of DNA thanks to its helicase activity. T-Ag promotes the bi-directional replication of DNA also by recruiting all the cellular proteins that are directly involved in the cell DNA synthetic process and by binding the replication protein A (RPA), that is a single-stranded DNA binding protein important for an efficient DNA replication [Melendy and Stillman, 1993].

Late mRNA transcription, processing and translation: once the viral DNA has been synthesized, T-Ag promotes the repression of early gene transcription and the progression of the virus to the late phase of its lifecycle, by activating the transcription of late genes. Virion proteins VP1, VP2, VP3 are synthesized in the cytoplasm of infected cells and transported to the nucleus for assembly into virions. Sequences near the amino *terminus* of VP1 and near the carboxyl-*termini* of VP2 and VP3 are essential for this nuclear accumulation [Wychowski et al., 1986; Moreland and Garcea, 1991]. These proteins may be transported to the nucleus as a complex as well as separately [Barouch and Harrison, 1994].

Virion assembly and release: once in the nucleus, VP1, VP2 and VP3 assembly into the typical capsid structure made up of 72 VP1 pentamers with one of the two minor proteins lying in the centre of each pentamer. The viral minichromosome, packaged with histones, is then inserted into the capsids [Sandalon et al., 1997]. It has been speculated that progeny virions are released by lytic disruption of their host cells. However, electron microscopy observations showed that SV40 virions are released directly from the plasma membranes of intact epithelial cells [Clayson et al., 1989]. Therefore, it remains to be elucidated whether cell lysis or at times intracellular vescicular transport is the preferred pathway for the release of polyomaviruses progeny virions.

1.1.7 BKV SUBTYPES DISTRIBUTION

BKV strains are classified into four subtypes using serological and genotyping methods [Knowles et al., 2001]. The first studies on the evolution of BKV have been hampered by the limited availability of BKV genomes from various human populations worldwide. In the last years, the introduction of the sensitive polymerase chain reaction (PCR) and the discovery that BKV DNA sequences could be amplified also from the urine of non- immunocompromised subjects, allowed to conduct a series of evolutionary studies on the BKV subtypes' distributions. In 1993, Jin and colleagues PCR-amplified and sequenced a 287 bp VP1 region, designed as the "typing region" , that contains a possible epitope region responsible for serological discrimination among subtypes, and the resultant sequences were used to detect subtypes-specific single nucleotide polymorphisms (SNPs) [Jin et al., 1993]. These sequence variations within this region have been used to classify BKV subtype strains in various laboratories. BKV isolates worldwide are classified into four subtypes (I–IV) [Knowles et al., 2001]. Subtype I (the most prevalent subtype) has been further divided into four subgroups (Ia, Ib-1, Ib-2, and Ic) (table 2) [Takasaka et al. 2004;

Nishimoto et al. 2006; Ikegaya et al. 2006; Zheng et al. 2007]. Interestingly, each of these subgroups has a unique geographic distribution pattern: Ia is prevalent in Africa, Ib-1 in Southeast Asia, Ib-2 in Europe, and Ic in Northeast Asia [Takasaka et al. 2004; Ikegaya et al. 2006; Zheng et al. 2007]. Recently it appears that a prototype of subtype I (probably emerging in Africa) diverged into various subgroups with the divisions of human populations that occurred after out-of-Africa migrations. In contrast, subtype IV (the second most prevalent subtype of BKV) shows a geographic distribution biased toward areas other than Africa, i.e., Europe and Asia [Zheng et al. 2007]. This finding may suggest that subtype IV originated outside Africa, although it is also possible that the original proportion of subtype IV might have been high in Africa but decreased thereafter, due to a change in the host susceptibility to subtype IV BKV.

Subgroup	Nucleotides at indicated positions*						
	1687	1698	1809	1860	1887	1908	1923
Ia	G	T	G	A	A	T	T
Ib-1	G	A	A	A	A	T	C
Ib-2	C	A	A/C†	A	A	A	C
Ic	G	A	G	G	C/A‡	T	T

*Nucleotide numbers are based on the BKV (DUN) sequence (Seif *et al.*, 1979).
†C was detected in some isolates (FIN-9 to -19, SJH-19 and -36, MAN-1 and -7 to -9). These isolates clustered together within subcluster Ib-2 (see Fig. 1).
‡A was detected in RYU-2 and KOM-20 and -24.

Table 2. BKV subgroups defined by nucleotide polymorphism [Ikegaya et al., 2006]

1.1.8 SEROEPIDEMIOLOGY

Serological surveys have shown that BKV infections are widespread in the general population with type-specific antibodies detectable in 60–80% of healthy adults [Taguchi et al., 1982; Knowles et al., 2003; Egli et al., 2009;

Antonsson et al., 2010]. Primary BKV infection occurs in early childhood. After primary infection, it persists in renal tissue, and probably also in B-lymphocytes and other locations [Dolei et al, 2000; Dörries et al.,1994]. Natural BKV transmission is not resolved, but likely occurs via the respiratory or fecal-oral route [Hirsch et al., 2003]. Primary infection is generally asymptomatic, and no definite clinical presentations have been attributed, although fever and non-specific upper respiratory symptoms have been suggested [Reploeg et al., 2001]. However, reactivation of these viruses in immunocompromised patients with relative or absolute cellular immunodeficiency has been associated clearly with serious complications [Major et al., 2001]. BKV reactivation is associated with interstitial nephritis [Nickeleit et al., 2000] and ureteral stenosis in renal allograft recipients, and late onset haemorrhagic cystitis in bone marrow transplant patients [Major et al., 2001]. BKV has also been detected in a variety of tumors such as the carcinoma of the urinary tract, prostate cancer and neuroblastoma renewing the interest about the BKV epidemiology [Carluccio et al., 2014; Flaegstad et al., 1999]. Reactivation of BKV may also occur up to 60% in healthy people in state of pregnancy, older age or immune dysfunction, leading to asymptomatic viruria [Hirsch 2005; Tsai et al., 1997; Kitamura et al., 1990]. Kean and colleagues demonstrated that BKV seroprevalence has an age specific trend from childhood to adulthood providing important data regarding the prevalence and the age-related timeline for infection (figure 7) [Kean et al., 2009]. Seroepidemiological studies, combined with virological and clinical data (i.e. the high prevalence of infection, low morbidity, asymptomatic reactivation and host specificity) suggested coevolutionary adaptation of BKV and the human host [Hirsch and Steiger 2003] and results therefore useful in determining past and current BKV exposure in patients at risk of BK-associated diseases or showing early signs of complications due to polyomavirus reactivation [Stolt et al., 2003].

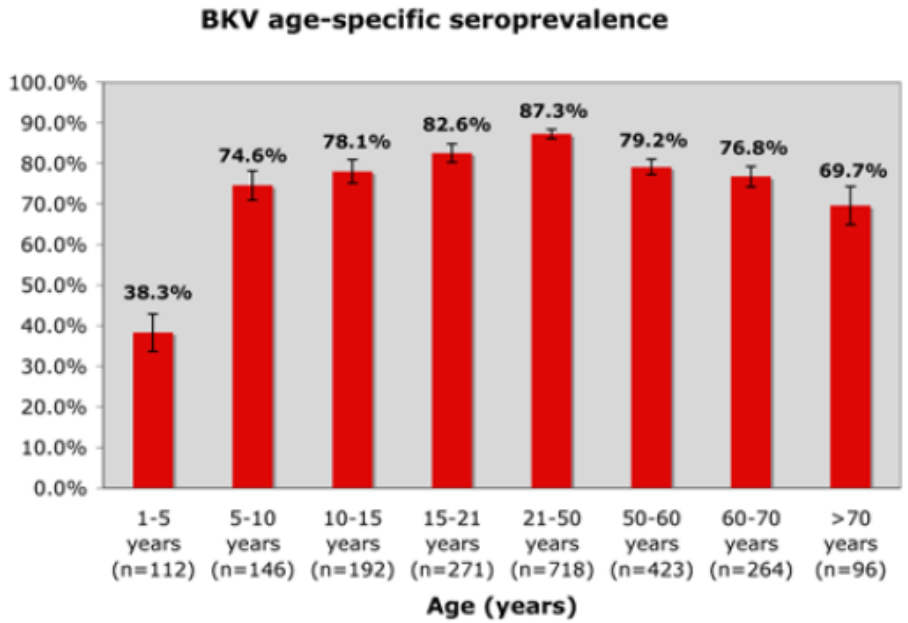

Figure 7. BKV seroprevalence [Kean et al., 2009]

1.2 POLYOMAVIRUS ASSOCIATED NEPHROPATHY (PVAN)

PVAN is one of the most common viral complication in renal transplant recipients and is an increasingly recognized cause of renal transplant dysfunction and graft loss [Costa and Cavallo, 2012]. PVAN characteristic were first described in 1978 by Mackenzie and colleagues as evidence of stenosis of the transplant ureter with virus infected cells in the ureteric epithelium and in one case also in the renal tubules [Mackenzie et al., 1978]. In 1995, Purighalla and colleagues first recognized and described PVAN as a serious complication after renal transplantation [Purighalla et al., 1995]. Since the first description of PVAN in 1995, an increasing prevalence rate from 1% to 10% has been evidenced [Hirsch et al., 2006]. The increase in prevalence data could be due to the introduction of new deeply immunosuppressive drugs and/or the relative decline in acute rejection rates. PVAN can lead to kidney graft loss in 10% up to 100% of

the cases, determining the return in hemodialysis, thus significantly and markedly reducing the graft survival.

1.2.1 CLINICAL AND HISTOLOGICAL FEATURES

PVAN clinical presentation may be inconspicuous and lacks of useful features. Varying degrees of renal dysfunction may be seen, although in early stages even normal serum creatinine levels may be detected. PVAN may consist in interstitial nephritis and/or ureteric stenosis with ureteric obstruction, hydronephrosis, and sometimes associated urinary tract infections [Costa and Cavallo, 2012]. Most of the cases are preceded by an asymptomatic phase of persistent and significant viruria. Sustained BKV viruria is typically followed within few weeks by viremia. A significant and sustained viremia identifies patients with uncontrolled viral replication potentially leading to parenchymal injury. Progression of PVAN leads to eventual deterioration of the kidney graft function. Usually, appearance of viruria and viremia precedes the increase in serum creatinine by weeks or months. Once the virus has reactivated, an ascending infection via cell-to-cell spread occurs [Meehan et al., 2006; Drachenberg et al., 2003; Nickeleit et al., 2000(a)]. Without appropriate immunologic control, a progressive lytic infection occurs resulting in large nuclear and perinuclear virus-containing inclusions in the tubule cells [Low et al., 2004; Bhol et al., 2007]. The infected cells have an enlarged nucleus with a gelatinous basophilic inclusion resulting from accumulation of the newly formed virions [Drachenberg and Papadimitriou, 2006]. Lysis of the infected cells results in viral seepage into the tubule lumen and urine but also to the interstitium and propagation to surrounding cells. Subsequent tubular cell necrosis leads to cast formation and denudation of the basement membrane. Destruction of tubular capillary walls results in vascular spread of the virus. A heterogeneous interstitial infiltration of inflammatory cells as well as tubulitis may be absent, intermixed with the active infection, or noted in

areas that lack cytopathic changes. Collateral damage with necrosis and apoptosis of noninfected tubule cells may occur. The resultant effect of continued intragraft inflammation, tubular injury, and upregulation of profibrotic mediators is allograft dysfunction and loss (figure 8).

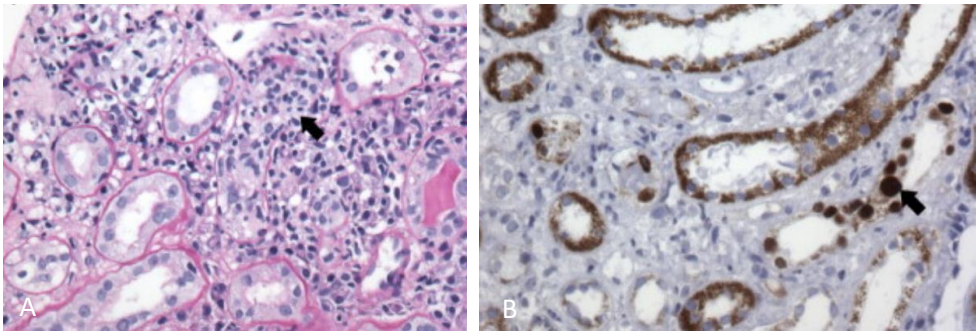

Figure 8: renal biopsies of a 62 years old man at 5 months from transplantation and 4 months before the starting of anti-graft loss therapy. A. Periodic acid–Schiff stain shows areas of tubular inflammation, focal tubular basement membrane disruption (arrow), and interstitial inflammation consisting of lymphocytes, plasma cells, and histiocytes affecting 30% of the total sampled renal parenchyma. B. Immunohistochemical staining for SV40 large T antigen shows numerous positively staining nuclei in tubular epithelial cells (arrow) in areas of less severe interstitial and tubular inflammation, indicating active polyomavirus infection Original magnification X400) [Wiseman, 2009]

1.2.2 VIROLOGICAL SCREENING

The pathogenesis of PVAN probably involves the interaction of multiple risk factors, which include immunosuppression and determinants of the patient, the transplanted organ, and the virus. Patient determinants increasing the risk for PVAN may include increased older age and male gender [Ramos et al., 2002; Awadalla et al., 2004; Wong et al., 2003; Trofe et al., 2003; Dadhania et al. 2004; Celik et al., 2003; Barri et al., 2001; Trofe et al., 2003(a)], white ethnicity [Ramos et al., 2003, Trofe et al., 2003(a)], diabetes mellitus [Randhawa et al., 1999; Trofe et al., 2003(a); Nickeleit et al., 1999] and a negative BKV serostatus in pediatric recipients [Ginevri et al., 2003; Smith et al., 2004]. However, a positive BKV serostatus prior to transplantation does not protect against polyomavirus replication, viremia or

PVAN [Hirsch et al., 2002; Brennan et al., 2005]. Viral replication is the single common feature of all patients at risk of nephropathy. In a kidney transplant recipient, BKV reactivation can come from the donor or the recipient. Recipients who had BKV infection and received a kidney from the same donor have been shown to have identical BKV genotypes, supporting donor transmission [Bohl et al., 2005; Vera-Sempere et al., 2006]. Recipients whose donors had higher BKV antibody titers were more likely to develop BKV infection than those with lower titers, also supporting donor transmission [Bohl et al., 2005; Andrews et al., 1988]. Injury is also believed to contribute to reactivation. Therefore, screening for viral replication is the most useful tool for the identification of patients at risk of developing nephropathy, thus allowing for earlier intervention, in particular a prevemptive reduction of immunosuppression, with improvement of outcome [Costa and Cavallo, 2012]. Screening for polyomavirus replication presents a high negative predictive value (>99%), as in the absence of virus replication PVAN is excluded [Mischitelli et al., 2007; Cavallo et al., 2009]. Screening for viral replication is also the most important tool for monitoring the response to treatment in patients with diagnosed PVAN. Different screening assays are available:

1) urine cytology, i.e. detection of epithelial cells termed “decoy cells” that are present in 40-60% of transplant recipients, although it is a good screening test with a negative predictive value (NPV) of 100%, positive predictive value (PPV) is very low (about 20%) [Hariharan et al., 2006];
2) quantification of urinary BKV-DNA, with a load 100-fold higher than plasma values evidenced in 30-40% of transplant recipients, that has a PPV of approximately 40% [Hariharan et al., 2006];
3) quantification of plasma BKV-DNA, with a viral load $>10^4$ copies/mL recommended for a presumed diagnosis of PVAN [Hirsch et al., 2005; Marchetti et al., 2007; Smith et al., 2007];

4) quantification of urinary VP1 mRNA that is likely to mirror active viral replication.

Considering that viral inclusions may be absent in the early stages of PVAN, inflammation may be scarce and the focal nature of renal involvement, the quantification of polyomavirus DNA on renal graft biopsies and/or ureteral specimens could also be taken into account besides histopathological evaluation. Polyomavirus-DNA quantitation could be useful in the presence of little evidence of viral cytopathy [Schmid et al., 2005]. The limited sensitivity of allograft biopsy is also critical for the definition of “resolved PVAN” as the goal of any intervention. Resolution of PVAN not only requires the disappearance of the histological signs of active disease (i.e., viral replication, inclusions, necrosis, inflammatory infiltrates) and negative immunohistochemistry, but should also include negative results of the surrogate replication markers such as BKV viremia and viruria.

1.2.3 DIAGNOSIS

PVAN is typically diagnosed within the first year post transplantation, although approximately 25% of the cases are seen later. When BKV nephropathy is diagnosed early within the first 6 months after transplantation and the creatinine is stable, survival is improved compared with when the diagnosis is made later and the creatinine is elevated. The definitive diagnosis of PVAN is made by histopathologic evaluation, however this form of diagnosis presents some drawbacks, including limited sensitivity due to focal involvement, thus accounting for sampling errors; varying presentations with cytopatic-inflammatory and/or fibrotic/scarring patterns; difficult differential diagnosis from acute rejection, that may coexist with an opposite impact on intervention strategies [Costa and Cavallo, 2012]. The diagnosis and the severity of BKV infection correspond to our understanding of the pathogenesis of nephropathy. Viral replication

begins early after transplantation and progresses through detectable stages: viruria then viremia then nephropathy (figure 9) [Hirsch et al., 2002; Brennan et al., 2005(a); Bressollette-Bodin et al., 2005; Limaye et al., 2001; Nickeleit et al., 2000]. Viruria can be detected by PCR for BKV DNA, reverse transcription PCR for BKV RNA, cytology for BKV inclusion bearing decoy cells, or electron microscopy for viral particles [Hirsch et al., 2002, Gardner et al., 1984,Brennan et al., 2005; Ding et al., 2002]. These tests are sensitive for detecting active BKV infections but lack specificity for nephropathy because the detected virus could originate anywhere along the urinary tract. Detection of BKV DNA in the plasma or viremia may be a better indicator of nephropathy. As the infection intensifies, the markers of viral replication increase. Threshold values have been suggested to predict BKV nephropathy, but considerable overlap of these values exists among recipients without BKV nephropathy, active BKV nephropathy, and solved BKV nephropathy [Randhawa et al., 2004]. Considering the main pathogenic factors of PVAN, i.e., viral replication and failure of immune surveillance, early diagnosis may be accomplished by virological and viro-immunological monitoring, consisting in monitoring of viral replication and evaluation of virus-specific immune response, respectively.

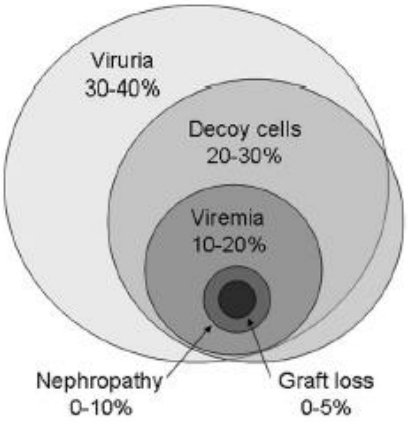

Figure 9: Type and prevalence of BKV infections in kidney transplant recipients [Bhol et al., 2007]

1.2.4 TREATMENT

The treatment of PVAN has three fundamental objectives: to eliminate the virus, to avoid the development of acute rejection, and to preserve the renal function [Cavallo et al., 2009]. At the moment, there is no approved and defined treatment for PVAN. The main line of intervention consist in reducing immunosuppression. This can be accomplished by three different approaches: reducing, stopping or switching the immunosuppressive drugs employed. More recently, the use of the immunomodulant agent leflunomide, together with the reduction of immunosuppression has been proposed. As the majority of cases of PVAN have been associated to triple immunosuppressive therapy including combinations of calcineurin inhibitors (tacrolimus, cyclosporine A), antiproliferative agents (mycophenolate mofetil, azathioprine) and corticosteroids, most of recommended strategies includes decreasing, switching or stopping the ongoing treatment [Costa and Cavallo, 2012]. Reduction of immunosuppression may prove insufficient to control viral replication or may not be appropriate in patients at high risk of rejection. Antiviral agents have been used, but no defined treatment is recommended and results are controversial. On the basis of in vitro activity against BKV, cidofovir, quinolones, and intravenous Ig (IVIG) have been reported as treatment options for BKV nephropathy. Cidofovir is a cytosine analogue and viral DNA polymerase inhibitor of BKV replication, but the mechanism is unclear because BKV lacks a viral polymerase gene [Farasati et al., 2005; Andrei et al., 1997; De Clercq et al., 2003]. Rather than a direct effect on BKV replication, cidofovir may restore the function of p53 and pRb, targets of the large T antigen, and permit BKV-infected cells to undergo apoptosis [Akan et al., 2006; De Clercq et al., 2003]. Despite this evidence, actually there is no randomized controlled study on the immusuppressive drugs and no selective antiviral target. The prevention of PVAN by regular monitoring of viremia/viruria remains the most appropriate approach and may prompt a preemptive reduction of immunosuppression.

1.3 HYPOXIA INDUCIBLE FACTOR

Hypoxia is defined as a reduction of oxygen amount available to a cell, tissue or organism. Oxygen deprivation creates significant stress in living cells linked to inappropriate accumulation of free radicals, which cause additional stress on proteins and DNA in the cell. The decline of oxygen level can also cause alteration in gene transcription or may result in posttranslational modifications of proteins, leading to changes of cell metabolism. Cells temporarily arrest in the cell cycle, reduce energy consumption and secrete survival and proangiogenic factors. The cellular response to hypoxia is focused on addressing the energy deficit created by the decrease in available oxygen. When aerobic metabolism is diminished due to the lack of molecular oxygen, cell utilizes the hypoxia inducible factors (HIFs) signaling cascade that drives the expression of a wide variety of genes essential for the adaptive response to hypoxia. HIFs are the master regulators of oxygen homeostasis and play a role in the development, postnatal physiology as well as disease pathogenesis. Since then, more than 70 targets genes regulated directly by HIFs have been identified and expression of over several hundred genes are known to be directly or indirectly influenced by HIF.

1.3.1 STRUCTURES AND ISOFORMS

HIF is a dimer composed of 120 kDa oxygen-regulated α-subunit and the constitutively expressed 91-94 kDa β-subunit (also known as the aryl hydrocarbon receptor nuclear translocator, ARNT). In mammals there are three isoform of the HIF-1α subunit (HIF-1α, HIF-2α also known as EPAS1 and HIF-3α or IPAS) and three isoform paralogues of HIF-1β (Arnt1, Arnt2 and Arnt3) [Zagorska and Dulak, 2004]. HIF-1α and HIF-2α are the best understood and described [Loboda et al., 2010, Majmundar et al., 2010]. HIF1 is the principal regulator of the hypoxic response in the mammalian cells [Semenza et al., 1998] and in particular, HIF-1α is recognized to

control more than 100 genes and this suggested that in endothelial cells more than 2% of all human genes may both directly or indirectly regulated by this factors [Manalo et al., 2005]. The role of HIF-3α is less well understood, but it is has been suggested that the alternative splice form of HIF-3α binds to and inhibits the transcriptional activity of HIF-1α [Makino et al., 2001]. HIF-2α has a similar structure to HIF-1α but the pattern of their expression varies: HIF-1α is widely present while HIF-2α is expressed only in certain tissues [Wiesener et al., 2003]. In particular, HIF-2α and HIF-3α are selectively expressed in vascular endothelial cells, type II pneumocytes, renal interstitial cells, liver parenchymal cells and cells of the myeloid lineage [Bertout et al., 2008]. Both α and β subunits are member of the family of the basic helix-loop-helix (bHLH) and PER-ARNT-SIM (PAS) domain-containing transcription factors [Wang et al., 1995]. Apart from those domains, which are important for DNA binding and dimerization, a central oxygen-dependent degradation domain (ODD) as well as two transactivation domains are also recognized: the N-terminal activation domain (NAD) and C-terminal activation domain (CAD) (located in the Transactivation and stability domain, TAD). The N-terminal transactivation domain of HIF-1α and HIF-2α is essential for targeting gene specificity [Dyan et al., 2006; Hu et al., 2007], while the CAD contributes to the regulation of most, but not all, HIF target genes (figure 10). HIF-α subunits heterodimerize with the stable HIF-1β subunit through their HLH and PAS domains. HIF heterodimers recognize and bind to hypoxia response elements (HREs) in the genome, which are similar to enhancer box (E box) motifs and have the consensus sequence G/ACGTG. Genome-wide chromatin immunoprecipitation experiments indicated that the correlation between HRE occupancy and hypoxic gene induction ranges from high for HIF1α upregulated genes to low for both HIF2α induced genes and HIF repressed genes [Mole et al., 2009; Xia et al., 2009]. In these latter cases, flanking sequences and additional regulatory elements appear to further

specify HIF binding and target gene regulation. Recent examples of additional modifiers of HIF dependent gene regulation include the forkhead box protein A2 (FOXA2) and the chromatin modifier Reptin [Qi et al., 2010; Lee et al., 2010].

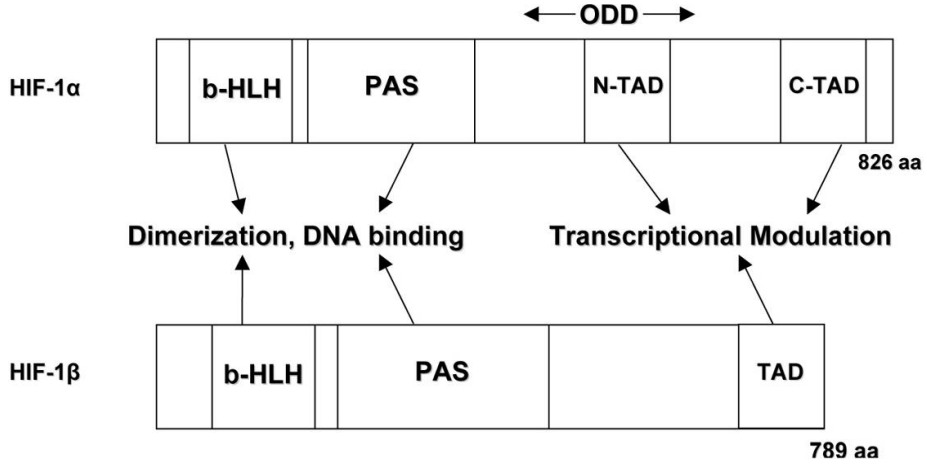

Figure 10: Schematic representation of HIF-1α and HIF-1β complex [Duffy et al., 2003]

1.3.2 MECHANISM OF REGULATION

1.3.2.1 OXIGEN DEPENDENT REGULATION

The HIF system is subject to a number of complex feedback mechanism. Regarding the HIF proteins, ARNT are constitutive nuclear proteins whereas the expression and activity of the α subunit is tightly regulated by oxygen concentration. It rapidly accumulates upon exposure to hypoxia and on reoxygenation is quickly degraded with a half-life of less than 5 min [Yu et al., 1998]. Given how detrimental hypoxia is to a cell, this rapid response time highlights the speed at which a cell must elicit a reaction to loss of oxygen tension. Equally important is the short half-life of the HIF protein following reoxygenation, and this time frame suggests that prolonged HIF activation might not be beneficial to the cell. The understanding of the mechanism that a cell uses to sense hypoxia and conveys this signal to the

alpha subunit has greatly increased over the last years. HIF-1α protein levels are tightly regulated by several mechanisms, but the most notable of these is the degradation pathway. Under aerobic conditions, HIF-1α undergoes proteasomal degradation via the ubiquitin-dependent pathway. This is due to the recent identification of a family of hydroxylases that modify the α subunit in an oxygen dependent manner [Lee et al., 2007]. These modifications are mediated by three hydroxylases, known as prolyl hydroxylase domain containing proteins (PHD) that posttranslational hydroxylate specific proline residues (Pro402 and Pro564) within the ODD of HIFα under normoxia [Bruick & McKnight, 2001; Epstein et al., 2001; Loboda et al., 2010]. Three PHDs proteins have been identified so far: PHD1, 2 and 3 [Epstein et al., 2001]. Although *in vitro*, all three hydroxylate HIF-1α [Bruick and McKnught, 2001], *in vivo* PHD2 isoform plays a major role in normoxic HIF-1α regulation [Appelhoff et al., 2004; Berra et al., 2003]. The proline hydroxylations are required for the interaction of HIFα with the von-Hippel Lindau tumor suppressor gene product (pVHL). pVHL serves as the recognition component of E3 ubiquitin-ligase that leads to HIFα ubiquitination and 26S proteosomal degradation [Bruick and McKnight, 2001; Epstein et al., 2001; Cockman et al., 2000; Maxwell et al., 1999]. During hypoxia, or in case of lack of PHDs cofactors, PHDs are inactive preventing binding of pVHL. Therefore, HIF-1α/2α escape ubiquitin and proteasomal degradation and can be transported to the nucleus where, after dimerization with HIF-1β and recruitment of numerous coactivators, they both bind to the same HRE at the target gene loci [Chilov et al., 1999]. HRE has a core of five-nucleotide sequence RCGTG (R:A/G) which is well conserved among numerous hypoxia responsive genes [Semenza et al., 1996]. The inactivation of PHDs during hypoxia and concomitant HIF-1α stabilization are also caused by PHDs degradation, which is mediated by E3 ubiquitin ligases Siah1a and Siah2 [Nakayama et al., 2004]. The mechanism of the PHDs degradation by Siah2 is dependent on p38 and

Akt kinases activity. Siah2 is subjected to phosphorylation by p38 that increases its activity under hypoxia conditions. Siah2 is upregulated when an active form of Akt is introduced in the cells [Nakayama et al., 2007]. HIFα subunits are also substrates for an asparaginyl hydroxylase: the Factor Inhibiting HIF-1α (FIH1). This enzyme is oxygen-dependent and represents another component of the oxygen-sensing machinery. Hydroxylation by FIH1 disrupts a critical interaction between HIFα and co-activators p300/CREB-binding protein (CBP), impairing HIF transcriptional activity [Webb et al., 2009; Mahon et al., 2001]. However, FIH1 has other targets [Webb et al., 2009; 2009(a)], indicating that it may have HIF-independent functions as well (figure 11).

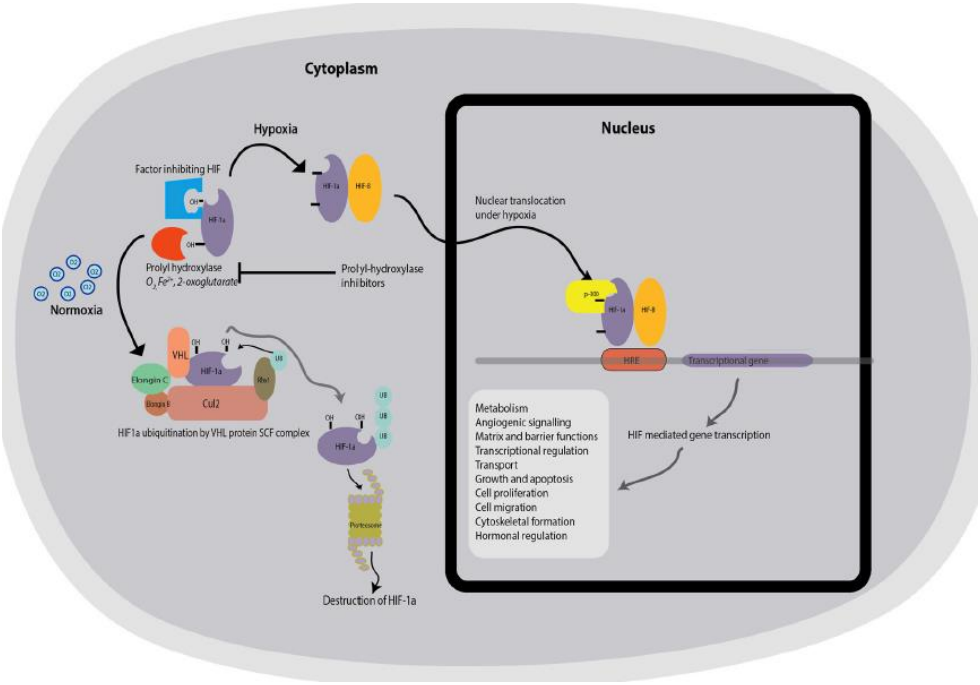

Figure 11: Schematic description of the HIF-1α pathway [Akhtar et al., 2014]

1.3.2.2 OTHER MECHANISMS OF REGULATION

Oxygen dependent regulation of HIF-1α degradation involves pVHL, however there has been increasing evidence of pVHL independent pathways of HIF-1α degradation [Koh et al., 2008; Liu et al., 2007a, 2007b; Luo et al., 2010]. Hypoxia-associated factor (HAF), detected both in normal and tumor derived cell lines and in proliferating tissues, but undetectable in normal non proliferating tissues, has been shown to regulate HIF-1α protein stability [Koh et al., 2008]. Koh et al. demonstrated that HAF promotes HIF-1α degradation independently of cellular oxygen tension. HAF overexpression diminishes HIF-1α, whereas HAF knockdown increased HIF-1α levels independently of pVHL or oxygen. Interestingly, the HAF action is selective for HIF-1α, as neither HAF knockdown nor overexpression caused any change in the levels of HIF-2α. This suggests that HAF is a novel HIF-1α isoform specific E3 ligase [Koh et al., 2008]. Extracellular heat shock protein 90 (Hsp90) is a molecular chaperone among whose client proteins is also HIF-1α. Accordingly, HIF-1α stability can be regulated by the receptor of activated protein kinase C (RACK1), which competes with Hsp90 for binding to HIF-1α and promotes the ubiquitination and degradation of HIF-1α in cells exposed to the Hsp90 inhibitor 17-allylaminogeldanamycin (17-AAG) [Liu et al., 2007a] or the calcineurin inhibitor cyclosporine A [Liu et al., 2007b]. Recently, also Hsp70 and carboxyl terminus of Hsc70-interacting protein (CHIP) were identified as HIF-1α interacting proteins that selectively regulate ubiquitination and degradation of HIF-1α, but not HIF-2α [Luo et al., 2010]. HIF-1α may also undergo other posttranslational modifications. The oxygen-dependent degradation of HIF-1α by pVHL can also be mediated by hypoxia induced HIF-1α small ubiquitin-like modifier (SUMO)ylation. Interestingly, SUMOylation can either positively [Bae et al., 2004; Carbia-Nagashima et al., 2007] or negatively [Berta et al., 2007; Cheng et al., 2007] regulate HIF-1α stability. It was also shown that SUMOylation promotes the binding of

pVHL to HIF-1α even when the latter is not hydroxy- lated on Pro402 or Pro564 [Cheng et al., 2007]. Recent data showed that also HIF-2α is a target protein of SUMO modifier [van Hagen 2009 Loboda]. Phosphorylation is another mechanism of HIF-α stabilization. HIF-1α undergoes phosphorylation by ERC/microtubule-associated proteins (ERK-MAPK), resulting in increased transcriptional activity [Richard et al., 1999]. It has been shown that p42/44 and p38 kinase phosphorylated HIF-1α and HIF-2α *in vitro* [Richard et al., 1999; Sodhi et al., 2000], whereas inhibitors of these pathway blocked HIF-1α mediated reporter gene expression [Hur et al., 2001].

1.3.3 TRANSCRIPTIONAL CO-ACTIVATORS

HIF-mediated transcription is dependent on the activity of several coactivators, which are recruited to form, together with HIF-α and β, an active HIF complex. This process is mediated by transactivation domains, the centrally located NAD, and the CAD, situated at the C-terminus end of the HIF-α proteins. The data obtained from many studies indicate that the p300/CBP is a central integrating coactivator [Arany et al., 1996] which, after binding with the HIF-1α or HIF-2α CAD helps to recruit the accessory coactivators like steroid receptor coactivator (SRC-1), transcription intermediary factor-2 (TIF-2) or the redox factor 1 (Ref-1), a nuclear protein possessing both redox and apurinic endonuclease DNA repair activities [Xanthoudakis and Curran, 1992]. The coactivators play two main roles: stabilizing the transcription initiation complex, that contains the RNA polymerase II, and also possessing histone acetyl- transferase activity that is required for the polymerase to access DNA within chromatin and transcribe it into RNA. SRC-1 and TIF-2 are the members of the SRC-1/p160 family of transcriptional coactivators harboring histone acetyltransferase activity, and are able to interact with HIF-1α and enhance its transactivation potential in a hypoxia-dependent manner [Carrero et al.,

2000]. Ruas and colleagues have found that SRC-1 does not interact directly with HIF-1α but is recruited to the complex by CBP in a hypoxia-dependent manner. By the use of different biochemical assays they showed that depletion of CBP from cell extracts abrogated the interaction between SRC-1 and HIF-1α [Ruas et al., 2005]. Ref-1 has also been shown to be involved in the formation of active HIF complex. Overexpression of Ref-1 enhances the transcriptional activity of HIF-1α [Huang et al., 1996] and the mechanism of this action relies on the redox-dependent interactions between HIF-1α and transcriptional coactivators, including p300 and CBP [Carrero et al., 2000]. Ref-1 takes an active part in the formation of hypoxia-inducible transcriptional complex regulating the main target gene of HIF-1α, the vascular endothelial growth factor (VEGF) expression in rat pulmonary artery endothelial cells [Ziel et al., 2004]. Interestingly, specific coactivators which bound only HIF-2α have been found. For example NF-KB essential modulator (NEMO) is unique for HIF-2α and enhances HIF-2α mediated transcription activity at normoxia [Bracken et al., 2005]. Similarly, the transcription factor Ets1 has been demonstrated to interact exclusively with HIF-2α for the transcription of VEGF receptor 2 [Elvert et al., 2003]. Another Ets family transcription factor, Elk-1, cooperates with HIF-2α to activate the target genes CITED-2, erythropoietin (EPO), insulin-like growth factor- binding protein-3 (IGFBP3), and plasminogen activator inhibitor-1 (PAI-1) [Aprelikova et al., 2006; Hu et al., 2007]. Another group of accessory molecules contains the factors which are required for transcription of specific HIF target genes. For example, hepatocyte nuclear factor 4 (HNF-4), acting together with HIF-1, is a liver and kidney specific transcription factor reported to be obligatory for EPO transcription [Zhang et al., 1999]. The deletion mutant of HNF-4, lacking the carboxyl terminal transactivation domain, which is essential for protein-protein interactions with HIF-1α, has been shown to prevent hypoxia induction of EPO [Tsuchiya et al., 2002]. The region of the transcriptional

coactivators binding is controlled by asparaginyl hydroxylase, also termed FIH-1, which was identified as a 2-oxoglutarate and Fe(II) dependent oxygenase, similarly as PHDs which modify proline residues in ODD domain [Lando et al., 2002]. FIH-1 modified the asparagine 803 of human HIF-1α, located in the CAD domain, what lead to blockage of p300/CBP coactivators recruitment to HIF-1α. Similarly, FIH-1 is capable of modifying the key asparagine residue (N851) within the HIF-2α CAD, thereby suppressing its activity [Lando et al., 2002].

1.3.4 HIF-1A STABILIZATION IN EXPERIMENTAL MODELS

The most recent model for oxygen sensing suggests that iron-mediated hydroxylation occurs via a group of HIF-specific proline hydroxylases [Yuan et al., 2003]. It was suggested that these hydroxylases have an iron binding-center and that iron is critical for its enzymatic activity. Epstein and colleagues [Yuan et al., 2003] further proposed that iron chelators can remove iron from the iron-binding center of the enzyme and that the iron can be replaced by cobalt at this site, which inactivates the hydroxylase activity. This model is consistent with the observations that cobalt (a transition metal) and iron chelators inhibit hydroxylation of HIF. It has been well documented that cobalt mimics hypoxia by causing the stabilization of HIF-α. The data available in the literature indicated that cobalt is cytotoxic to many cell types, including neural cells [Wang et al., 2000; Olivieri et al., 2001; Yang et al., 2004] and can induce cell death by apoptosis and necrosis [Huk et al., 2004]. Cobalt can cause DNA fragmentation [Zou et al., 2001; Araya et al., 2002; Graham et al., 2004], activation of caspases [Zou et al., 2002], increased production of reactive oxygen species (ROS) [Olivieri et al., 2001; Zou et al., 2001; Chandel et al., 2000], augmented phosphorylation of mitogen activated protein (MAP) kinases [Yang et al., 2004; Zou et al., 2002] and elevated levels of p53 [Chandel et al., 2000]. Some of the characteristic effects of cobalt are thought to be mediated by

interaction with the cellular oxygen-sensing machinery. Like low oxygen tension, cobalt at normoxic conditions is able to stabilize the α-subunit of hypoxia-inducible factor HIF-1 by blocking its ubiquitination and proteasomal degradation [Epstein et al., 2001]. Increased levels of HIF-1α result in higher transcription of a set of genes that encode several proteins, i.e. glycolytic enzymes, erythropoietin and heat shock proteins, important for the adaptation of cells to hypoxic stress [Wiesener et al., 2003; Sharp et al., 2004]. Like HIF-1α, the levels of HIF-2α protein are low during normoxia and accumulate when cells are exposed to hypoxia, proteasomal inhibitors, transition metals (i.e. cobalt), iron chelators, or reducing agents [Yuan et al., 2003]. However, the biochemical mechanism by which cobalt stabilizes HIF-α remains unknown. A recent model suggested that the hydroxylation of HIF-α is mediated by a group of HIF-specific hydroxylases and that cobalt can inactivate the enzymes by occupying an iron-binding site on the proline hydroxylases [Yuan et al., 2003]. More recently, Yuan and colleagues showed that cobalt inhibits the interaction between pVHL and hydroxylated HIF-α and that inhibits the hydroxylation of a key proline residue within the ODD domain of HIF-2α. This is the first report that cobalt stabilizes cellular HIF-2α by occupying the pVHL-binding domain. This model suggests that cobalt also stabilizes HIF-α proteins by binding directly to the ODD and that cobalt inhibits both hydroxylation and the interaction between hydroxylated HIF-α and pVHL. This conclusion is supported by MALDI data, which revealed that cobalt binds directly to a synthetic HIF peptide with a nonhydroxylated proline residue [Yuan et al., 2003]. In addition, results of Yuan and colleagues showed that cobalt inhibits the HIF-pVHL interaction even after the proline residue becomes hydroxylated. Thus, cobalt can bind to HIF regardless of the hydroxylation state of the proline residue within the ODD. The study was carried out *in vitro* and does not necessarily reflect how cobalt functions within cells. One possible model to explain how cobalt could stabilize HIF-α in cells is illustrated in

figure 12. Cobalt may occupy the iron center of a HIF-α specific proline hydroxylase, thereby inactivating the enzyme. Even if a subset of HIF-α does undergo hydroxylation, hydroxylated HIF-α could still bind to cobalt. Cobalt could thereby prevent the interaction between pVHL and hydroxylated HIF-α, which would prevent the subsequent ubiquitination and degradation of HIF-α.

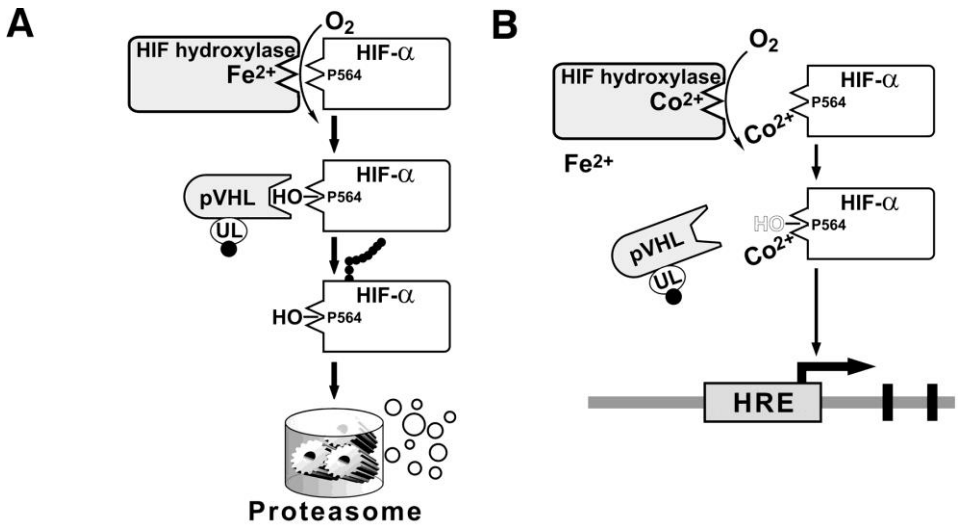

Figure 12. Proposed model for oxygen sensing. **A**, the current model for oxygen sensing. The HIF-specific hydroxylase is thought to be an iron-binding protein. In the presence of oxygen, it catalyzes the hydroxylation of proline 564 within HIF. Hydroxylated HIF is then ubiquitinated by pVHL. Ubiquitinated HIF is degraded by proteasomal mechanism. Cobalt inhibits the hydroxylation of HIF by binding to the iron-binding domain of HIF hydroxylase. **B**, revised model based on the new in vitro data. Hydroxylation of HIF-α is mediated by a HIF-specific hydroxylase. Cobalt binds to the iron center of this enzyme to inactive the hydroxylase activity. Even if a portion of HIF-α becomes hydroxylated, cobalt can also bind directly to the hydroxylated proteins to prevent the interaction between HIF-α and pVHL, thereby preventing the degradation of HIF-α [Yuan et al., 2003]

1.3.5 HIF-1A ACTIVATION DURING KYDNEY TRANSPLANTATION

During the process of transplantation, organs are subjected to hypoxic and ischemic injury at the moment of procurement, preservation and following reperfusion. This process of ischemia reperfusion injury (IRI) is recognized as being detrimental for organ function and long-term graft survival. In particular, in renal transplantation, acute tubular necrosis (ATN) contributes significantly to the development of delayed graft function. This has led to propose ex vivo machine preservation in attempt to reduce the impact of IRI [Moers et al., 2009]. As a consequence, the transplant scientific community has focused its attention in order to reducing and ameliorating the effects of organ ischemia through different approaches: modulating donor management, improving ex vivo organ preservation and minimizing reperfusion injury. It is recognized that all mammalian cells have the intrinsic ability to sense oxygen and the capacity to activate protective genes in the face of hypoxia [Maxwell et al., 1993]. For these reasons, better understanding of the role of the HIF pathway in the context of organ donation and transplantation could be of importance in improving the quality of older and ‘‘high-risk’’ donor organs. Conde and colleagues [Conde et al., 2012] have investigated both in the *in vitro* and *in vivo* settings the effect of stabilizing HIF-1α on the outcomes of IRI models. They exposed a proximal tubular HK-2 cell line to a period of 6 h of hypoxia and nutrient deprivation to mimic ischemia, followed by re-oxygenation in a complete medium as an analogue of reperfusion [Conde et al., 2012]. They identified HIF-1α stabilization during hypoxia and again following 3 h of reperfusion, with lower signals being detected between the two periods. Conde and colleagues [Conde et al., 2012] demonstrated also that the response was mediated by an Akt/mTOR signaling pathway and the protective effects could be ameliorated by siRNA for HIF-1α or YC-1 (a pharmacological inhibitor of HIF-1α). Analysis on biopsies taken during transplantation have demonstrated that the HIF system was activated as a

result of the procurement process and correlated with the degree of exposure of kidneys to warm and cold ischemia [Baan et al., 2003]. Rosenberger and colleagues demonstrated, using high-amplification immunohistochemistry in human kidney biopsies, that immediately following engraftment, HIF-1α was detectable with low HIF detection scores correlating with primary nonfunction [Rosenberger et al., 2006]. The authors demonstrated that HIF-1α was detectable both in the renal cortex and in the medulla with collecting ducts and glomeruli showing a high signal. At 2-weeks post engraftment analysis of biopsies showed widespread HIF-1α induction and the authors attributed the presence of HIF to the effects of posttransplant hyperfiltration, hypertrophy and calcineurin inhibitor induced toxicity. At 3 months, HIF expression was no longer detectable except in kidneys, demonstrating clinical and sub-clinical rejection. The authors hypothesized that the increased HIF expression was due to the rejection induced hypoxia. However, inflammatory cell induction of HIF remains a possibility, and the relation between HIF levels and allograft rejection requires further evaluation.

1.3.6 HIF-1A AND VIRAL INFECTIONS

To control viral and other microbiological infections, the host has developed a broad arsenal of innate defense mechanisms, including physical barrier functions, soluble effectors such as complement and antimicrobial peptides and phagocytic cells. The critical role of phagocytes in host defense lies in their rapid mobilization and ability to recognize and inactivate pathogens independently of prior encounter, as required by adaptive immunity. The principal phagocytes of mammalian innate immunity are cells of the myeloid lineage, monocyte/macrophages and neutrophils. These short-lived cells are recruited in response to alterations of tissue integrity, whether the byproduct of chemical or physical injury or the spread of infectious microorganisms [Zinkernagel et al., 2007]. To maintain energy homeostasis

and carry out their biological activities in these specialized environments, phagocytic cell types must generate adenosine triphosphate (ATP) via glycolysis. Because upregulation of virtually every enzyme in the glycolytic pathway is mediated almost exclusively by HIF-1α [Semenza et al., 1994], a role for this transcription factor in supporting phagocyte function during inflammation was intuitive. In the last few years, genetic tools provided not only experimental validation of this concept, but uncovered profound implications of the HIF-1α control pathway in the overall regulation of mammalian innate immunity [Zinkernagel et al., 2007]. Activation of HIF-1α pathway during the life cycle of viral pathogens has been the subject of various investigation, revealing a diversity of functional outcomes in disease progression and critical linkages to viral oncogenesis. Viral infection is generally appreciated to induce stabilization of HIF-1α in target cells, which consequently contributes to local inflammation. For example, the common pathogen of the upper respiratory tract, the respiratory syncytial virus (RSV), induces HIF-1α in primary human bronchial epithelial cells via a NO-dependent pathway [Kilani et al., 2004]. Increased HIF-1α levels stimulate VEGF production, enhancing monolayer permeability, which may play a role in the airway edema of acute RSV infection. In some cases, HIF-1α may help coordinate a host defense program to limit cell damage secondary to viral infection. This scenario might particularly apply to viruses which exert an acute cytolytic effect, such as the vesicular stomatitis virus (VSV). Several years ago, it was noticed that hypoxia reduced the cytopathogenicity and replication of VSV, with measured antiviral effects of interferons α and γ potentiated under the low oxygen conditions [Naldini et al., 1993]. Interferons in turn have been shown to upregulate the expression of HIF-1α [de Veer et al., 2001]. The significance of HIF in the antiviral response to VSV was recently established by a pharmacological approach for the inhibition of HIF activity by a small molecule antagonist (chemotin) or RNA interference enhanced VSV

cytotoxicity and replication, whereas the treatment with the hypoxia mimetic cobalt chloride promoted cellular resistance to infection [Hwang et al., 2006]. Furthermore, expression profiling showed HIF enhancement of interferon β and other antiviral genes during VSV infection [Hwang et al., 2006]. For a number of persistent viral infections, when induction of HIF-1α is insufficient to conduct the eradication, the accompanying proangiogenic program can contribute to oncogenesis. For example, chronic infections with the hepatitis B and C viruses (HBV and HCV) are epidemiologically associated with the development of hepatocellular carcinoma (HCC), a highly vascularized solid tumor. The X protein of HBV (HBx) is felt to play an important role in angiogenesis and metastasis of HCC [Wang et al., 1994]. HIF-1α levels and nuclear translocation are increased in cultured liver cells by expression of HBx via p42/p44 mitogen-activated protein kinase (MAPK) pathways, leading to transcriptional activation of HIF-1α target genes including VEGF, a finding corroborated *in vivo* in the livers of HBx transgenic mice [Yoo et al., 2003]. HBx was found to interact directly with the bHLH/PAS domain of HIF-1α, blocking its association with pvHL and thus preventing its ubiquitin-mediated degradation [Moon et al., 2004]. Moreover, HIF-1α activation induced by HBx was found to increase the multi-drug resistance 1 (MDR1) transporter activity in a hepatoma cell line, thereby contributing to increase the resistance of the cancer cells to chemotherapeutic agents [Han et al., 2007]. Recently, HCV infection has also been found to stabilize HIF-1α with contributions from MAPK and other cellular activation pathways (NF-kB, STAT-3, PI3-K/AkT), stimulating VEGF production and neovascularization in a chick chorioallantioic membrane surrogate assay system [Nasimuzzaman et al., 2007]. Another example linking viral activation of HIF-1α to proangiongenesis and tumor development can be found in the case of human papillomavirus-16 (HPV-16), the etiologic agent of cervical interstitial neoplasia that, undetected, can progress to cervical carcinoma. In advanced cervical cancer lesions,

many of which are hypoxic, increased HIF-1α levels can be correlated to poor prognosis [Hockel et al., 1996, Birner et al., 2000]. Transfection of human cervical cancer cell lines with HPV-16 oncoproteins E6 and E7 can induce VEGF expression and capillary formation in vitro; however, this proangiogenic effect is abolished when the cells are cotransfected with siRNA targeting HIF-1α [Tang et al., 2007]. Together, these new studies suggested a synergism of HIF-1α with viral oncogenes in premalignant lesions to promote gene activation programs favoring neovascularization and cancer development. Increased HIF-1α protein levels and VEGF expression are detected in T-cell lines infected with the human T-cell leukemia virus type 1 (HTLV-1), via a process involving activation of PI3K/Akt signaling by the HTLV-1 protein Tax [Tomita et al., 2007]. The major oncoprotein of the Epstein Barr virus (EBV), latent membrane protein 1 (LMP1), increases HIF-1α levels and stimulates VEGF expression in nasopharyngeal epithelial cells through a mechanism dependent both upon hydrogen peroxide (H_2O_2) production and p42/p44 MAPK activity [Wakisaka et al., 2004]. Co-immunoprecipation studies indicate EBV LMP1 enhances the stability of Siah1 E3 ubiquitin ligase, inducing proteasomal degradation of PHD-1 and PHD-3 that normally tag HIF-1α for degradation. LMP1 thus prevents formation of the VHL/HIF-1α complex, providing a mechanism for HIF-1α stabilization during EBV nasopharyngeal cell infection [Kondo et al., 2006]. A fascinating crosstalk between viral genes and the HIF- 1α pathway has been elucidated for the human herpesvirus 8 (HHV-8). HHV-8 infection of endothelial cells in vitro leads to increased stabilization of the two HIF-α subunits and increased HIF responsive gene expression [Carroll et al., 2006]. The HHV-8 latency-associated nuclear antigen (LANA), which plays a critical role in modulating viral and target cell gene expression, increases HIF-1α mRNA levels, and also physically interacts with the transcription factor to enhance its promoter activities [Cai et al., 2006]. HIF-1α induction and co-activation during HHV-8 infection can

then lead to activation of target genes in the genome of the virus itself, which is involved in transition of the virus from latency to a lytic replication phase. Another potential example of viral HIF crosstalk, is for the parvovirus B19 replication that results enhanced under hypoxic conditions. HIF-1α binding to an HRE located in the B19 promoter region can be demonstrated; however, the full implications of this finding for viral pathogenesis remain unclear [Pillet et al., 2004].

1.3.7 HIF-1A AND HUMAN POLYOMAVIRUS JC

The recent research above described has highlighted the importance of hypoxic response and HIF signaling in controlling immune responses towards infectious agents. Like for the other viruses, HIF-1α resulted involved also in the activation of JCV, an opportunistic human neurotropic polyomavirus that, in case of immunosuppression, can cause the Progressive Multifocal Leukoencephalopathy (PML). The first demonstration of the mechanism by which JCV crosses the blood-brain barrier (BBB) was given by Chapagain and colleagues in 2007 [Chapagain et al., 2007]. In particular, they reported that cell-free JCV entry into the brain by infecting human brain microvascular endothelial cells and replicated efficiently producing infectious virions. JCV is capable to promoting cellular stress and is known that several transcription factors have been implicated in the activation of the JCV promoter. A work of Piña-Oviedo and colleagues investigate this aspect and demonstrate the implication of HIF-1α in the activation of JCV and the role in the development of PML in human oligodendrocytes. HIF-1α was found up regulated in glial cells where JCV replication takes place, bizzare astrocytes and oligodendrocytes. The increase level of HIF-1α is probably due to the response of cellular stress caused by the infection with JCV. They observed an up regulation of HIF-1α in endothelial cells from small capillaries within areas of demyelination [Piña-Oviedo et al., 2009]. These

data, taken together with the discovery of Chapagain and colleagues, lead to a novel model to explain the rising of PML: JCV replication in endothelial cells in association with the enormous stress of these areas caused by demyelinating process are responsible for the up-regulation of HIF-1α in these cells. Furthermore, with transcription activation assay they found JCV promoter activation by HIF-1α both for the early and the late promoters. Interestingly, the activation was potentiated in the presence of Smads (pathway downstream effectors of the transforming growth factor-beta TGF-β), which suggests cooperation between HIF-1α and other proteins in the stimulation of JCV transcription and replication. Finally, with others set of experiments, they demonstrate the co-localization of HIF-1α and Smads in the nuclei of JCV affected glial cells in cases of PML and *in vitro*, as well as their physical interaction by co-immunoprecipitation and the binding of HIF-1α to the JCV control region by a chromatin immunoprecipitation assay. These evidences also open another topic about HIF-1α and JCV latency and reactivation. It is well established that after a subclinical primary infection, JCV remains in a latent state in the kidney, one of the organs that has the capability to detect hypoxia [Beckmann and Shah 1983]. Hypoxic conditions can activate glycolysis resulting in the increased synthesis of pyrimidines and purines required for JCV viral replication.

2. AIM OF THE STUDY

The human polyomavirus BK (BKV) is a member of the *Polyomaviridae* family detected in 1971 in the urine of an immunosuppressed renal transplant recipient who developed ureteric stenosis [Gardner et al., 1971]. BKV has a worldwide seroprevalence of about 90%. After the primary infection, BKV establishes a life-long latency within the urogenital tract. The severe immunological impairment occurring in transplant kidney recipients leads to BKV reactivation that may result in the polyomavirus associated nephropathy (PVAN). During transplantation, kidney is subjected to hypoxic conditions, driven by the action of Hypoxia Inducible Factor (HIF). It has been proved that the HIF isoform 1-α (HIF-1α) may interact with several viruses, but till now there are no evidences regarding the interaction between BKV and HIF-1α. In the present study, we aimed to achieve a better understanding about the relation between BKV infection and hypoxia condition in kidney cells in case of transplantation. In order to achieve this aim the experimental design of the study was organized as follow: a) analysis of HIF-1α expression level in kidney tissues, from both PVAN and not PVAN transplanted patients, b) study of the physical interaction between BKV promoter (NCCR) and HIF-1α, c) study of the effect of hypoxia on BKV replication in an *in vitro* model of BKV infection.

3. MATHERIALS AND METHODS

3.1 HIF-1A MRNA EXPRESSION IN PVAN TISSUES

3.1.1 STUDY PARTICIPANTS AND SAMPLE COLLECTION

From January 2003 to August 2007, a total of 17 kidney tissue samples were collected at the Department of Pathology, Ospedale Maggiore della Carità, Novara, Italy at different time points from transplantation. The samples were immediately formalin-fixed for a minimum of two hours, paraffin-embedded and routinely stained by Hematoxylin & Eosin and immunohistochemistry using anti-SV40 antibody (Lee Biomolecular Research Labs, San Diego CA) and screened for BKV positivity for diagnostic purpose. Patients were divided into three groups, PVAN patients (PVAN) that underwent a kidney transplant and developed PVAN after transplantation, patients that underwent a kidney transplant without developing PVAN (NOT PVAN) and a control group (CTRL) that underwent a renal biopsy for a clinical needs/reasons not related to renal transplant. The biopsies belonging to the first two groups resulted positive for BKV screening, while in the third group all the specimens were negative for BKV screening (table 3). The study was performed in accordance with the requirements of the local Ethics Committee, and all patients or their patients' parents provided informed consent.

GROUP	N°	M/F	AGE (years±SD)	MEAN TIME FROM TRANSPLANT (months±SD)	BKV
PVAN	7	4/3	60.6 ± 10.5	9.2 ± 6.0	+
NOT PVAN	4	3/1	46.2 ± 13.3	24.5 ± 16.1	+
CTRL	6	3/3	50.6 ± 20.8	2.4 ± 3.1	-

Table 3. Case study. PVAN, Polyomavirus Associated Nephropathy; NOT PVAN, patients that underwent a kidney transplant without developing PVAN; CTRL, control group

3.1.2 RNA ISOLATION

Total RNA was isolated from the paraffin embedded biopsies using the RNeasy FFP kit (Qiagen, Germany) according to the manufacturer's guidelines (Appendix C). Total RNA was then quantified using nanodrop technology (Thermo Scientific, Lithuania).

3.1.3 RETROTRANSCRIPTION

Reverse transcription of total RNA was performed by the QuantiTect Reverse Transcription Kit (Qiagen, Germany) according to the manufacturer's guidelines. RNA sample is retrotranscribed using a master mix prepared from Quantiscript Reverse Transcriptase (RT), Quantiscript RT Buffer, and RT Primer Mix. The entire reaction takes place at 42°C and is then inactivated at 95°C. The mix reaction is showed in table 4. cDNA was then quantified using spectrophotometric technology (Biorad, USA).

COMPONENT	VOLUME/ REACTION
Quantiscript Reverse Transcriptase*	1 µl
Quantiscript RT buffer, 5x**	4 µl
RT primer Mix	1 µl
Template RNA	≤ 14 µl (50 ng/µl)
Total volume	20 µl

Table 4. Reverse-transcription reaction components. * Contains RNase inhibitor. ** Includes Mg^{2+} and dNTPs

3.1.4 REAL TIME POLYMERASE CHAIN REACTION (REAL TIME PCR)

Real time polymerase chain reaction (Real Time PCR) was performed on an Applied Biosystems 7500 Real-Time PCR System (Applied Biosystems, Carlsbad, USA), using the QuantiTect SYBR Green PCR kit (Qiagen, Germany) according to the manufacturer's instructions. The assay was a relative quantification of HIF-1α expression compared to the expression of

the housekeeping glyceraldehyde-3-phosphate dehydrogenase gene (GAPDH), as previously reported [Landry and Mager, 2003].

The primer set targeting the HIF-1α and GAPDH genes was previously published by Wang and colleagues and Landry and colleagues (table 5) [Wang et al., 2014, Landry and Mager, 2003].

GENE	PRIMERS	SEQUENCE
GAPDH	GAPDH Forward	5'-GCCCAGGATGCCCTTGA-3'
	GAPDH Reverse	5'-GTGTCCCCACTGCCAAC-3'
HIF-1α	HIF-1α Forward	5'- TGAAGTGTACCCTAACTAGCCGA -3'
	HIF-1α Reverse	5'- AATCAGCACCAAGCAGGTCATAG -3'

Table 5. Sequence of GAPDH and HIF-1α primers used in the Real Time PCR analysis

The reaction mix was prepared as follows (table 6):

COMPONENT	VOLUME/ REACTION	FINAL CONCENTRATION
2x QuantiTect SYBR Green PCR Master Mix*	12,5 µL	1x
Forward Primer (70 µM)	0,11 µL	0,3 µM
Reverse Primer (70 µM)	0,11 µL	0,3 µM
Template cDNA	5 µL	(≤ 500 ng/reaction)
RNasi-free water	7,3 µL	
Total reaction volume	**25 µL**	

Table 6. Reaction mix setup. *Provides a final concentration of 2.5 mM $MgCl^2$ and containing ROX passive reference dye

For both the assays the cycling conditions were as follow (table 7) :

STEP	TIME	TEMPERATURE
UNG*	2 min	50 °C
PCR initial activation step	15 min	95 °C
Denaturation	15 sec	94°C
Annealing	30 sec	54°C
Extension	30 sec	72°C
Number of cycles	**45**	

Table 7. Real Time PCR cycler conditions. *Uracil-N-glycosylase, eliminate any resulting from carryover contamination (carryover dUMP-containing PCR products prevention)

3.2 CELL CULTURE CONDITIONS

African green monkey kidney cell culture (VERO, Amercian Type Culture Collection; ATCC) was mantained with Dulbecco's Modified Eagle Medium (DMEM, Euroclone, Italy) supplemented with 10% heat inactivated Fetal Bovine Serum (FBS) (Euroclone, Italy), antibiotics (50 U/mL penicillin; 50 µg/mL streptomycin (Euroclone, Italy) and L-Glutamine (2mM) (Euroclone, Italy), and icubated at 37°C in a humified environment with 5% CO2.

3.3 SUBCLONING

3.3.1 BKV NCCR SUBCLONING

In a previously study, BKV NCCR (380 bp) Dunlop strain was cloned in the BamHI site (G^GATCC) of the pBLCAT3 plasmid. In the present work, BKV NCCR was isolated from the pBLCAT3 plasmid by digestion with BamHI, purificated by gel electrophoresis and cloned within the pMetLuc2-Reporter vector (Clontech, USA) in early and late orientation in the BamHI site of the vector, upstream the coding sequence of the reporter gene *Metridia longa*. For high copy expression of plasmids, the DH5αF' strain of Escherichia Coli (Invitrogen, USA) was transformed with the fresh products of ligation.

Plasmid DNA was extracted from bacterial cells using the QIAGEN Plasmid Minikit (QIAGEN, Germany) (Appendix A), following the manifacturer's instructions. To confirm the right orientation of the DNA fragments automatic sequencing was performed by an external facility (Primm, Italy). Sequences were analyzed using BLAST at NCBI. After sequencing two clones were choosen with the BKV NCCR linked to the Metridia Luciferase (MetLuc) gene in the early (pNCCRLucE) and late (pNCCRLucL) orientations respectively (Appendix A).

3.3.2 HIF-1A SUBCLONING

In another previously study, HIF-1α gene was cloned in the BamHI site (G^GATCC) of the pcDNA3 vector, a mammalian expression vector with the Cytomegalovirus (CMV) promoter and a neomycin-resistance marker. The resulting plasmid was named pHIF (Appendix A).

3.4 LUCIFERASE ASSAY

Three hundred thousands of VERO cells were seeded in a M6 multiwell plate and transiently transfected using FuGENE® 6 Transfection Reagent (Promega, USA), following manufacturer's instructions. 2 µg of each plasmid were used for transfection in each well, maintaining the FuGENE:DNA ratio 5:2. Cells were transfected with: pNCCRLucE or pNCCRLucE co-transfected with pHIF; pNCCRLucL or pNCCRLucL co-transfected with pHIF; pHIF and pMetLuc2-Reporter vector without BKV NCCR inserted. The positive control was constructed using VERO cells transfected with pMetLuc2-Control vector (Clontech, USA), containing the MetLuc reporter gene transcriptionally regulated by the strong CMV promoter. After 48 hours post-transfection cell culture's supernatant were analyzed using Ready-To-Glow Secreted Luciferase Reporter System (Clontech, USA) according to the manufacturer's instructions. Briefly, 5 µL of freshly 1X substrate were added to 50 µL of cell culture's supernatant and luciferase activity was assed recording light signal with a Modulus

luminometer, according to the manufacturer's protocol (Turner BioSystems, USA). All experiments were performed in triplicates.

3.5 CHROMATIN IMMUNOPRECIPITATION (CHIP) ASSAY

Two million and a half of VERO cells were grown overnight in 100 mm dishes and then transiently co-transfected with pHIF plasmid, and with pBKV (ATCC) plasmid that contains the whole BKV strain Dunlop genome molecularly cloned into the pBR322 vector through its BamHI unique restriction site. Briefly, transfection was performed using the FuGENE 6 transfection reagent (Promega, USA) as previously described. In particular, 11,5 µg of each plasmid were used for transfection in each dish, mantaining the FuGENE:DNA ratio 5:2. Plates were returned to the incubator until reaching a 100% confluence. Cells were harvested and used for total protein extraction and cross-linking. To evaluate the effective plasmid expression, extracted protein were analyzed by western blot targetin HIF-1α protein (97-120 kDa) and Tubulin protein (46-48 kDa) (Appendix B). In parallel, to perform the ChIP assay, cell were cross-linked and immunoprecipitated using protein G-Sepharose beads (Protein G Mag Sepharose™, GE Healthcare, UK), according to manifacturer's instructions (Appendix B).

Purified DNA samples obtained downstream the ChIP procedure were analyzed through primer-specific PCR set. The primer set spanning the BKV NCCR were the following (table 8):

	NUCLEOTIDE	SEQUENCE
NCCR.F	5082-5102	5'-GATCGAATTCGGCCTCAGAAAAAGCCTCCA-3'
NCCR.R	390-411	5'-TATAGGATCCCCCGTCTACACTGTCTTCACC-3'

Table 8. Sequence of primers used in the PCR analysis. NCCR.F primer forward, NCCR.R primer reverse

The reaction mix was prepared as follows (table 9):

COMPONENT	VOLUME/ REACTION
5x Buffer*	10,0 µL
dNTPs (10mM)	2,0 µL
$MgCl_2$ (25mM)*	4,0µL
NCCR.F (10 pmol/µL)	2,5 µL
NCCR.R (10 pmol/µL)	2,5 µL
Taq polymerase (5U/µL)*	0,4
Template DNA	5 µL
RNasi-free water	23,6 µL
Total reaction volume	**50 µL**

Table 9. Reaction mix setup. *Promega (USA)

The amplification was performed on a GeneAmp PCR System 9700 (Applied Biosystems, USA) running the following protocol (table 10):

STEP	TIME	TEMPERATURE
Initial denaturation	5 min	95°C
Denaturation	40 sec	95°C
Annealing	40 sec	60°C
Extension	40 sec	72°C
Final extension	5 min	72°C
Number of cycles	**40**	

Table 10. PCR cycler conditions.

The products of amplification were then analyzed after running a 2% agarose gel electrophoresis in 0.5X TBE buffer at 90 Volt for 30 minutes and stained with GelStar Gel Stain (Lonza Rockland Inc., USA).

In parallel, to clarify the nature of the interaction between HIF-1α and BKV NCCR, both gene sequences have been in silico analyzed using BLASTN 2.2.32+ software to find whether one or more HRE core sequences were present in the BKV NCCR.

3.6 BKV INFECTION AND HYPOXIA SIMULATION

3.6.1 BKV WW URINE PRECIPITATION

Viral suspension was previously obtained by precipitation from a pool of 5 human urine samples positive for BKV strain WW virions, using PEG-it Virus Precipitation solution (System Biosciences, USA) according to the manufacturer's instructions. No other viruses than BKV strain WW were detected by quantitative Real Time PCR (qPCR) analysis in the pooled urine samples. PEG-it Virus Precipitation Solution provides a simple and highly effective means to concentrate lentiviral particles. PEG-it is a formulation of polyethylene glycol optimized for the precipitation of all lentiviral-based particles. Briefly, 1 volume of cold PEG-it Virus Precipitation Solution (4ºC) was added to every 4 volumes of urine pool. After an incubation at 4°C over night, the solution was centrifugated at 1500 × g for 30 minutes at 4ºC. After centrifugation, the Lentivector particles may appear as a beige or white pellet at the bottom of the vessel. Viral DNA was isolated from the lentiviral pellet using the commercial Nucleospin RNAvirus kit (Macherey Nagels, Germany), according to themanufacturer's protocol (Appendix C) and tested in a BKV-specific qPCR (Appendix B). Viral stock suspension was conserved at -20°C for subsequent infection.

3.6.2 BKV WW INFECTION

One million of VERO cells were plated in each T75 flask. After 24 hours, cells (at approximately 80% confluence) were infected with 10^7 copies of BKV strain WW stock. The infection was performed by adsorption in serum free medium for 90 minutes at 37°C. The inoculum was then removed, cells were washed twice with PBS to eliminate unbound virus, and DMEM

containing 2% FBS was added. Mock infected cells, that were used as negative controls, were given the same treatment, but without the addition of virus. After infection with the BKV WW virions, cells were continuously cultured in 10% FBS DMEM. The efficiency of viral gene expression and viral replication in the infected cell cultures was evaluated by light-microscope observation of emerging cytopathic effects and by BKV-specific qPCR and β-globin qPCR (Appendix B) on DNA isolated from cell cultures' pellets and supernatants, collected at different time-points (days 3, 7, 10 post infection) and processed with QIAmp DNA blood Mini kit (Qiagen, Germany) and NucleoSpin RNA virus kit (Macherey Nagel, Germany) respectively, according to the manufacturer's protocol (Appendix C). The detection limit of the BKV qPCR assay was determined at 5 copies/reaction. Data were expressed as BKV copies per one thousand of cells.

3.6.3 MTT ASSAY

From the literature is known that cobalt chloride ($CoCl_2$) mimics hypoxia by causing the stabilization of HIF-α. To evaluate $CoCl_2$ cytotoxicity, $1{,}1 \cdot 10^4$ VERO cells were seeded in 96-well culture plates and maintained at 37°C in a 5% CO_2 humidified atmosphere to allow adherence and initiation of proliferation. When cells reached ~90% confluence, culture medium was removed and $CoCl_2$ containing medium was added to the cells to reach final concentrations of 50 μM, 100 μM, 150 μM and 200 μM. Then, cells were incubated for 24 hours, 48 hours and 72 hours at 37°C in a 5% CO_2 humidified atmosphere. Culture medium without $CoCl_2$ served as the control in each experiment. Cytotoxicity was determined by MTT (3-[4,5-dimethylthiazol-2-yl]-2,5-diphenyltetrazolium bromide; thiazolyl blue) (Sigma-Aldrich, Germany) assay. The MTT assay is a colorimetric assay for assessing cell metabolic activity. NAD(P)H-dependent cellular oxidoreductase enzymes are capable of reducing the tetrazolium dye MTT

to its insoluble formazan, which has a purple color. Briefly, at the end of exposure periods, 20µL MTT solution (0,5 mg/mL in Phosphate Buffer Saline, PBS) were added to the each well, and the cells were incubated 3h at 37°C. The dark blue formazon crystals formed in intact cells were solubilized with Dimethyl Sulfoxide (DMSO) (Sigma-Aldrich, Germany). At the end of the incubation, absorbance values of each sample were measured at 550 nm using micro plate reader BioTek Synergy™ 4 Hybrid Microplate Reader (BioTek, USA). Furthermore, to evaluate the effective stabilization on HIF-1α, a western blot analysis targeting HIF-1α protein (97-120 kDa) and Tubulin protein (46-48 kDa) was conducted on total proteins extracted from $CoCl_2$ treated and untreated cells (Appendix B).

3.6.4 HYPOXIA SIMULATION

At day 3 post-infection, corresponding to the viral replication peak level, as revealed by BKV-specific qPCR analysis, hypoxic stress was simulated by exposing the infected cells to 100µM $CoCl_2$. After 24 hours of exposition, cells were collected and nucleic acids were isolated using the QIAmp DNA Blood Mini kit (Qiagen, Germany) according to the manufacturer's instructions (Appendix C). This test was performed in duplicate, and included a control of infected cells non subjected to $CoCl_2$ treatment. BKV and β-globin gene were quantified by specific qPCR assays (Appendix B).

3.7 STATISTICAL ANALYSIS

Analysis of HIF-1α qPCR results were analysed by the $2^{-\Delta\Delta Ct}$ method and expressed as fold of difference between HIF-1α and GAPDH.

Results of luminometric assays and MTT assay were expressed as means ± standard deviation.

For statistical comparison, significance was evaluated using the Student t test. Values of $p < 0.05$ were considered statistically significant.

4. RESULTS

4.1 HIF-1A MRNA EXPRESSION IN PVAN TISSUES

To evaluate HIF-1α expression level *in vivo* and its cellular behavior in the process of transplantation, 17 kidney paraffin-embedded tissue samples from BKV+ PVAN patients (tissues from kidney transplant patients who developed PVAN after transplantation), BKV+ NOT PVAN patients (tissues from kidney transplant patients who did not developed PVAN after transplantation) and a BKV- control group (group that underwent a renal biopsy for clinical needs/reasons not related to renal transplant) were collected. Total RNA was extract from paraffin embedded tissues, reverse transcripted into cDNA and analyzed in a qualitative Real Time PCR to evaluate HIF-1α expression, compared to GAPDH expression. The mRNA expression levels of HIF-1α gene in PVAN tissues and NOT PVAN tissues were presented in comparison with the control group. Analysis of Real Time PCR data were conducted with the $2^{-\Delta\Delta Ct}$ method and expressed as fold differences between HIF-1α and GAPDH. Expression level resulted 13.6 folds higher in PVAN tissues than its expression in the control group. No differences were observed in the HIF-1α expression between the NOT PVAN and the control group (figure 13). These results show that HIF-1α is stabilized in PVAN tissue BKV positive.

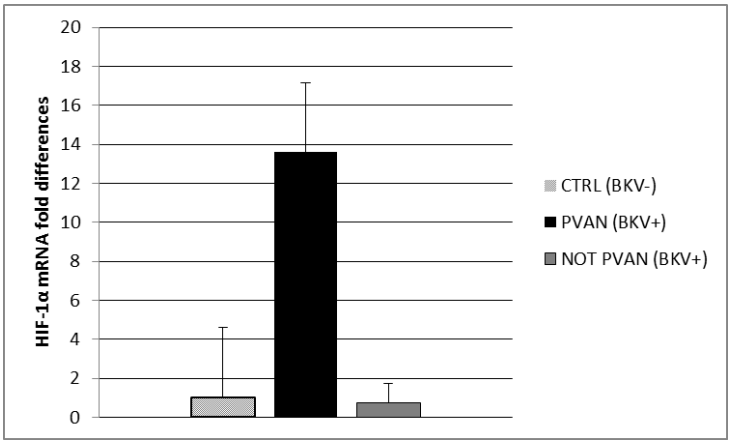

Figure 13. Fold differences of HIF-1α mRNA expression in the groups of study. CTRL: control group. PVAN (BKV+): Polyomavirus Associated Nephropathy samples. NOT PVAN (BKV-): tissue samples not showing Polyomavirus Associated Nephropathy

After these *in vivo* evidences, the study was designed to evaluate the interaction between HIF-1α and BKV in an *in vitro* model. The first step was setted up to evaluate the potential functional interaction between HIF-1α and BKV NCCR performing a Luciferase assay. After this, we performed a ChiP assay to evaluate a possible interaction between HIF-1α and BKV NCCR. At the ends, we create an *in vitro* model of hypoxia and BKV infection to corroborate the previously results.

4.2 LUCIFERASE ASSAY

Different sets of luminometric assays were performed to determine the potential involvement of HIF-1α in the regulation of BKV NCCR with both early and late orientations. BKV NCCR (Dunlop strain) was cloned in the BamHI site of pMetLuc2-reporter vector (Clontech, USA) in early and late orientation and HIF-1α gene was cloned in the BamHI site of the pcDNA3 vector. The resulting vectors were named respectively: pNCCRLucE, pNCCRLucL and pHIF. These plasmid where used to transiently transfect VERO cells with the following setting: pNCCRLucE or pNCCRLucE co-transfected with pHIF; pNCCRLucL or pNCCRLucL co-transfected with

pHIF; pHIF and pMetLuc2-Reporter vector without BKV NCCR inserted. The positive control was constructed using the VERO cells transfected with pMetLuc2-Control vector (Clontech, USA), containing the MetLuc reporter gene transcriptionally regulated by the strong CMV promoter. After 48h of incubation, supernatants of transfected cells were used to asses luciferase activity. As shown in figure 14, experimental results demonstrated that the transcriptional activity of both NCCR early and late configurations was enhanced by HIF-1α. Interestingly, in the presence of HIF-1α plasmid, transcriptional activity of the BKV NCCR early was increased 6-folds ($p<0.05$), while the BKV NCCR late activity was increased 2-folds ($p<0.05$) respect BKV NCCR early and late activity alone. These result show that the presence of HIF-1α stabilize BKV NCCR increasing its activity as promoter of *Metridia Luciferase* gene indicating a functional interaction between HIF-1α and NCCR.

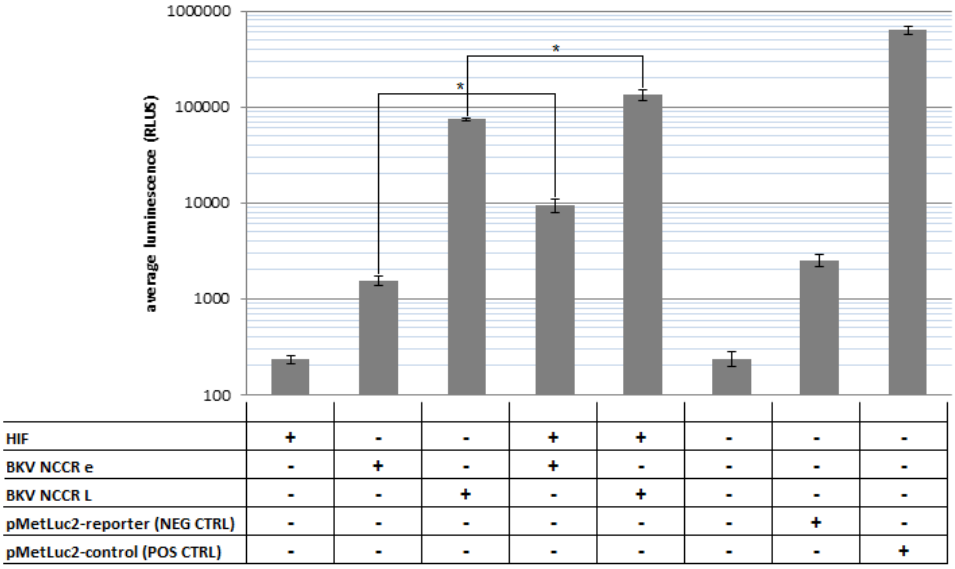

Figure 14. Luciferase assay results showed as average luminescence (RLUs). HIF: pHIF plasmid. BKV NCCR e: pNCCRLucE plasmid. BKV NCCR L: pNCCRLucL plasmid. pMetLuc2-resporter: pMetLuc2-resporter vector without BKV NCCR insert. pMetLuc2-control: pMetLuc2-control vector containing the MetLuc reporter gene transcriptional regulated by CMV promoter

4.3 CHROMATIN IMMUNOPRECIPITATION (CHIP) ASSAY

Once the activation of BKV NCCR by HIF-1α was established, a ChIP assay was conducted to determine whether HIF-1α binds the BKV NCCR *in vitro*. VERO cells were transiently co-transfected with pHIF plasmid and pBKV plasmid (pBR322 vector containing the entire genome of BKV strain Dunlop in BamHI site). After reaching 100% confluence, cells were harvested and used in parallel for total protein extraction and ChIP assay. Proteins were analyzed in a western blot targeting HIF-1α protein and Tubulin protein. Western blot analysis confirmed that HIF-α protein is stabilized in the presence of BKV plasmid. Autoradiography film showed that HIF-1α signal is slightly present in the lane corresponding to the mock control not transfected. In transfected cells, HIF-1α signal resulted moderate in the lane corresponding to VERO cells transfected with pBKV Dunlop plasmid alone while a stronger signal is present in the lane corresponding to VERO cells transfected with pBKV Dunlop plasmid and pHIF plasmid. Tubulin signal resulted comparable in all the lanes (figure 15).

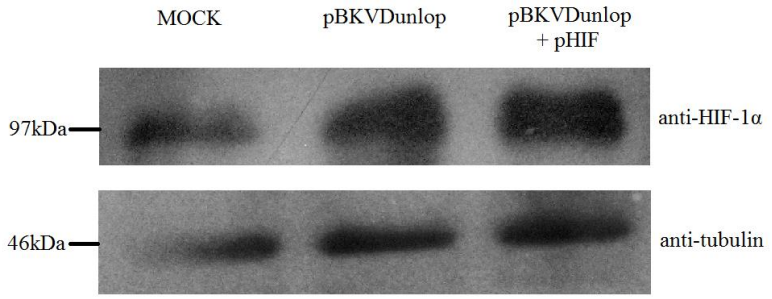

Figure 15. Western blot on protein lysate from transfected cells. MOCK: VERO cells not transfected. pBKVDunlop: VERO cells transfected with pBKV Dunlop plasmid. pBKVDunlop + pHIF: VERO cells transfected with pBKV Dunlop plasmid and pHIF plasmid

Purified DNA obtained downstream the ChIP procedures were analyzed in a PCR specific for BKV NCCR. A 490 bp PCR product, corresponding to the BKV NCCR, was detectable in the lanes corresponding to the cross-

linked and sonicated chromatine before (IP input) and after (IP anti-HIF-1α) immunoprecipitation assay, respectively. The same PCR fragment was not visible when using the non-specific anti-mouse IgG (mouse IgG control) or in the negative control without any antibody (beads only control) (figure 16). This result show that there is a physical interaction between HIF-1α and the BKV NCCR.

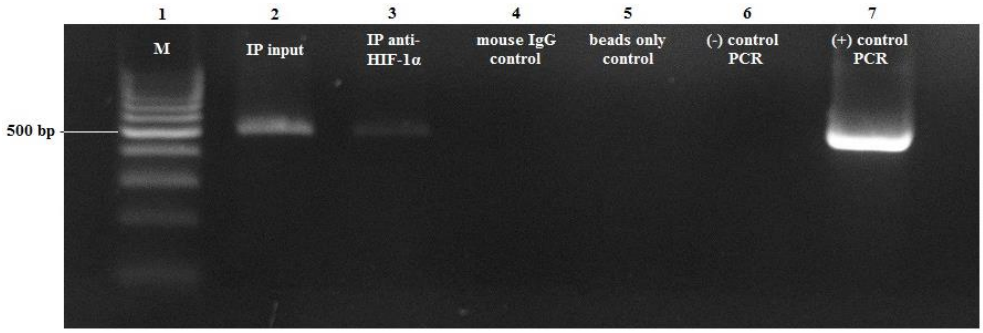

Figure 16. PCR results on 2% agarose gel. Approximate size of the PCR product: 490 bp. Lane 1: DNA ladder (100 bp). Lane 2: DNA cross-linked and sonicated before immunoprecipitation. Lane 3: DNA cross-linked and sonicated after immunoprecipitation with the specific mouse monoclonal anti-HIF-1α antibody. Lane 4: immunoprecipitation negative control with a non-specific mouse IgG. Lane 5: no specific antibody used as another negative control. Lane 6: negative PCR control. Lane 7: positive PCR control (pBKVDunlop)

Finally, BLASTN analysis showed no match between HRE sequence and BKV NCCR sequences demonstrated that no binding sites for HIF-1α are present, confirming what have been previously described in literature.

4.4 MTT ASSAY

Before achieving the last step of the study, an MTT assay was performed to evaluate the $CoCl_2$ toxicity in VERO cells. VERO cells were treated with increasing concentration of $CoCl_2$ and subjected to different time of incubation. In particular, cells were treated with 50 μM, 100 μM, 150 μM and 200 μM of $CoCl_2$ for 24h, 48h and 72h at 37°C in a 5% CO_2 humidified atmosphere. MTT assay revealed that $CoCl_2$ reduced the number of viable cells in a concentration and time-dependent manner. As shown in figure 17,

at 24 hours of incubation, all doses of $CoCl_2$ showed a modest cytotoxicity. High concentration of $CoCl_2$ (100 µM, 150 µM and 200 µM) were significantly cytotoxic at 48 and 72 hours of incubation. Lower concentration of $CoCl_2$ (50 µM) showed a moderate cytotoxicity that slightly reduce cell viability in all the time points tested. For these regions, incubations with 100 µM of $CoCl_2$ for 24 hours and 50 µM of $CoCl_2$ for 48 hours were then chosen for the subsequent experiments.

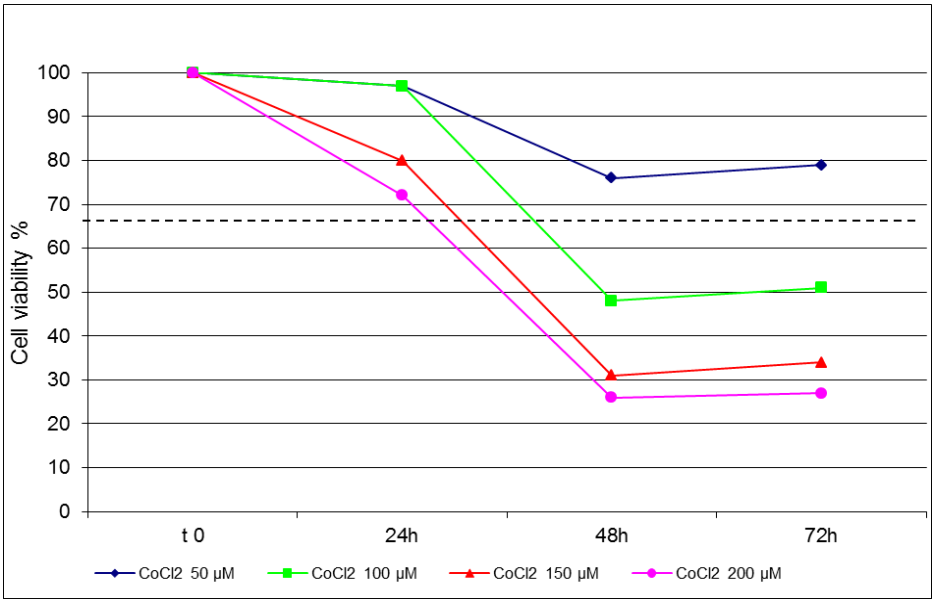

Figure 17. Cell viability of VERO cells determined by MTT assay after treatment with increasing dose of $CoCl_2$ at different time of incubation

Furthermore, to investigate if $CoCl_2$ stabilize HIF-1α protein, a western blot analysis on protein extracted from VERO cells treated with 100 µM of $CoCl_2$ for 24 hours and with 50 µM was conducted. Western blot results confirmed that $CoCl_2$ stabilized HIF-α protein in both the $CoCl_2$ treatment (figure 18). In particular, incubation with 100 µM of $CoCl_2$ for 24 hours showed a slightly intense HIF-1α protein signal. For this reason, in accordance with MTT results and experimental conditions, incubation with 100 µM of $CoCl_2$ for 24

hours was considered the optimal treatment for the subsequent experiments.

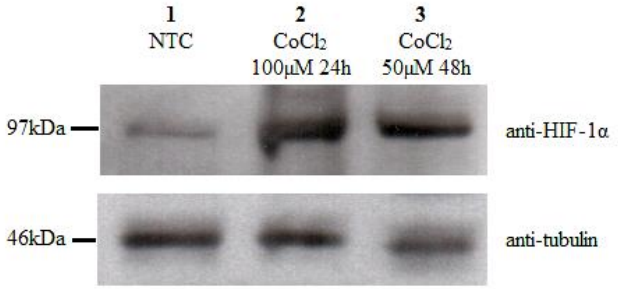

Figure 18. Western blot results. 1: VERO cells not treated with $CoCl_2$. 2: VERO cells treated with 100 μM of $CoCl_2$ for 24 hours. 3. VERO cells treated with 50 μM of $CoCl_2$ for 48 hours

4.5 BKV INFECTION AND HYPOXIA SIMULATION

To obtain an *in vitro* model of infection, VERO cells were infected with BKV strain WW virions, previously isolated from a pool of human urine. The isolated fraction was tested in a qPCR assay targeting the most frequent human polyomaviruses and no other viruses than BKV strain WW were detected. In particular, the BKV viral load resulted $5{,}0 \cdot 10^8$ viral copies/mL. The efficiency of viral replication in infected cell cultures was evaluated by light microscopy at days 5 and 10 post infection and by qPCR specific for BKV and β-globin gene on nucleic acids extracts from cellular pellet and cellular supernatants at days 3, 7, 10 post infection. Light microscopy analysis showed that at days 5 and 10 post infection no relevant cytopathic effects were detectable. The infected cells looked healthy and didn't show any morphological change (figure 19). These data were in accordance with qPCR results that showing an infection peak at day 3 post infection ($1{,}27 \cdot 10^5$ viral copies/mL) in the cellular pellet that rapidly decrease after 7 and 10 days post infection ($3{,}62 \cdot 10^3$ and $3{,}34 \cdot 10^2$ viral copies/mL respectively) (figure 20). qPCR on cellular supernatants showed that BKV genome was detectable only at day 3 post infection with a viral load of $2{,}44 \cdot 10^5$ viral copies/mL (data not shown). Negative control of infection

resulted negative for morphological changes and for virological qPCR screening at the same time points. At day three post infection, corresponding to the viral replication peak, cells were treated with 100 μM of $CoCl_2$. After 24h of incubation nucleic acids were extract from cellular pellet and tested in a qPCR specific for BKV and β-globin gene. Data obtained by qPCR experiment reveled that BKV viral load was 3.1 virions/1000 cells in not treated cells and 15 virions/1000 cells in treated cells. In particular, the mean viral load resulted 5-folds increased in $CoCl_2$ treated cells compared to not treated infected cells (figure 21).

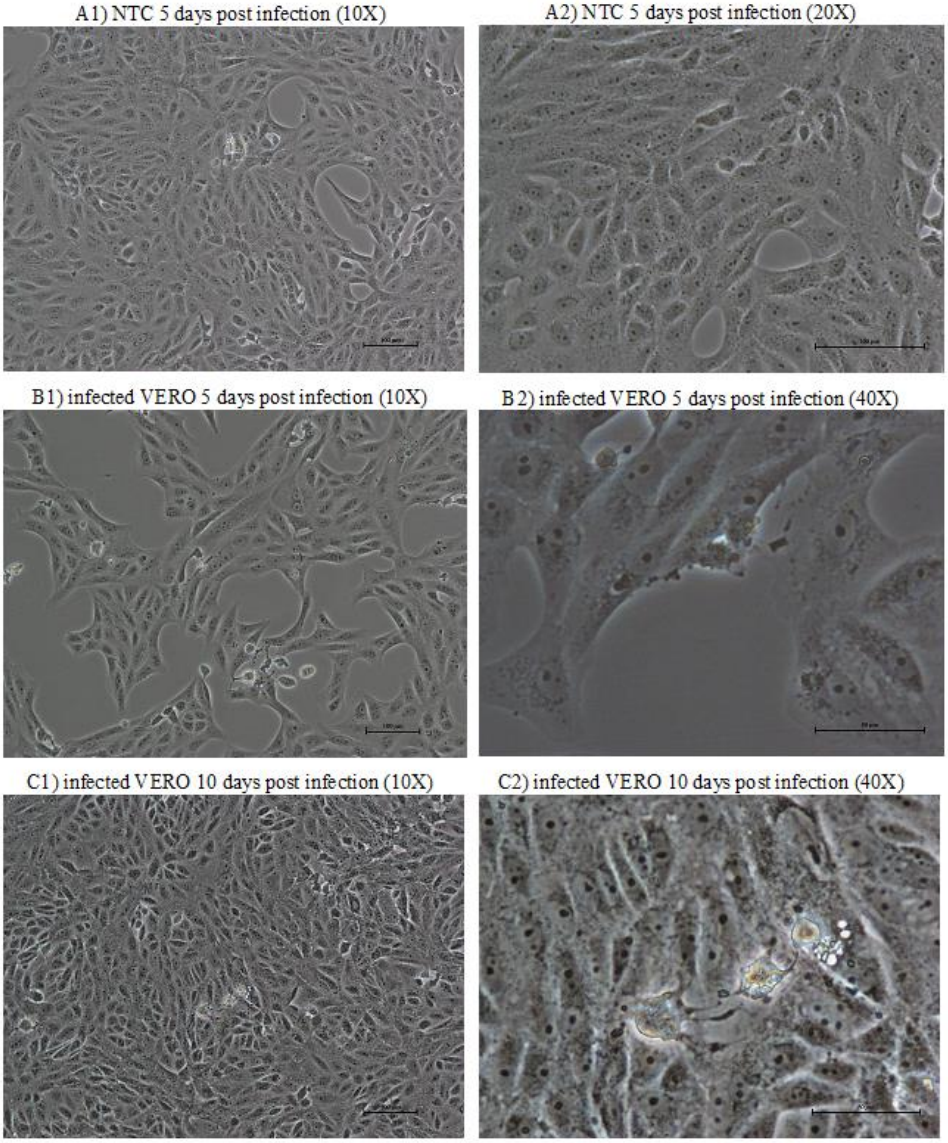

Figure 19. Light microscopy analysis. **A1**: VERO cells not infected (negative control NTC) at day 5 post infection, magnification 10X. **A2**: NTC at day 5 post infection magnification 20X. **B1**. VERO cells infected with BKV WW at day 5 post infection, magnification 10X. **B2**: VERO cells infected with BKV WW at day 5 post infection, magnification 40X. **C1**: VERO cells infected with BKV WW at day 10 post infection, magnification 10X. **C2**: VERO cells infected with BKV WW at day 10 post infection, magnification 40X

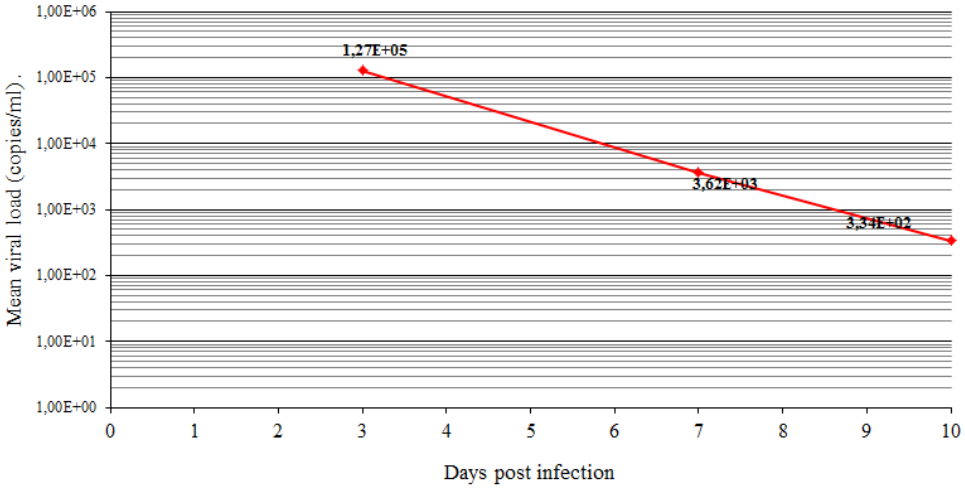

Figure 20. Mean viral load (copies/mL) determined by qPCR analysis on DNA extracted from cellular pellets and normalized on β-globin gene at days 3, 7 and 10 post infection

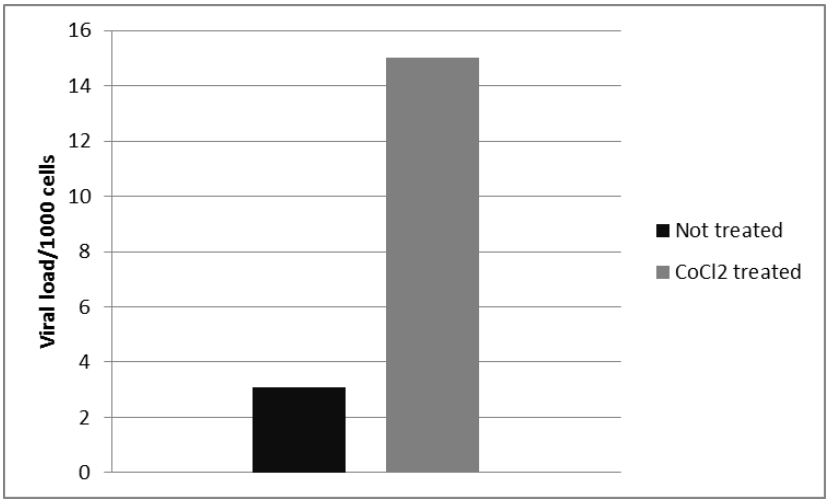

Figure 21. Viral load/1000 of infected cells after $CoCl_2$ treatment. Mean viral load resulted 5-folds increased in $CoCl_2$ treated cells compared to not treated infected cells

5. DISCUSSION

The human polyomavirus BK (BKV) is a member of the Polyomaviridae family detected in 1971 in the urine of an immunosuppressed renal transplant recipient who developed ureteric stenosis; the virus was named as the initials of the patient, BK [Gardner et al., 1971]. Polyomaviruses are nonenveloped viruses with an icosahedral capsid of about 40-45 nm in diameter. BK virions consist of 88% proteins and 12% DNA. BKV and the strictly related JC polyomavirus (JCV) were the first human viruses isolated that strongly resembled the morphology and genomic organization of the previously described oncogenic polyomaviruses simian virus 40 (SV40) and mouse polyomavirus. The viral genome is composed by a single copy of a circular double-stranded DNA molecule of about 5 kilobase pairs [Khalili and Stoner, 2001]. The genome can be divided into three functional regions: the genetically conserved early and late regions and a hypervariable regulatory region called Non Coding Control Region (NCCR) that contains the bidirectional promoter for both the early and late regions [Cole and Conzen, 2001; Moens and Rekvig, 2001]. The early region encodes for the two viral regulatory proteins: the large tumor antigen (T-Ag) and the small tumor antigen (t-Ag). The late coding region, expressed only after the initiation of DNA replication, contains the genetic information for the major capsid protein VP1 and the two minor capsid proteins, VP2 and VP3 and for a small protein called agnoprotein. Serological surveys have shown that BKV infection is widespread in the general population with type-specific antibodies detectable in 60-80% of healthy adults [Taguchi et al., 1982] [Knowles et al., 2003; Egli et al., 2009; Antonsson et al., 2010]. Natural BKV transmission is not resolved, but likely occurs via the respiratory or fecal-oral route [Hirsch et al., 2003] and the primary infection occurs predominantly during childhood. After the primary infection, often asymptomatic, no defined clinical presentations have been attributed, although fever and non-specific upper respiratory symptoms have been

suggested [Reploeg et al., 2001]. BKV establishes a life-long subclinical latency mostly within the kidney, the urogenital tract and probably also in B lymphocytes and other body district of immunocompetent individuals [Dörries et al.,1997; Shah 1996; Dolei et al., 2000; Dörries et al.,1994]. Intermittent or chronic BKV reactivation can occur in individuals with perturbed immune conditions leading to different symptomatology with various degrees of severity. Reactivation of BKV can occur in up to 60% of healthy pregnant woman, eldery or immune deficient subjects, leading to asymptomatic viruria [Hirsch 2005; Tsai et al., 1997; Kitamura et al., 1990]. In immunocompromised patients with relative or absolute cellular immunodeficiency, BKV reactivation has been associated with interstitial nephritis [Nickeleit et al., 2000], ureteral stenosis in renal allograft recipients and late onset of hemorrhagic cystitis in bone marrow transplant patients [Major et al., 2001]. BKV has also been detected in a variety of tumors such as the carcinoma of the urinary tract, prostate cancer and neuroblastoma renewing the interest about the BKV epidemiology Carluccio et al., 2014; Flaegstad et al., 1999]. For these reasons, during the recent years, BKV has drawn the attention of the scientific and medical communities because of its potential to cause human diseases.

Polyomavirus-associated nephropathy (PVAN) is one of the most common viral complications in renal transplant recipients and is an increasingly recognized cause of renal transplant dysfunction and graft loss [Costa and Cavallo, 2012]. Since the first description of PVAN in 1995, an increasing prevalence rate from 1% to 10% has been evidenced [Hirsch et al., 2006]. PVAN can lead to kidney graft loss in 10% up to 100% of the cases, determining the return in hemodialysis, thus significantly and markedly reducing the graft survival. PVAN clinical presentation may be inconspicuous and lacks of useful features. Varying degrees of renal dysfunction may be observed, such as interstitial nephritis and/or ureteric stenosis with ureteric obstruction, hydronephrosis, and sometimes

associated urinary tract infections [Costa and Cavallo, 2012]. Progression of PVAN leads to eventual deterioration of the kidney graft function. Viral replication is the single common feature of all patients at risk of nephropathy and it is well known that BKV is the etiological agent of PVAN. Most of the cases are preceded by an asymptomatic phase of persistent and significant viruria that is typically followed by viremia within few weeks. A significant and sustained viremia identifies patients with uncontrolled viral replication that may potentially lead to parenchymal injury. Once the virus has reactivated, an ascending infection via cell-to-cell spread occurs [Meehan et al., 2006; Drachenberg et al., 2003; Nickeleit et al., 2000(a)]. The infected cells have an enlarged nucleus with a gelatinous basophilic inclusion resulting from accumulation of the newly formed virions [Drachenberg and Papadimitriou, 2006]. Lysis of the infected cells results in viral seepage into the tubule lumen and urine but also to the interstitium and propagation to surrounding cells. Subsequent tubular cell necrosis leads to cast formation and denudation of the basement membrane. Destruction of tubular capillary walls results in vascular spread of the virus. Heterogeneous interstitial infiltration of inflammatory cells as well as tubulitis may be absent, intermixed with the active infection, or observed in areas that lack cytopathic changes. Collateral damage with necrosis and apoptosis of noninfected tubule cells may occur. The resultant effect of continued intragraft inflammation, tubular injury, and upregulation of profibrotic mediators is allograft dysfunction and loss.

The intense immunosuppressive therapy required to prevent the organ rejection after transplantation, is considered the major risk factor for PVAN development [Hirsch et al., 2002]. This condition may predispose to the reactivation of the latent BKV, which may cause the necrosis of tubular cells and therefore the functional impairment of the kidney [Nickeleit et al., 2002]. For these reasons, a screening for viral replication is the most useful tool for the identification of patients at risk of developing nephropathy,

allowing for early intervention, such as the preventive reduction of immunosuppression, with improvement of outcome [Costa and Cavallo, 2012]. Screening for polyomavirus replication presents a high negative predictive value (>99%), as in the absence of virus replication PVAN is excluded [Mischitelli et al., 2007; Cavallo et al., 2009]. The screening for viral replication is also the most important tool for monitoring the response to the treatment in patients with diagnosed PVAN.

The observation that PVAN is rare in transplant recipients of other solid organs such as liver, heart and lung, despite exposure to the same classes, combination and concentrations of immunosuppressive drugs leads to believe that there are some other determinants of disease related to the allogenic renal graft, pathogenically important for the PVAN development. It has been suggested that ischemic injury during organ implantation might play a role in creating the appropriate environment for viral reactivation/replication leading to nephropathy [Bohl et al., 2007; Trofe et al., 2003]. It is well known that under hypoxic conditions, like those that are defined during the ischemic time, cells specifically respond through a finely regulated mechanism mediated by the hypoxia inducible factors (HIFs) [Loboda et al., 2010]. HIFs take part to a signaling cascade that drives the expression of a wide variety of genes essential for the adaptive response to hypoxia. HIFs are the master regulators of oxygen homeostasis and play a role in the development, postnatal physiology as well as disease pathogenesis. Since then, more than 70 target genes regulated directly by HIFs have been identified and expression of over hundred genes are known to be directly or indirectly influenced by HIF. HIF is a dimer composed of 120 kDa oxygen-regulated α-subunit and the constitutively expressed 91-94 kDa β-subunit. There are three different isoforms of each subunit and HIF1 is the principal regulator of the hypoxic response in the mammalian cells [Semenza et al., 1998], able to control more than 100 genes, suggesting that more than 2% of the human genes may be both

directly or indirectly regulated by this factor [Manalo et al., 2005]. HIF-1α, which is ubiquitous, is constitutively expressed within cells, but under normoxia this protein is targeted for proteosomal degradation. During hypoxia, HIF-1α ubiquitination is inhibited and therefore this factor can translocate to the nucleus where, after dimerization with HIF-1β and recruitment of numerous co-activators, can trigger the transcription of target genes. HIF-activated genes include VEGF, which promotes angiogenesis, Glucose Transporter-1 (GLUT1), Lactate Dehydrogenase (LDHA), and Epo, which induces erythropoiesis.

During the process of transplantation, organs are subjected to hypoxic and ischemic injury at the moment of procurement, preservation and following reperfusion. This process of ischemia reperfusion injury (IRI) is recognized as being detrimental for organ function and long-term graft survival. In particular, in renal transplantation, acute tubular necrosis (ATN) contributes significantly to the development of delayed graft function. For these reasons, better understanding of the role of the HIF pathway in the context of organ donation and transplantation could be of importance in improving the quality of older and ‘‘high-risk’’ donor organs. In vitro experiments showed that HIF-1α is stabilized during hypoxia and analysis of biopsies taken during transplantation have shown that the HIF system was activated as result of the procurement process and correlated with the degree of exposure of the kidneys to ischemia [Baan et al., 2003]. Finally, Rosenberg and colleagues demonstrated that HIF-1α was detectable with low scores correlating with primary nonfunction immediately after the engraftment [Rosenberger et al., 2006]. The authors showed that HIF-1α was detectable both in the renal cortex and in the medulla with collecting ducts and glomeruli showing a high signal that disappeared at 3 months. The authors hypothesized that inflammatory cells induction of HIF, opening a new side of research about the relation between HIF levels and allograft rejection.

Because the upregulation of the enzymes in the glycolytic pathway is mediated almost exclusively by HIF-1α [Semenza et al., 1994], its role in supporting phagocyte function during inflammation was intuitive. In the last few years, genetic tools provided not only experimental validation of this concept, but uncovered profound implications of the HIF-1α control pathway in the overall regulation of mammalian innate immunity [Zinkernagel et al., 2007]. Activation of HIF-1α pathway during the life cycle of viral pathogens has been the object of various investigation, revealing a diversity of functional outcomes in disease progression and critical linkages to viral oncogenesis. Viral infection is generally induces stabilization of HIF-1α in target cells, which consequently contribute to local inflammation. In literature there are many examples of viral HIF crosstalk. The first example is the respiratory syncytial virus (RSV), that induces HIF1-α in primary human bronchial epithelial cells via a NO-dependent pathway [Kilani et al., 2004]. This scenario might apply to that viruses which exert an acute cytolytic effect, such as the vesicular stomatitis virus (VSV). Several years ago, it was noticed that hypoxia reduced the cytopathogenicity and replication of VSV, with measured antiviral effects of interferons α and γ potentiated under the low oxygen conditions [Naldini et al., 1993]. For a number of persistent viral infections, when induction of HIF-1α is insufficient to conduct the eradication, the accompanying proangiogenic program can contribute to oncogenesis. For example, chronic infections of the hepatitis B and C viruses (HBV and HCV) are epidemiologically associated with the development of hepatocellular carcinoma (HCC), a highly vascularized solid tumor [Wang et al., 1994]. Another example linking viral activation of HIF-1α to proangiongenesis and tumor development can be found in the case of human papillomavirus-16 (HPV-16), the etiologic agent of cervical interstitial neoplasia that, if undetected, can progress to cervical carcinoma. Increased HIF-1α levels can be correlated to poor prognosis in advanced cervical cancer lesions, many of which are hypoxic [Hockel et al., 1996,

Birner et al., 2000]. Furthermore, increased HIF-1α protein levels and VEGF expression are detected in T-cell lines infected with the human T-cell leukemia virus type 1 (HTLV-1) [Tomita et al., 2007] and in nasopharyngeal epithelial cells infected by Epstein Barr virus (EBV) [Wakisaka et al., 2004]. Finally, HIF-1α was stabilized in endothelial cells infected with Human Herpes Virus 8 (HHV-8) and replication of parvovirus B19 was enhanced under hypoxic condition due to the binding of HIF-1α to the HRE located in the B19 virus promoter [Pillet et al., 2004]. As it happens for the other viruses, HIF-1α was involved also in the activation of JCV, an opportunistic human neurotropic polyomavirus that, in case of immunosuppression, can cause the Progressive Multifocal Leukoencephalopathy (PML). A work of Piña-Oviedo and colleagues demonstrate the implication of HIF-1α in the activation of JCV and its role in the development of PML in human oligodendrocytes. HIF-1α was found up regulated in glial, bizzare astrocytes and oligodendrocytes cells where JCV replication takes place. The increase level of HIF-1α was probably due to the response of cellular stress caused by the infection of JCV. The authors observed an up regulation of HIF-1α in endothelial cells from small capillaries within areas of demyelination. JCV replication in endothelial cells in association with the enormous stress of these areas caused by demielinating process were responsible for the up-regulation of HIF-1α. Furthermore, with transcription activation assay, they showed the JCV early and late promoter activation by HIF-1α. These evidences open the topic about HIF-1α and BKV/JCV latency and reactivation. It is well established that after a subclinical primary infection, BKV and JCV remains in a latent state in the kidney, one of the organs that has the capability to detect hypoxia [Beckmann and Shah 1983]. Hypoxic conditions can activate glycolysis resulting in the increased synthesis of pyrimidines and purines required for BKV and JCV viral replication. For these reasons further investigation will be necessary to corroborate the information about the interaction between HIF-1α and JCV

promoter and new investigation will be necessary to investigate wether there is a similar HIF-1α – BKV crosstalk in renal cells.

6. CONCLUSION

Viral replication is the single common feature of all patients at risk of nephropathy, and it is well known that BKV is the etiological agent of PVAN. The intense immunosuppressive therapy that is required to prevent organ rejection after transplantation is considered the major risk factor for developing PVAN [Hirsch et al., 2002]. This condition may predispose an individual to reactivation of latent BKV, which may cause necrosis of tubular cells and therefore functional impairment of the kidney [Nickeleit et al., 2002]. However, PVAN is rare in transplant recipients of non-kidney solid organs such as livers, hearts and lungs, despite exposure of the patients to the same classes, combination and concentrations of immunosuppressive drugs. Consequently, some other determinants of disease related to the allogenic renal graft may be pathogenically important for PVAN development. It has been suggested that ischemic injury during organ implantation might play a role in creating the appropriate environment for viral reactivation/replication that leads to nephropathy [Bohl et al., 2007; Trofe et al., 2003]. It is well known that under hypoxic conditions, such as those experienced during the ischemic period, cells specifically respond through a finely regulated mechanism mediated by the HIFs [Loboda et al., 2010]. HIF-1α, which is ubiquitous, is constitutively expressed within cells, but under normoxia this protein is targeted for proteasomal degradation. During hypoxia, HIF-1α ubiquitination is inhibited allowing this factor to translocate to the nucleus where, after dimerization with HIF-1β and recruitment of numerous co-activators, it can trigger the transcription of target genes. HIF-activated genes include VEGF, which promotes angiogenesis, Glucose Transporter-1 (GLUT1), Lactate Dehydrogenase (LDHA), and Epo, which induces erythropoiesis. HIF-1α may also influence the replication of several viruses. A recent study demonstrated the important role of HIF-1α in the activation of the JCV promoter [Piña -Oviedo

et al., 2009]. In particular, Piña -Oviedo and colleagues provided evidence of direct binding between HIF-1α and the JCV control region and of the ensuing early promoter activation. Hypoxic conditions may increase the expression of an immediate early protein of Epstein - Barr virus (EBV), thus mediating the switch to a lytic form of infection in cells latently infected with the virus [Kondo et al., 2006]. In addition, it has been demonstrated that low levels of oxygen can up-regulate the replication of human parvovirus B19 [Pillet et al., 2004] and that HIF-1α is highly expressed in Human T cell leukemia virus type 1 (HTLV-1) infected cells [Tomita et al., 2007]. Based on the observation that the HIF-1α mRNA expression level was up-regulated almost 14-fold in the PVAN kidney biopsies compared to both BKV positive non PVAN kidney tissues and normal kidney tissues, we attempted to find an explanation for these results by a series of *in vitro* experiments. We demonstrated the functional interaction between HIF-1α and the BKV promoter because both the early and late viral NCCR were up-regulated in conjunction with the over-expression of HIF-1α. This effect was probably due to a physical interaction between the BKV NCCR and HIF-1α, as shown by the results of the ChiP assay. To finally corroborate the findings collected so far, we designed an *in vitro* model of infection and hypoxia resembling as effectively as possible what really occurs in the human body. Aiming to optimally simulate an in vivo infection, this model was examined using virions directly pooled from human urine samples and belonging to the BKV archetypal strain (WW). The normalized viral load was determined after hypoxia simulation, demonstrating that HIF-1α stabilization induces a 5-fold increase in the viral replication rate. Several conclusions can be drawn based on these observations. Patient determinants that increase the risk for PVAN may include increased older age. In contrast, controversial data are present in the literature regarding age-related HIF-1α expression. Liu and colleagues demonstrated that HIF-1α mRNA levels were significantly greater in young mice compared to

mature mice. On the contrary, impaired HIF-1α activation is also observed in hypoxic skin wounds of aged diabetic mice [Liu et al., 2008], and Rosenberger et al. [2007] showed that HIF-1α levels are higher in older kidneys. These findings underscore the importance of aging as a modulator of ischemic responses and may perhaps partially explain the findings in the cohort of patients we studied because the average age of the recipients with PVAN was 60.6 years, while the average ages of the recipients with no PVAN and the control group were 46.2 and 50.6 years, respectively. Additionally, Rosenberger and colleagues [2007] observed a strong correlation between the abundance of HIF-1α and the time elapsed since the transplant. In our cohort of patients, this correlation could not be confirmed, because in the control BKV negative group of patients, low levels of HIF-1α mRNA were observed at a mean time of 2.4 months after the transplant; on the contrary in the PVAN BKV positive group of patients, high levels of HIF-1α mRNA were observed at a mean time of 9.0 months after the transplant. This observation could further corroborate the association between the virus and HIF-1α and their synergetic involvement in the development of PVAN. Regarding the physical interaction of HIF-1α with the NCCR DNA, to the best of our knowledge, no known binding sites for HIF-1α have been previously described. The BKV NCCR strain WW and Dunlop sequences have been analyzed in silico using BLASTN 2.2.32+ software to determine whether one or more HRE core sequences are present. (5'-[A/G]CGT-3') [Wenger et al., 1997]. However, no match was found between the HRE sequence and BKV NCCR sequences (data not shown); therefore, further functional analyses should be conducted in the future to better understand the link between the BKV promoter and HIF-1α.

These data, taken together, are important in defining the role of hypoxic stress in BKV re-activation after renal transplantation. In particular, it can be concluded that opportunistic viral replication, which is mainly due to immunosuppressive therapy, is further stimulated and favored by HIF-1α

activation that is driven by hypoxic conditions during transplantation. The experimental results obtained suggest a hypothetical molecular mechanism underling this thesis, which can be outlined as follows: the cellular response to a hypoxic environment prevents HIF-1α proteasomal degradation, allowing the binding of HIF-1α to HIF-1β. The HIF-1 active complex can translocate to the nucleus, where it binds to the BKV NCCR, thus promoting the transcription of viral genes and stimulating BKV replication. If confirmed by further experiments, this scenario may have important clinical implications: exposure to hypoxia during the renal transplantation process should be considered a crucial risk factor for the development of PVAN. These findings could be translated into clinical practice by replacing modulation of the HIF system with ex-vivo organ preservation technologies, such as extra-corporeal membrane oxygenation [Akhtar et al., 2014], or by considering HIF-1α as a target for inhibition, perhaps using RNA interference technology.

7. REFERENCES

Abend JR, Joseph AE, Das D, Campbell-Cecen DB, Imperiale MJ. A truncated T antigen expressed from an alternatively spliced BK virus early mRNA. *J Gen Virol*. 2009;90(Pt 5):1238-45

Ahuja D, Sáenz-Robles MT, Pipas JM. SV40 large T antigen targets multiple cellular pathways to elicit cellular transformation. *Oncogene.* 2005;21;24(52):7729-45. Review

Akan I, Sariyer IK, Biffi R, Palermo V, Woolridge S, White MK, Amini S, Khalili K, Safak M. Human polyomavirus JCV late leader peptide region contains important regulatory elements. *Virology*. 2006;349(1):66-78

Akhtar MZ, Sutherland AI, Huang H, Ploeg RJ, Pugh CW. The role of hypoxia-inducible factors in organ donation and transplantation: the current perspective and future opportunities. *Am J Transplant*. 2014;14(7):1481-7

Ali SH, Kasper JS, Arai T, DeCaprio JA. Cul7/p185/p193 binding to simian virus 40 large T antigen has a role in cellular transformation. *J Virol*. 2004;78(6):2749-57

Anderson HA, Chen Y, Norkin LC, Bound simian virus 40 translocates to caveolin-enriched membrane domains, and its entry is inhibited by drugs that selectively disrupt caveolae. *Mol Biol Cell*. 1996; 7: 1825-34

Andrei G, Snoeck R, Vandeputte M, De Clercq E. Activities of various compounds against murine and primate polyomaviruses. *Antimicrob Agents Chemother*. 1997;41(3):587-93

Andrews CA, Shah KV, Daniel RW, Hirsch MS, Rubin RH: A serological investigation of BK virus and JC virus infections in recipients of renal allografts. *J Infect Dis*. 1988;158: 176–181

Antonsson A, Green AC, Mallitt KA, O'Rourke PK, Pawlita M, Waterboer T, Neale RE. Prevalence and stability of antibodies to the BK and JC polyomaviruses: a long-term longitudinal study of Australians. *J Gen Virol*. 2010;91(Pt7):1849-53

Appelhoff RJ, Tian YM, Raval RR, Turley H, Harris AL, Pugh CW, Ratcliffe PJ, Gleadle JM. Differential function of the prolyl hydroxylases PHD1, PHD2, and PHD3 in the regulation of hypoxia-inducible factor. *J Biol Chem*. 2004;279(37):38458-65

Aprelikova O, Wood M, Tackett S, Chandramouli GV, Barrett JC. Role of ETS transcription factors in the hypoxia-inducible factor-2 target gene selection. *Cancer Res*. 2006;66(11):5641-7

Araya J, Maruyama M, Inoue A, Fujita T, Kawahara J, Sassa K, Hayashi R, Kawagishi Y, Yamashita N, Sugiyama E, Kobayashi M. Inhibition of proteasome activity is involved in cobalt-induced apoptosis of human alveolar macrophages. *Am J Physiol Lung Cell Mol Physiol.* 2002;283(4):L849-58

Arany Z, Huang LE, Eckner R, Bhattacharya S, Jiang C, Goldberg MA, Bunn HF, Livingston DM. An essential role for p300/CBP in the cellular response to hypoxia. *Proc Natl Acad Sci U S A*. 1996;93(23):12969-73

Arroyo JD, Hahn WC. Involvement of PP2A in viral and cellular transformation. *Oncogene*. 2005;24(52):7746-55. Review.

Awadalla Y, Randhawa P, Ruppert K, et al. HLA Mismatching increases the risk of BK virus nephropathy in renal transplant recipients. *Am J Transplant*. 2004; 4:1691

Azzi , De Santis R, Salotti V, Di Pietro N, Ginevri F, Comoli P, BK virus regulatory region sequence deletions in a case of human polyomavirus associated nephropathy (PVAN) after kidney transplantation. *J Clin Virol*. 2006; 35(1):106-8

Baan C, van Gelder T, Peeters A, Mol W, Niesters H, Weimar W, IJzermans J. Living kidney donors and hypoxia-inducible factor-1alpha. *Transplantation*. 2003;75(4):570-1

Bárcena-Panero A, Echevarría JE, Van Ghelue M, Fedele G, Royuela E, Gerits N, Moens U. BK polyomavirus with archetypal and rearranged non-coding control regions is present in cerebrospinal fluids from patients with neurological complications. *J Gen Virol*. 2012;93(Pt 8):1780-94

Bae SH, Jeong JW, Park JA, Kim SH, Bae MK, Choi SJ, Kim KW. Sumoylation increases HIF-1alpha stability and its transcriptional activity. *Biochem Biophys Res Commun*. 2004;324(1):394-400

Barouch D, Harrison S, Interaction among the major and minor coat proteins of polyomavirus. *J Virol*. 1994; 68:3982-89

Barri YM, Ahmad I, Ketel BL, et al. Polyoma viral infection in renal transplantation: the role of immunosuppressive therapy. *Clin Transplant*. 2001;15:240

Beckmann AM, Shah KV. Propagation and primary isolation of JCV and BKV in urinary epithelial cell cultures. *Prog Clin Biol Res*. 1983;105:3-14

Berra E, Benizri E, Ginouvès A, Volmat V, Roux D, Pouysségur J. HIF prolyl hydroxylase 2 is the key oxygen sensor setting low steady-state levels of HIF-1alpha in normoxia. *EMBO J*. 2003;22(16):4082-90

Berta MA, Mazure N, Hattab M, Pouysségur J, Brahimi-Horn MC. SUMOylation of hypoxia-inducible factor-1alpha reduces its transcriptional activity. *Biochem Biophys Res Commun*. 2007;360(3):646-52

Bertout JA, Patel SA, Simon MC. The impact of O2 availability on human cancer. *Nat Rev Cancer*. 2008;8(12):967-75

Birner P, Schindl M, Obermair A, Plank C, Breitenecker G, Oberhuber G. Overexpression of hypoxia-inducible factor 1alpha is a marker for an unfavorable prognosis in early-stage invasive cervical cancer. *Cancer Res*. 2000;60(17):4693-6

Bohl DL, Storch GA, Ryschkewitsch C, Gaudreault-Keener M, Schnitzler MA, Major EO, Brennan DC: Donor origin of BK virus in renal transplantation and role of HLA C7 in susceptibility to sustained BK viremia. *Am J Transplant*. 2005;5:2213–2221

Bohl DL, Brennan DC. BK virus nephropathy and kidney transplantation. *Clin J Am Soc Nephrol*. 2007;2 Suppl 1:S36-46. Review

Bollag B, Chuke WF, Frisque RJ. Hybrid genomes of the polyomaviruses JC virus, BK virus, and simian virus 40: identification of sequences important for efficient transformation. *J Virol*. 1989;63(2):863-72

Bracken CP, Whitelaw ML, Peet DJ. Activity of hypoxia-inducible factor 2alpha is regulated by association with the NF-kappaB essential modulator. *J Biol Chem*. 2005;280(14):14240-51

Brady JN, Winston VD, Consigli RA, Dissociation of polyomavirus by the chelation of calcium ions found associated with purified virions. *J Virol*. 1997; 23: 717-24

Brennan DC, Agha I, Bohl DL, et al. Incidence of BK with tacrolimus versus cyclosporine and impact of preemptive immunosuppression reduction. *Am J Transplant*. 2005; 5: 582

Brennan DC, Agha I, Bohl DL, Schnitzler MA, Hardinger KL, Lockwood M, Torrence S, Schuessler R, Roby T, Gaudreault-Keener M, Storch GA. Incidence of BK with tacrolimus versus cyclosporine and impact of preemptive immunosuppression reduction. *Am J Transplant*. 2005(a);5(3):582-94

Bressollette-Bodin C, Coste-Burel M, Hourmant M, Sebille V, Andre-Garnier E, Imbert-Marcille BM. A prospective longitudinal study of BK virus infection in 104 renal transplant recipients. *Am J Transplant*. 2005;5(8):1926-33

Bruick RK, McKnight SL. A conserved family of prolyl-4-hydroxylases that modify HIF. *Science*. 2001 Nov 9;294(5545):1337-40

Cai Q, Lan K, Verma SC, Si H, Lin D, Robertson ES. Kaposi's sarcoma-associated herpesvirus latent protein LANA interacts with HIF-1 alpha to upregulate RTA expression during hypoxia: Latency control under low oxygen conditions. *J Virol*. 2006;80(16):7965-75

Campbell KS, Mullane KP, Aksoy IA, Stubdal H, Zalvide J, Pipas JM, Silver PA, Roberts TM, Schaffhausen BS, DeCaprio JA. DnaJ/hsp40 chaperone domain of SV40 large T antigen promotes efficient viral DNA replication. *Genes Dev*. 1997;11(9):1098-110

Carbia-Nagashima A, Gerez J, Perez-Castro C, Paez-Pereda M, Silberstein S, Stalla GK, Holsboer F, Arzt E. RSUME, a small RWD-containing protein, enhances SUMO conjugation and stabilizes HIF-1alpha during hypoxia. *Cell*. 2007;131(2):309-23

Carluccio S, Signorini L, Elia F, Villani S, Delbue S and Ferrante P. A Potential Linkage Between the JC and BK Polyomaviruses and Brain and Urinary Tract Tumors: A Review of the Literature. *Advances in Tumor Virology*. 2014:4 17–24

Carrero P, Okamoto K, Coumailleau P, O'Brien S, Tanaka H, Poellinger L. Redox-regulated recruitment of the transcriptional coactivators CREB-binding protein and SRC-1 to hypoxia-inducible factor 1alpha. *Mol Cell Biol*. 2000;20(1):402-15

Carroll PA, Kenerson HL, Yeung RS, Lagunoff M. Latent Kaposi's sarcoma-associated herpesvirus infection of endothelial cells activates hypoxia-induced factors. *J Virol*. 2006;80(21):10802-12

Cavallo R, Bergallo M, Sidoti F, Astegiano S, Terlizzi ME, Costa C. Polyomavirus-associated nephropathy: critical issues in virological monitoring. *New Microbiol*. 2009;32(3):235-43

Cavender JF, Conn A, Epler M, Lacko H, Tevethia MJ. Simian virus 40 large T antigen contains two independent activities that cooperate with a ras oncogene to transform rat embryo fibroblasts. *J Virol*. 1995;69(2):923-34

Celik B, Shapiro R, Vats A, Randhawa PS. Polyomavirus allograft nephropathy: sequential assessment of histologic viral load, tubulitis, and graft function following changes in immunosuppression. *Am J Transplant*. 2003; 3:1378

Chandel NS, Vander Heiden MG, Thompson CB, Schumacker PT. Redox regulation of p53 during hypoxia. Oncogene. 2000;19(34):3840-8

Chang D, Cai X, Consigili RA, Characterization of the DNA binding properties of polyomavirus capsid proteins. *J Virol*. 1993; 67: 6327-31

Chapagain ML, Verma S, Mercier F, Yanagihara R, Nerurkar VR, Polyomavirus JC infects human brain microvascular endothelial cells independent of serotonin receptor 2A. *Virology*, 2007;364:55-63

Chen PL, Wang WC, Ou CK, Chen LS, Chang D, Disulfide bonds stabilize JC virus capsid-like structures by protecting calcium ions from chelation. FEBS Lett. 2001; 500:109-13

Cheng J, Kang X, Zhang S, Yeh ET. SUMO-specific protease 1 is essential for stabilization of HIF1alpha during hypoxia. Cell. 2007;131(3):584-95

Chilov D, Camenisch G, Kvietikova I, Ziegler U, Gassmann M, Wenger RH. Induction and nuclear translocation of hypoxia-inducible factor-1 (HIF-1): heterodimerization with ARNT is not necessary for nuclear accumulation of HIF-1alpha. *J Cell Sci*. 1999;112 (Pt 8):1203-12

Clever J, Dean DA, Kasamatsu H, Identification of a DNA binding domain in simian virus 40 capsid proteins VP2 and VP3. *J Biol Chem*. 1993; 268: 20877-83

Clayson ET, Brando LV, Compans RW. Release of simian virus 40 virions from epithelial cells is polarized and occurs without cell lysis. *J Virol*. 1989; 63: 2278-88

Clever J, Yamada M, Kasamatsu H. Import of simian virus 40 virions through nuclear pore complexes. *Proc Natl Acad Sci USA*. 1991; 88:7333-37

Cockman ME, Masson N, Mole DR, Jaakkola P, Chang GW, Clifford SC, Maher ER, Pugh CW, Ratcliffe PJ, Maxwell PH. Hypoxia inducible factor-alpha binding and ubiquitylation by the von Hippel-Lindau tumor suppressor protein. *J Biol Chem*. 2000;275(33):25733-41

Cole C, Conzen SD. Polyomaviridae: the viruses and their replication. In: Fundamental Virology, 2001. Vol.1, pp. 985-1018, Knipe DM and Howley PM (editors). Lippincott Williams and Wilkins, Philadelphia

Conde E, Alegre L, Blanco-Sánchez I, Sáenz-Morales D, Aguado-Fraile E, Ponte B, Ramos E, Sáiz A, Jiménez C, Ordoñez A, López-Cabrera M, del Peso L, de Landázuri MO, Liaño F, Selgas R, Sanchez-Tomero JA, García-Bermejo ML. Hypoxia inducible factor 1-alpha (HIF-1 alpha) is induced during reperfusion after renal ischemia and is critical for proximal tubule cell survival. PLoS One. 2012;7(3)

Costa C, Cavallo R. Polyomavirus-associated nephropathy. *World J Transplant*. 2012;2(6):84-94

Cotsiki M, Lock RL, Cheng Y, Williams GL, Zhao J, Perera D, Freire R, Entwistle A, Golemis EA, Roberts TM, Jat PS, Gjoerup OV. Simian virus 40 large T antigen targets the spindle assembly checkpoint protein Bub1. *Proc Natl Acad Sci U S A*. 2004;101(4):947-52

Dadhania D, Muthukumar T, Snopkowski C, et al. Epidemiology of BK virus replication in renal allograft recipients and identification of corticosteroid maintenance therapy as an independent risk factor. *Am J Transplantation*. 2004;4:S198

Dayan F, Roux D, Brahimi-Horn MC, Pouyssegur J, Mazure NM. The oxygen sensor factor-inhibiting hypoxia-inducible factor-1 controls expression of distinct genes through the bifunctional transcriptional character of hypoxia-inducible factor-1alpha. *Cancer Res*. 2006;66(7):3688-98

DeCaprio JA, Ludlow JW, Figge J, Shew JY, Huang CM, Lee WH, Marsilio E, Paucha E, Livingston DM. SV40 large tumor antigen forms a specific complex with the product of the retinoblastoma susceptibility gene. *Cell*. 1988;54(2):275-83

De Clercq E. Clinical potential of the acyclic nucleoside phosphonates cidofovir, adefovir, and tenofovir in treatment of DNA virus and retrovirus infections. *Clin Microbiol Rev*. 2003;16(4):569-96. Review

de Veer MJ, Holko M, Frevel M, Walker E, Der S, Paranjape JM, Silverman RH, Williams BR. Functional classification of interferon-stimulated genes identified using microarrays. *J Leukoc Biol*. 2001;69(6):912-20. Review

Ding R, Medeiros M, Dadhania D, Muthukumar T, Kracker D, Kong JM, Epstein SR, Sharma VK, Seshan SV, Li B, Suthanthiran M. Noninvasive diagnosis of BK virus nephritis by measurement of messenger RNA for BK virus VP1 in urine. *Transplantation.* 2002;74(7):987-94

Dohner K, Sodeik B. The role of the cytoskeleton during viral infection. *Curr Top Microbiol Immunol*. 2005; 285: 67-108

Dolei A, Pietropaolo V, Gomes E, Di Taranto C, Zicchedda M, Spanu MA, Lavorino C, Manca M, Degener AM. Polyomavirus persistence in lymphocytes: prevalence in lymphocytes from blood donors and healthy personnel of a blood transfusion centre. *J Gen Virol*. 2000;81(Pt 8):1967-73

Dörries K, Vogel E, Günther S, Czub S. Infection of human polyomaviruses JC and BK in peripheral blood leukocytes from immunocompetent individuals. *Virology*. 1994;198(1):59-70

Dörries K. New aspects in the pathogenesis of polyomavirus-induced disease. Adv *Virus Res*. 1997;48:205-61

Drachenberg CB, Papadimitriou JC, Wali R, Cubitt C, Ramos E. BK polyomavirus allograft nephropathy: ultrastructural features from viral cell entry to lysis. *Am J Transplant*. 2003; 3: 1383-92

Drachenberg CB, Papadimitriou JC. Polyomavirus-associated nephropathy: update in diagnosis. Transpl Infect Dis. 2006;8(2):68-75. Review

Duffy JP, Eibl G, Reber HA, Hines OJ. Influence of hypoxia and neoangiogenesis on the growth of pancreatic cancer. *Mol Cancer*. 2003;2:12. Review

Dugan A, Eash S, Atwood WJ, A N-linked glycoprotein with alpha(2,3)-linked sialic acid is a receptor of BK virus. *J Virol*. 2005; 79: 14442-45

Eash S, Querbes W, Atwood WJ, Infection of Vero cells by BK virus is dependent on caveolae. *J Virol*. 2004; 78:11583-90

Egli A, Infanti L, Dumoulin A, Buser A, Samaridis J, Stebler C, Gosert R, Hirsch HH. Prevalence of polyomavirus BK and JC infection and replication in 400 healthy blood donors. *J Infect Dis*. 2009;199(6):837-46

Elvert G, Kappel A, Heidenreich R, Englmeier U, Lanz S, Acker T, Rauter M, Plate K, Sieweke M, Breier G, Flamme I. Cooperative interaction of hypoxia-inducible factor-2alpha (HIF-2alpha) and Ets-1 in the transcriptional activation of vascular endothelial growth factor receptor-2 (Flk-1). *J Biol Chem*. 2003;278(9):7520-30

Epstein AC, Gleadle JM, McNeill LA, Hewitson KS, O'Rourke J, Mole DR, Mukherji M, Metzen E, Wilson MI, Dhanda A, Tian YM, Masson N, Hamilton DL, Jaakkola P, Barstead R, Hodgkin J, Maxwell PH, Pugh CW, Schofield CJ, Ratcliffe PJ. C. elegans EGL-9 and mammalian homologs define a family of dioxygenases that regulate HIF by prolyl hydroxylation. Cell. 2001;107(1):43-54

Farasati NA, Shapiro R, Vats A, Randhawa P. Effect of leflunomide and cidofovir on replication of BK virus in an in vitro culture system. *Transplantation*. 2005;79(1):116-8

Flaegstad T, Andresen PA, Johnsen JI, Asomani SK, Jørgensen GE, Vignarajan S, Kjuul A, Kogner P, Traavik T. A possible contributory role of BK virus infection in neuroblastoma development. *Cancer Res*. 1999;59(5):1160-3

Gardner SD, Field AM, Coleman DV, Hulme B. New human papovavirus (B.K.) isolated from urine after renal transplantation. *Lancet*. 1971;1(7712):1253-7

Gardner SD, MacKenzie EF, Smith C, Porter AA. Prospective study of the human polyomaviruses BK and JC and cytomegalovirus in renal transplant recipients. *J Clin Pathol*. 1984;37(5):578-86

Gharakhanian E, Takahashi J, Clever J, Kasamatsu H, In vitro assay for protein-protein interaction: Carboxyl-terminal 40 residues of simian virus 40 structural protein VP3 contain a determinant for interaction with VP1. *Proc Natl Acad Sci USA*. 1988; 85: 6607-11

Ginevri F, De Santis R, Comoli P, et al. Polyomavirus BK infection in pediatric kidney-allograft recipients: a single-center analysis of incidence, risk factors, and novel therapeutic approaches. *Transplantation*. 2003;75:1266

Gosert R, Rinaldo CH, Funk GA, Egli A, Ramos E, Drachenberg CB, Hirsch HH. Polyomavirus BK with rearranged noncoding control region emerge in vivo in renal transplant patients and increase viral replication and cytopathology. *J Exp Med*. 2008;205(4):841-52

Graham RM, Frazier DP, Thompson JW, Haliko S, Li H, Wasserlauf BJ, Spiga MG, Bishopric NH, Webster KA. A unique pathway of cardiac myocyte death caused by hypoxia-acidosis. *J Exp Biol*. 2004;207(Pt 18):3189-200. Review

Griffith JP, Griffith DL, Rayment WT, Caspar DL, Inside polyomavirus at 25 Å resolution. *Nature*. 1992; 355: 652-54

Han HK, Han CY, Cheon EP, Lee J, Kang KW. Role of hypoxia-inducible factor-alpha in hepatitis-B-virus X protein-mediated MDR1 activation. *Biochem Biophys Res Commun*. 2007;357(2):567-73

Hariharan S. BK virus nephritis after renal transplantation. *Kidney Int*. 2006;69(4):655-62. Review

Harris KF, Christensen JB, Imperiale MJ. BK virus large T antigen: interactions with the retinoblastoma family of tumor suppressor proteins and effects on cellular growth control. *J Virol*. 1996;70(4):2378-86

Hirsch HH, Knowles W, Dickenmann M, et al. Prospective study of polyomavirus type BK replication and nephropathy in renal-transplant recipients. *N Engl J Med*. 2002;347:488

Hirsch HH, Steiger J. Polyomavirus BK. *Lancet Infect Dis*. 2003;3: 611–623

Hirsch HH. BK virus: opportunity makes a pathogen. *Clin Infect Dis*. 2005 Aug 1;41(3):354-60. Epub 2005. Review

Hirsch HH, Drachenberg CB, Steiger G, Ramos E. Polyomavirus-associated nephropathy in renal transplantation: critical issues of screening and management. In: Ahsan N, editor. Polyomaviruses and human diseases. Georgetown: Landes Bioscience, 2006: 117-147

Hockel M, Schlenger K, Aral B, Mitze M, Schaffer U, Vaupel P. Association between tumor hypoxia and malignant progression in advanced cancer of the uterine cervix. *Cancer Res*. 1996;56(19):4509-15

Hu CJ, Sataur A, Wang L, Chen H, Simon MC. The N-terminal transactivation domain confers target gene specificity of hypoxia-inducible factors HIF-1alpha and HIF-2alpha. *Mol Biol Cell*. 2007;18(11):4528-42

Huang LE, Arany Z, Livingston DM, Bunn HF. Activation of hypoxia-inducible transcription factor depends primarily upon redox-sensitive stabilization of its alpha subunit. *J Biol Chem*. 1996;271(50):32253-9

Huk OL, Catelas I, Mwale F, Antoniou J, Zukor DJ, Petit A. Induction of apoptosis and necrosis by metal ions in vitro. J Arthroplasty. 2004;19(8 Suppl 3):84-7

Hur E, Chang KY, Lee E, Lee SK, Park H. Mitogen-activated protein kinase kinase inhibitor PD98059 blocks the trans-activation but not the stabilization or DNA binding ability of hypoxia-inducible factor-1alpha. *Mol Pharmacol*. 2001;59(5):1216-24

Hwang II, Watson IR, Der SD, Ohh M. Loss of VHL confers hypoxia-inducible factor (HIF)-dependent resistance to vesicular stomatitis virus: role of HIF in antiviral response. *J Virol*. 2006;80(21):10712-23

Ikegaya H, Saukko PJ, Tertti R, Metsärinne KP, Carr MJ, Crowley B, Sakurada K, Zheng HY, Kitamura T, Yogo Y. Identification of a genomic subgroup of BK polyomavirus spread in European populations. *J Gen Virol*. 2006;87(Pt11):3201-8

Jin L, Gibson PE, Booth JC, Clewley JP. Genomic typing of BK virus in clinical specimens by direct sequencing of polymerase chain reaction products. *J Med Virol*. 1993;41(1):11-7

Jorgensen GE, Hammarin AL, Bratt G, Grandien N, Flaegstad T, Johnsen JI, Identification of a unique BK virus variant in the CNS of a patient with AIDS. *J Med Virol*. 2003; 70(1): 14-9

Kean JM, Rao S, Wang M, Garcea RL. Seroepidemiology of human polyomaviruses. *PLoS Pathog*. 2009;5(3):e1000363

Kelley WL, Georgopoulos C. The T/t common exon of simian virus 40, JC, and BK polyomavirus T antigens can functionally replace the J-domain of the Escherichia coli DnaJ molecular chaperone. *Proc Natl Acad Sci U S A*. 1997;94(8):3679-84

Khalili K and Stoner GL: Human Polyomaviruses: molecular and clinical perspectives, 2001, Kahlili K and Stoner GL (editors). Wiley-Liss, New York

Khalili K, White MK, Sawa H, Nagashima K, Safak M. The agnoprotein of polyomaviruses: a multifunctional auxiliary protein. *J Cell Physiol*. 2005;204(1):1-7

Kierstead TD, Tevethia MJ. Association of p53 binding and immortalization of primary C57BL/6 mouse embryo fibroblasts by using simian virus 40 T-antigen mutants bearing internal overlapping deletion mutations. *J Virol*. 1993;67(4):1817-29

Kilani MM, Mohammed KA, Nasreen N, Tepper RS, Antony VB. RSV causes HIF-1alpha stabilization via NO release in primary bronchial epithelial cells. *Inflammation*. 2004;28(5):245-51

Kitamura T, Aso Y, Kuniyoshi N, Hara K, Yogo Y. High incidence of urinary JC virus excretion in nonimmunosuppressed older patients. *J Infect Dis.* 1990;161:1128–1133

Knowles WA. The epidemiology of BK virus and the occurrence of antigenic and genomic subtypes. In Human Polyomaviruses: Molecular and Clinical Perspectives, Khalili K, Stoner GL (eds). John Wiley & Sons: New York, 2001; 527–559

Knowles WA, Pipkin P, Andrews N, Vyse A, Minor P, Brown DW, Miller E. Population-based study of antibody to the human polyomaviruses BKV and JCV and the simian polyomavirus SV40. *J Med Virol*. 2003;71(1):115-23

Koh MY, Darnay BG, Powis G. Hypoxia-associated factor, a novel E3-ubiquitin ligase, binds and ubiquitinates hypoxia-inducible factor 1alpha, leading to its oxygen-independent degradation. *Mol Cell Biol*. 2008;28(23):7081-95

Kohrman DC, Imperiale MJ. Simian virus 40 large T antigen stably complexes with a 185-kilodalton host protein. *J Virol*. 1992;66(3):1752-60

Kondo S, Seo SY, Yoshizaki T, Wakisaka N, Furukawa M, Joab I, Jang KL, Pagano JS. EBV latent membrane protein 1 upregulates hypoxia-inducible factor 1α through Siah1-mediated down-regulation of prolyl hydroxylases 1 and 3 in nasopharyngeal epithelial cells. *Cancer Res*. 2006;66:9870–9877

Lando D, Peet DJ, Gorman JJ, Whelan DA, Whitelaw ML, Bruick RK. FIH-1 is an asparaginyl hydroxylase enzyme that regulates the transcriptional activity of hypoxia-inducible factor. *Genes Dev*. 2002;16(12):1466-71

Landry JR, Mager DL. Functional analysis of the endogenous retroviral promoter of the human endothelin B receptor gene. *J Virol*. 2003;77(13):7459-66

Lee K A, Roth RA, LaPres JJ. Hypoxia, drug therapy and toxicity. *Pharmacol Ther*. 2007;113(2):229-46. Epub 2006 Oct 12. Review

Lee JS, Kim Y, Kim IS, Kim B, Choi HJ, Lee JM, Shin HJ, Kim JH, Kim JY, Seo SB, Lee H, Binda O, Gozani O, Semenza GL, Kim M, Kim KI, Hwang D, Baek SH. Negative regulation of hypoxic responses via induced Reptin methylation. *Mol Cell*. 2010;39(1):71-85

Li D, Zhao R, Lilyestrom W, Gai D, Zhang R, DeCaprio JA, Fanning E, Jochimiak A, Szakonyi G, Chen XS. Structure of the replicative helicase of the oncoprotein SV40 large tumour antigen. *Nature*. 2003; 423(6939):512-8

Li TC, Takeda N, Kato K, Nilsson G, Xing L, Haag L, Chen RH, Miyamura T, Characterization of self-assembled virus-like particles of human polyomavirus BK generated by recombinant baculoviruses. *Virology*. 2003; 311 (1): 115-24

Liang B, Tikhanovich I, Nasheuer HP, Folk WR. Stimulation of BK virus DNA replication by NFI family transcription factors. *J Virol*. 2012;86(6):3264-75

Liddington RC, Yan Y, Moulai J, Sahli R, Benjamin TL, Harrison SC. Structure of simian virus 40 at 3.8-Å resolution. *Nature*. 1991; 354(6351):278-84

Limaye AP, Jerome KR, Kuhr CS, Ferrenberg J, Huang ML, Davis CL, Corey L, Marsh CL. Quantitation of BK virus load in serum for the diagnosis of BK virus-associated nephropathy in renal transplant recipients. *J Infect Dis*. 2001;183(11):1669-72

Liu CK, Wei G, Atwood WJ, Infection of glial cells by the human polyomavirus JC is mediated by a N-linked glycoprotein containing terminal alpha 2-6 linked sialic acids. *J Virol*. 1998; 72:4643-49

Liu YV, Baek JH, Zhang H, Diez R, Cole RN, Semenza GL. RACK1 competes with HSP90 for binding to HIF-1alpha and is required for O(2)-independent and HSP90 inhibitor-induced degradation of HIF-1alpha. *Mol Cell*. 2007(a);25(2):207-17

Liu YV, Hubbi ME, Pan F, McDonald KR, Mansharamani M, Cole RN, Liu JO, Semenza GL. Calcineurin promotes hypoxia-inducible factor 1alpha expression by dephosphorylating RACK1 and blocking RACK1 dimerization. *J Biol Chem*. 2007;282(51):37064-73

Lo YM, Tein MS, Lau TK, Haines CJ, Leung TN, Poon PM, Wainscoat JS, Johnson PJ, Chang AM, Hjelm NM. Quantitative analysis of fetal DNA in maternal plasma and serum: implications for noninvasive prenatal diagnosis. *Am J Hum Genet*. 1998;62(4):768-75

Loboda A, Jozkowicz A, Dulak J. HIF-1 and HIF-2 transcription factors—similar but not identical. *Mol Cells*. 2010;29(5):435-42

Low J, Humes HD, Szczypka M, Imperiale M. BKV and SV40 infection of human kidney tubular epithelial cells in vitro. *Virology.* 2004;323:182–188

Luo W, Zhong J, Chang R, Hu H, Pandey A, Semenza GL. Hsp70 and CHIP selectively mediate ubiquitination and degradation of hypoxia-inducible factor (HIF)-1alpha but Not HIF-2alpha. *J Biol Chem*. 2010;285(6):3651-63

Mackenzie EF, Poulding JM, Harrison PR, Amer B, Human polyoma virus (HPV)--a significant pathogen in renal transplantation. *Proc Eur Dial Transplant Assoc*. 1978;15:352-60

Mahon PC, Hirota K, Semenza GL. FIH-1: a novel protein that interacts with HIF-1alpha and VHL to mediate repression of HIF-1 transcriptional activity. *Genes Dev*. 2001;15(20):2675-86

Majmundar AJ, Wong WJ, Simon MC. Hypoxia-inducible factors and the response to hypoxic stress. *Mol Cell*. 2010;40(2):294-309

Major EO. Human polyomaviruses. In: Fields BN, Howley PM, eds. Fields virology, 4th edn. Philadelphia: Lippincot-William and Wilkins, 2001; 2175–2196

Makino Y, Cao R, Svensson K, Bertilsson G, Asman M, Tanaka H, Cao Y, Berkenstam A, Poellinger L. Inhibitory PAS domain protein is a negative regulator of hypoxia-inducible gene expression. *Nature*. 2001;414(6863):550-4

Manalo DJ, Rowan A, Lavoie T, Natarajan L, Kelly BD, Ye SQ, Garcia JG, Semenza GL. Transcriptional regulation of vascular endothelial cell responses to hypoxia by HIF-1. *Blood*. 2005;105(2):659-69

Marchetti S, Graffeo R, Siddu A, Santangelo R, Ciotti M, Picardi A, Favalli C, Fadda G, Cattani P. BK virus DNA detection by real-time polymerase chain reaction in clinical specimens. *New Microbiol*. 2007;30(2):119-26

Maxwell PH, Pugh CW, Ratcliffe PJ. Inducible operation of the erythropoietin 3' enhancer in multiple cell lines: evidence for a widespread oxygen-sensing mechanism. *Proc Natl Acad Sci U S A*. 1993;90(6):2423-7

Maxwell PH, Wiesener MS, Chang GW, Clifford SC, Vaux EC, Cockman ME, Wykoff CC, Pugh CW, Maher ER, Ratcliffe PJ. The tumour suppressor protein VHL targets hypoxia-inducible factors for oxygen-dependent proteolysis. *Nature*. 1999;399(6733):271-5

Meehan SM, Kraus MD, Kadambi PV, Chang A: Nephron segment localization of polyoma virus large T antigen in renal allografts. *Hum Pathol* 2006; 37: 1400–1406

Melendy T, Stillman B. An interaction between replication protein A and SV40 T antigen appears essential forprimosome assmbly during SV40 DNA replication. *J Biol Chem*. 1993;268: 3389-95

Mischitelli M, Fioriti D, Anzivino E, Bellizzi A, Ferretti G, Gussman N, Mitterhofer AP, Tinti F, Barile M, Dal Maso M, Chiarini F, Pietropaolo V. BKV QPCR detection and infection monitoring in renal transplant recipients. *New Microbiol*. 2007;30(3):271-4

Moens U, Johansen T, Johnsen JI, Seternes OM, Traavik T. Noncoding control region of naturally occurring BK virus variants: sequence comparison and functional analysis. *Virus Genes*. 1995;10(3):261-75. Review

Moens U, Rekvig P, Molecular biology of BK virus and clinical and basic aspects of BK virus renal infection. In: Human Polyomaviruses: molecular and clinical perspectives, 2001. Vol. 1, pp. 359-408, Kahlili K and Stoner GL (editors). Wiley-Liss, New York

Moens U, Van Ghelue M, Johannessen M. Oncogenic potentials of the human polyomavirus regulatory proteins. *Cell Mol Life Sci*. 2007;64(13):1656-78. Review.

Moers C, Pirenne J, Paul A, Ploeg RJ; Machine Preservation Trial Study Group. Machine perfusion or cold storage in deceased-donor kidney transplantation. *N Engl J Med*. 2012;366(8):770-1

Mole DR, Blancher C, Copley RR, Pollard PJ, Gleadle JM, Ragoussis J, Ratcliffe PJ. Genome-wide association of hypoxia-inducible factor (HIF)-1alpha and HIF-2alpha DNA binding with expression profiling of hypoxia-inducible transcripts. *J Biol Chem*. 2009;284(25):16767-75

Moon EJ, Jeong CH, Jeong JW, Kim KR, Yu DY, Murakami S, Kim CW, Kim KW. Hepatitis B virus X protein induces angiogenesis by stabilizing hypoxia-inducible factor-1alpha. *FASEB J*. 2004;18(2):382-4

Moreland RB, Garcea R. Characterization of a nuclear localization sequence in the polyomavirus capsid protein VP1. *Virol*. 1991; 185: 513-18

Nakayama K, Frew IJ, Hagensen M, Skals M, Habelhah H, Bhoumik A, Kadoya T, Erdjument-Bromage H, Tempst P, Frappell PB, Bowtell DD, Ronai Z. Siah2 regulates stability of prolyl-hydroxylases, controls HIF1alpha abundance, and modulates physiological responses to hypoxia. *Cell*. 2004;117(7):941-52

Nakayama K, Gazdoiu S, Abraham R, Pan ZQ, Ronai Z. Hypoxia-induced assembly of prolyl hydroxylase PHD3 into complexes: implications for its activity and susceptibility for degradation by the E3 ligase Siah2. *Biochem J*. 2007;401(1):217-26

Nakanishi A, Clever J, Yamada M, Li PP, Kasamatsu H. Association with capsid proteins promotes nuclear targeting of simian virus 40 DNA. *Proc Natl Acad Sci USA*. 1996; 93: 96-100

Nasimuzzaman M, Waris G, Mikolon D, Stupack DG, Siddiqui A. Hepatitis C virus stabilizes hypoxia-inducible factor 1alpha and stimulates the synthesis of vascular endothelial growth factor. *J Virol*. 2007;81(19):10249-57

Naldini A, Carraro F, Fleischmann WR Jr, Bocci V. Hypoxia enhances the antiviral activity of interferons. *J Interferon Res*. 1993;13(2):127-32

Nickeleit V, Hirsch HH, Binet IF, et al. Polyomavirus infection of renal allograft recipients: from latent infection to manifest disease. *J Am Soc Nephrol*. 1999;10:1080.

Nickeleit V, Klimkait T, Binet IF, Dalquen P, Del Zenero V, Thiel G, Mihatsch MJ, Hirsch HH. Testing for polyomavirus type BK DNA in plasma to identify renal-allograft recipients with viral nephropathy. *N Engl J Med*. 2000;342(18):1309-15

Nickeleit V, Hirsch HH, Zeiler M, Gudat F, Prince O, Thiel G, Mihatsch MJ: BK-virus nephropathy in renal transplants-tubular necrosis, MHC-class II expression and rejection in a puzzling game. *Nephrol Dial Transplant*. 2000(a);15: 324–332

Nickeleit V, Steiger J, Mihatsch MJ. 2002. BK virus infection after kidney transplantation. *Graft* 5: S46-S57

Nilsson J, Miyazaki N, Xing L, Wu B, Takeda N, Miyamura T, Cheng RH, Structure and assembly of a T=1 virus-like particle in BK polyomavirus. *J Virol*. 2005; 79(9):5337-45

Nishimoto Y, Zheng HY, Zhong S, Ikegaya H, Chen Q, Sugimoto C, Kitamura T, Yogo Y. An Asian origin for subtype IV BK virus based on phylogenetic analysis. *J Mol Evol*. 2007;65(1):103-11

Nomura S, Khoury G, Jay G. Subcellular localization of the simian virus 40 agnoprotein. *J Virol*. 1983;45(1):428-33

Okada Y, Endo S, Takahashi H, Sawa H, Umemura T, Nagashima K. Distribution and function of JCV agnoprotein. *J Neurovirol*. 2001;7(4):302-6

Olivieri G, Hess C, Savaskan E, Ly C, Meier F, Baysang G, Brockhaus M, Müller-Spahn F. Melatonin protects SHSY5Y neuroblastoma cells from cobalt-induced oxidative stress, neurotoxicity and increased beta-amyloid secretion. *J Pineal Res*. 2001;31(4):320-5

Olsen GH, Andresen PA, Hilmarsen HT, Bjørang O, Scott H, Midtvedt K, Rinaldo CH. Genetic variability in BK Virus regulatory regions in urine and kidney biopsies from renal-transplant patients. *J Med Virol*. 2006;78(3):384-93

Pillet S, Le Guyader N, Hofer T, NguyenKhac F, Koken M, Aubin JT, Fichelson S, Gassmann M, Morinet F. Hypoxia enhances human B19 erythrovirus gene expression in primary erythroid cells. Virology. 2004;327(1):1-7

Piña-Oviedo S, Khalili K, Del Valle L. Hypoxia inducible factor-1 alpha activation of the JCV promoter: role in the pathogenesis of progressive multifocal leukoencephalopathy. *Acta Neuropathol*. 2009;118(2):235-47

Purighalla R, Shapiro R, McCauley J, Randhawa P, BK virus infection in a kidney allograft diagnosed by needle biopsy. *Am J Kidney Dis*, 1995;26:671-73

Qi J, Nakayama K, Cardiff RD, Borowsky AD, Kaul K, Williams R, Krajewski S, Mercola D, Carpenter PM, Bowtell D, Ronai ZA. Siah2-dependent concerted activity of HIF and FoxA2 regulates formation of neuroendocrine phenotype and neuroendocrine prostate tumors. *Cancer Cell*. 2010;18(1):23-38

Ramos E, Drachenberg CB, Papadimitriou JC, et al. Clinical course of polyoma virus nephropathy in 67 renal transplant patients. *J Am Soc Nephrol.* 2002;13: 2145

Ramos E, Drachenberg CB, Portocarrero M, et al. BK virus nephropathy diagnosis and treatment: experience at the University of Maryland Renal Transplant Program. *Clin Transpl*. 2003; 143

Randhawa PS, Finkelstein S, Scantlebury V, et al. Human polyomavirus-associated interstitial nephritis in the allograft kidney. *Transplantation.* 1999;67: 103

Randhawa PS, Finkelstein S, Scantlebury V, et al. Human polyomavirus-associated interstitial nephritis in the allograft kidney. Transplantation. 1999;67: 103

Randhawa PS, Zygmunt D, Shapiro R, Vats A, Weck K, Swalsky P, Finkelstein S, Viral regulatory region sequence variations in kidney tissue obtained from patients with BK virus nephropathy. *Kidney Int*. 2003; 64(2):743-7

Randhawa P, Ho A, Shapiro R, Vats A, Swalsky P, Finkelstein S, Uhrmacher J, Weck K. Correlates of quantitative measurement of BK polyomavirus (BKV) DNA with clinical course of BKV infection in renal transplant patients. *J Clin Microbiol*. 2004;42(3):1176-80

Reploeg MD, Storch GA, Clifford DB. BK virus: a clinical review. *Clin Infect Dis* 2001; 33: 191–202

Richard DE, Berra E, Gothié E, Roux D, Pouysségur J. p42/p44 mitogen-activated protein kinases phosphorylate hypoxia-inducible factor 1alpha (HIF-1alpha) and enhance the transcriptional activity of HIF-1. *J Biol Chem*. 1999;274(46):32631-7

Rosenberger C, Rosen S, Heyman SN. Renal parenchymal oxygenation and hypoxia adaptation in acute kidney injury. *Clin Exp Pharmacol Physiol*. 2006;33(10):980-8. Review

Ruas JL, Poellinger L, Pereira T. Role of CBP in regulating HIF-1-mediated activation of transcription. *J Cell Sci*. 2005;118(Pt 2):301-11

Rundell K, Parakati R. The role of the SV40 ST antigen in cell growth promotion and transformation. *Semin Cancer Biol*. 2001;11(1):5-13. Review

Safak M, Khalili K. Physical and functional interaction between viral and cellular proteins modulate JCV gene transcription. *J Neurovirol*. 2001;7(4):288-92. Review

Sandalon Z, Dalyot-Herman N, Oppenheim AB, Oppenheim A. In vitro assembly of SV40 virions and pseudovirions: vector development for gene therapy. *Hum Gene Ther*. 1997; 8: 843-49

Schmid H, Nitschko H, Gerth J, Kliem V, Henger A, Cohen CD, Schlöndorff D, Gröne HJ, Kretzler M. Polyomavirus DNA and RNA detection in renal allograft biopsies: results from a European multicenter study. *Transplantation.* 2005;80(5):600-4

Seif I, Khoury G, Dhar R, The genome of human papovavirus BKV. *Cell*. 1979; 18: 963-77

Semenza GL, Roth PH, Fang HM, Wang GL. Transcriptional regulation of genes encoding glycolytic enzymes by hypoxia-inducible factor 1. *J Biol Chem*. 1994;269(38):23757-63

Semenza GL, Jiang BH, Leung SW, Passantino R, Concordet JP, Maire P, Giallongo A. Hypoxia response elements in the aldolase A, enolase 1, and lactate dehydrogenase A gene promoters contain essential binding sites for hypoxia-inducible factor 1. *J Biol Chem*. 1996;271(51):32529-37

Semenza GL. Hypoxia-inducible factor 1: master regulator of O2 homeostasis. *Curr Opin Genet Dev*. 1998;8(5):588-94. Review

Shah KV. Polyomaviruses. In Fields BN, Knipe DM,Howley PM, Eds; Fields Virology; Lippincot-Raven: Philadelphia, pp 2027-2043

Sharp FR, Bernaudin M. HIF1 and oxygen sensing in the brain. Nat Rev Neurosci. 2004;5(6):437-48. Review

Smith JM, McDonald RA, Finn LS, et al. Polyomavirus nephropathy in pediatric kidney transplant recipients. *Am J Transplantation*. 2004;4:2109

Smith TF, Espy MJ, Mandreakar J, Jones MF, Cockerill FR, Patel R. Quantitative realtime polymerase chain reaction for evaluating DNAemia due to cytomegalovirus, Epstein-Barr virus, and BK virus in solid-organ transplant recipients. *Clin. Infect. Dis*. 2007; 45,1056-1061

Sodhi A, Montaner S, Patel V, Zohar M, Bais C, Mesri EA, Gutkind JS. The Kaposi's sarcoma-associated herpes virus G protein-coupled receptor up-regulates vascular endothelial growth factor expression and secretion through mitogen activated protein kinase and p38 pathways acting on hypoxia-inducible factor 1alpha. *Cancer Res*. 2000;60(17):4873-80

Sontag JM, Sontag E. Regulation of cell adhesion by PP2A and SV40 small tumor antigen: an important link to cell transformation. *Cell Mol Life Sci*. 2006;63(24):2979-91. Review

Stehle T, Gamblin SJ, Yan Y, Harrison S, The structure of simian virus 40 refined at 3.1 Å resolution. *Structure*. 1996; 4:165-82

Stolt A, Sasnauskas K, Koskela P, Lehtinen M, Dillner J. Seroepidemiology of the human polyomaviruses. *J Gen Virol*. 2003;84(Pt 6):1499-504

Taguchi F, Kajioka J, Miyamura T. Prevalence rate and age of acquisition of antibodies against JC virus and BK virus in human sera. *Microbiol Immunol*. 1982;26(11):1057-64

Takasaka T, Goya N, Tokumoto T, Tanabe K, Toma H, Ogawa Y, Hokama S, Momose A, Funyu T, Fujioka T, Omori S, Akiyama H, Chen Q, Zheng HY, Ohta N, Kitamura T, Yogo Y. Subtypes of BK virus prevalent in Japan and variation in their transcriptional control region. *J Gen Virol*. 2004;85(Pt 10):2821-7

Tang X, Zhang Q, Nishitani J, Brown J, Shi S, Le AD. Overexpression of human papillomavirus type 16 oncoproteins enhances hypoxia-inducible factor 1 alpha protein accumulation and vascular endothelial growth factor expression in human cervical carcinoma cells. Clin Cancer Res. 2007;13(9):2568-76

Tavis JE, Walker DL, Gardner SD, Frisque RJ. Nucleotide sequence of the human polyomavirus AS virus, an antigenic variant of BK virus. J Virol. 1989;63(2):901-11

Tomita M, Semenza GL, Michiels C, Matsuda T, Uchihara JN, Okudaira T, Tanaka Y, Taira N, Ohshiro K, Mori N. Activation of hypoxia-inducible factor 1 in human T-cell leukaemia virus type 1-infected cell lines and primary adult T-cell leukaemia cells. *Biochem J*. 2007;406(2):317-23

Trofe J, Roy-Chaudhury P, Gordon J, et al. Early cessation/avoidance regimens are associated with lower incidence of polyomavirus nephropathy. *Am J Transplantation*. 2003; 3:371

Trofe J, Gaber LW, Stratta RJ, et al. Polyomavirus in kidney and kidney-pancreas transplant recipients. *Transpl Infect Dis*. 2003(a);5:21

Tsai R, Wang M, Ou W et al. Incidence of JC viruria is higher than that of BK viruria in Taiwan. *J Med Virol* 1997;52: 253–257

Tsuchiya T, Kominato Y, Ueda M. Human hypoxic signal transduction through a signature motif in hepatocyte nuclear factor 4. *J Biochem*. 2002;132(1):37-44

Vera-Sempere FJ, Rubio L, Felipe-Ponce V, Garcia A, Sanahuja MJ, Zamora I, Ramos D, Beneyto I, Sanchez-Plumed J: Renal donor implication in the origin of BK infection: Analysis of genomic viral subtypes. *Transplant Proc*. 2006;38: 2378–2381

Wakisaka N, Kondo S, Yoshizaki T, Murono S, Furukawa M, Pagano JS. Epstein-Barr virus latent membrane protein 1 induces synthesis of hypoxia-inducible factor 1α. *Mol Cell Biol.*2004;24:5223–5234

Wang XW, Forrester K, Yeh H, Feitelson MA, Gu JR, Harris CC. Hepatitis B virus X protein inhibits p53 sequence-specific DNA binding, transcriptional activity, and association with transcription factor ERCC3. *Proc Natl Acad Sci U S A*. 1994;91(6):2230-4

Wang GL, Jiang BH, Rue EA, Semenza GL. Hypoxia-inducible factor 1 is a basic-helix-loop-helix-PAS heterodimer regulated by cellular O2 tension. *Proc Natl Acad* Sci U S A. 1995;92(12):5510-4

Wang G, Hazra TK, Mitra S, Lee HM, Englander EW. Mitochondrial DNA damage and a hypoxic response are induced by CoCl(2) in rat neuronal PC12 cells. *Nucleic Acids Res*. 2000;28(10):2135-40

Wang B, Ding YM, Fan P, Wang B, Xu JH, Wang WX. Expression and significance of MMP2 and HIF-1α in hepatocellular carcinoma. *Oncol Lett*. 2014;8(2):539-546

Webb JD, Coleman ML, Pugh CW. Hypoxia, hypoxia-inducible factors (HIF), HIF hydroxylases and oxygen sensing. *Cell Mol Life Sci*. 2009 Nov;66(22):3539-54. Review

Webb JD, Murányi A, Pugh CW, Ratcliffe PJ, Coleman ML. MYPT1, the targeting subunit of smooth-muscle myosin phosphatase, is a substrate for the asparaginyl hydroxylase factor inhibiting hypoxia-inducible factor (FIH). *Biochem J*. 2009(a);420(2):327-33

Wenger RH, Gassmann M. Oxygen(es) and the hypoxia-inducible factor-1. *Biol Chem*. 1997;378(7):609-16. Review

Wychowski C, Benichou D, Girard M, A domain of SV40 capsid polypeptide VP1 that specifies migration into the cells nucleus. EMBO J. 1986; 5: 2569-76

Wiesener MS, Maxwell PH. HIF and oxygen sensing; as important to life as the air we breathe? *Ann Med*. 2003;35(3):183-90. Review

Wiseman AC. Polyomavirus nephropathy: a current perspective and clinical considerations. *Am J Kidney Dis*. 2009;54(1):131-42

Wong W, Hirsch HH, Pascual M, et al. BK virus replication in kidney transplant recipients who received thymoglobulin induction. *J Am Soc Nephrol*. 2003;14:SU-PO539

Yang SJ, Pyen J, Lee I, Lee H, Kim Y, Kim T. Cobalt chloride-induced apoptosis and extracellular signal-regulated protein kinase 1/2 activation in rat C6 glioma cells. J Biochem Mol Biol. 2004;37(4):480-6

Yoo YG, Oh SH, Park ES, Cho H, Lee N, Park H, Kim DK, Yu DY, Seong JK, Lee MO. Hepatitis B virus X protein enhances transcriptional activity of hypoxia-inducible factor-1alpha through activation of mitogen-activated protein kinase pathway. *J Biol Chem*. 2003;278(40):39076-84

Yu AY, Frid MG, Shimoda LA, Wiener CM, Stenmark K, Semenza GL. Temporal, spatial, and oxygen-regulated expression of hypoxia-inducible factor-1 in the lung. *Am J Physiol*. 1998;275(4 Pt 1):L818-26

Yuan Y, Hilliard G, Ferguson T, Millhorn DE. Cobalt inhibits the interaction between hypoxia-inducible factor-alpha and von Hippel-Lindau protein by direct binding to hypoxia-inducible factor-alpha. *J Biol Chem*. 2003;278(18):15911-6

Xanthoudakis S, Curran T. Identification and characterization of Ref-1, a nuclear protein that facilitates AP-1 DNA-binding activity. *EMBO J*. 1992;11(2):653-65

Xanthoudakis S, Curran T. Identification and characterization of Ref-1, a nuclear protein that facilitates AP-1 DNA-binding activity. EMBO J. 1992;11(2):653-65

Xia X, Lemieux ME, Li W, Carroll JS, Brown M, Liu XS, Kung AL. Integrative analysis of HIF binding and transactivation reveals its role in maintaining histone methylation homeostasis. Proc Natl Acad Sci U S A. 2009;106(11):4260-5

Zagórska A, Dulak J. HIF-1: the knowns and unknowns of hypoxia sensing. *Acta Biochim Pol*. 2004;51(3):563-85. Review

Zhang W, Tsuchiya T, Yasukochi Y. Transitional change in interaction between HIF-1 and HNF-4 in response to hypoxia. *J Hum Genet*. 1999;44(5):293-9

Zheng HY, Nishimoto Y, Chen Q, Hasegawa M, Zhong S, Ikegaya H, Ohno N, Sugimoto C, Takasaka T, Kitamura T, Yogo Y. Relationships between BK virus lineages and human populations. *Microbes Infect*. 2007;9(2):204-13

Ziel KA, Campbell CC, Wilson GL, Gillespie MN. Ref-1/Ape is critical for formation of the hypoxia-inducible transcriptional complex on the hypoxic response element of the rat pulmonary artery endothelial cell VEGF gene. *FASEB J*. 2004;18(9):986-988

Zinkernagel AS, Johnson RS, Nizet V. Hypoxia inducible factor (HIF) function in innate immunity and infection. J Mol Med (Berl). 2007;85(12):1339-46. Review

Zou W, Zeng J, Zhuo M, Xu W, Sun L, Wang J, Liu X. Involvement of caspase-3 and p38 mitogen-activated protein kinase in cobalt chloride-induced apoptosis in PC12 cells. *J Neurosci Res*. 2002;67(6):837-43

Zou W, Yan M, Xu W, Huo H, Sun L, Zheng Z, Liu X. Cobalt chloride induces PC12 cells apoptosis through reactive oxygen species and accompanied by AP-1 activation. *J Neurosci Res*. 2001;64(6):646-53

http://www.hindawi.com/journals/jir/2013/373579/fig2/

APPENDIX A – MOLECULAR CLONING

A.1 pNCCRLucE AND pNCCRLucL CREATION

In a previously study, BKV NCCR (380 bp) Dunlop strain was cloned in the BamHI site (G^GATCC) of the pBLCAT3 plasmid. In the present work, BKV NCCR Dunlop strain was isolated from the pBLCAT3 plasmid by digestion with BamHI, purificated by gel electrophoresis and cloned within the pMetLuc2-Reporter vector (Clontech, USA) in early and late orientation in the BamHI site of the the multiple cloning site of the vector (nt 48-85), upstream the coding sequence of the reporter gene *Metridia longa.*

A.2 pBLCAT3 DIGESTION

The digestion reaction mix was prepared as follow:

COMPONENT	VOLUME/ REACTION
NEB buffer (10x)*	2,0 µL
BamHI-HF (10U/µL)*	1,0 µL
pBLCAT3 plasmid (~1µg/µL)	2,0 µL
DNAsi-free water	15,0 µL
Total volume	**20 µL**

Table A1. Digestion reaction mix setup. * New England Biolabs

The reaction was incubated at 37°C over night.

The product of digestion was analyzed after running a 2% agarose gel electrophoresis in 0.5X TBE buffer at 90 Volt for 30 minutes and stained with GelStar Gel Stain (Lonza Rockland Inc., USA). Gel DNA purification was performed with the QIAquick Gel Extraction and PCR Purification kit (Qiagen, Germany) according to manufacturer's instructions.

A.3 pMetLuc2-Reporter DIGESTION

pMetLuc2-Reporter is a promoter reporter vector that allows the analysis of promoter function in cell-based assays. The vector encodes a sequence-optimized, secreted luciferase from the marine copepod *Metridia longa*. The 24 kDa Metridia luciferase (MetLuc) reporter protein contains a 17 amino acid, N-terminal signal peptide that allows efficient secretion of the reporter. When a functional promoter is cloned into the MCS, located upstream of the MetLuc reporter gene, MetLuc is expressed and secreted into the medium surrounding the transfected cells. SV40 polyadenylation signals downstream of the MetLuc gene direct proper processing of the 3' end of the MetLuc mRNA. The vector backbone contains an SV40 origin for replication in mammalian cells expressing the SV40 large T antigen, a pUC origin of replication for propagation in E. coli, and an f1 origin for single-stranded DNA production. A neomycin resistance cassette (Neor) allows stably transfected eukaryotic cells to be selected using G418. This cassette consists of the SV40 early promoter, the Tn5 kanamycin/neomycin resistance gene, and polyadenylation signals from the herpes simplex virus thymidine kinase (HSV TK) gene. The vector also contains a synthetic transcription blocker (TB), composed of adjacent polyadenylation and transcription pause sites, that reduces background readthrough transcription. A bacterial promoter (P_{Kan^r}) upstream of the cassette allows kanamycin resistance in E. coli (figure A1).

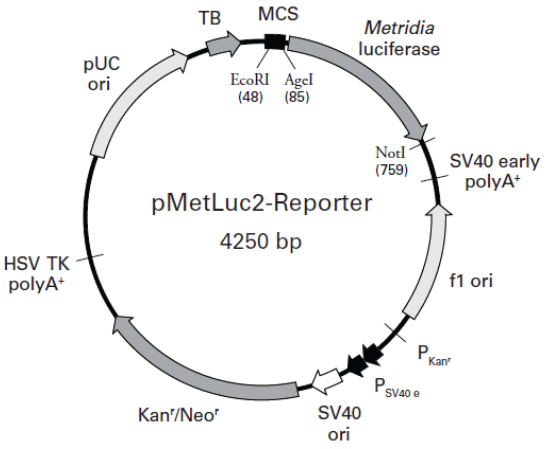

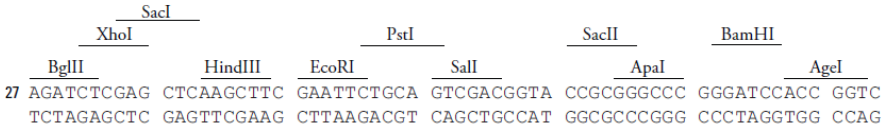

Figure A1. pMetLuc2-Reporter Vector Map and Multiple Cloning Site (MCS)

The digestion reaction mix was prepared as follow:

COMPONENT	VOLUME/ REACTION
NEB buffer (10x)*	2,0 µL
BamHI-HF™ (10U/µL)*	1,0 µL
pMetLuc2-Reporter vector (500ng/µL)	2,0 µL
DNAsi-free water	15,0 µL
Total volume	**20 µL**

Table A2. Digestion reaction mix setup. * New England Biolabs

The reaction was incubated at 37°C over night.

Digested pMetLuc2-resporter vector was then treated with Calf Intestine Phosphtase (CIP) (BioSigma, Italy). CIP nonspecifically catalyzes the dephosphorylation of 5´ and 3´ ends of DNA and RNA phosphomonoesters. In cloning, dephosphorylation prevents religation of linearized plasmid DNA. The enzyme acts on 5´ protruding, 5´ recessed and blunt ends.

The reaction mix was prepared as follow:

COMPONENT	VOLUME/ REACTION
Buffer (10x)*	3,0 µL
CIP (10U/µL)*	0,5 µL
Digested pMetLuc2-Reporter vector	20 µL
DNAsi-free water	6,5 µL
Total volume	**30 µL**

Table A3. Reaction mix setup. * BioSigma

The reaction was incubated at 37°C for 90 minutes.

The product of CIP treatment was purified using the QIAquick PCR Purification kit (Qiagen, Germany) (Appendix C), according to manufacturer's instructions and then visualized in a 2% agarose gel.

A.4 LIGATION

For the insertion of BKV NCCR in the pMetLuc2-Reporter vector digested and CIP treated was used the T4 DNA Ligase (Promega, Italy) that catalyzes the joining of two strands of DNA between the 5´-phosphate and the 3´-hydroxyl groups of adjacent nucleotides in either a cohesive-ended or blunt-ended configuration.

The ligation mix was prepared as follow:

COMPONENT	VOLUME/ REACTION
Buffer (10x)*	1,0 µL
T4 DNA ligase (5U/µL)*	1,0 µL
BKV NCCR (15ng/µL)	5,0 µL
pMetLuc2-Reporter vector (50ng/µL)**	2,0 µL
DNAsi-free water	11 µL
Total volume	**20 µL**

Table A4. Reaction mix setup. * Promega. ** Previously BamHI digested and CIP tretaed

The reaction was incubated at 16°C over night.

A.5 PLASIMD AMPLIFICATION

The ligation product was then used to transform the plasmid into *E.coli DH5α* cells using the heat shock method. 10 µL of ligation reaction were added to 1 µL of TCM (100mM Tris-HCl pH7.5, 100mM CaCl2, 100mM MgCl2) and added to 50 µL of *E.coli DH5α* cells in ice. After an incubation of 30 minutes in ice, the mixture of chemically competent bacteria and DNA is placed at 42°C for 1 minute (heat shock) and then placed back in ice for 5 minutes. Immediately after, 800 µL SOC media (Bacto-Tryptone 20g/L, yeast extract 5g/L, NaCl 10mM, KCl 2,5mM, $MgCl_2$ 10mM, glucose 20mM) were added and the transformed cells are incubated at 37°C for 1 hour with agitation. 100 µL of transformed cells were then plated on Luria-Bertani (LB) agar plates (LB Medium + 1,5% agar + kanamycin 30µg/mL for selective growth) and incubated at 37°C over night. At the end, one bacterial colony is picked up and suspended over night at 37°C in LB broth for subsequent plasmid purification.

A.6 PLASIMD PURIFICATION

The extraction of plasmid DNA was carried out using the QIAGEN Plasmid Minikit that contains three buffers: resuspending buffer P1, the lysis buffer P2 and the neutralization buffer P3 (Qiagen, Germany) (Appendix C). The bacterial culture is centrifuged at 3000 rpm for 15 minutes. After pouring off the supernatant the pellet is resuspended in 200 µL of buffer P1. The lysis is allowed by adding 200 µL of buffer P2 and incubating the resuspended pellet for 2-3 minutes. The lysis is stopped by adding 200 µL of buffer P3. After centrifugation of the mix at 14000 rpm for 5 minutes at 4°C, the clear supernatant is taken and isopropanol is added (1:1) in order to allow the precipitation of DNA (-20°C, 1 hour). The reaction is then centrifuged at 14000 rpm for 5 minutes and the supernatant is removed. The air-drying of the pellet is required in order to remove residual isopropanol. The pellet is resuspended in DNAsi free water (50 µL-150 µL).

The resulting plasmids were then sent for sequencing to PrimmBiotech (Milano, Italy) in order to asses the presence of the insert using a reverse sequencing primer that is complementary to the 5' region of the *Metridia* reporter gene region into the upstream MCS (5'-CACGATGTCGATGTTGGGG-3', nt 183-165).

A.7 pHIF CREATION

In another previously study, HIF-1α gene was cloned in the BamHI site (G^GATCC) of the pcDNA3 vector, a mammalian expression vector with the CMV promoter and a neomycin-resistance marker. The resulting plasmid was named pHIF.

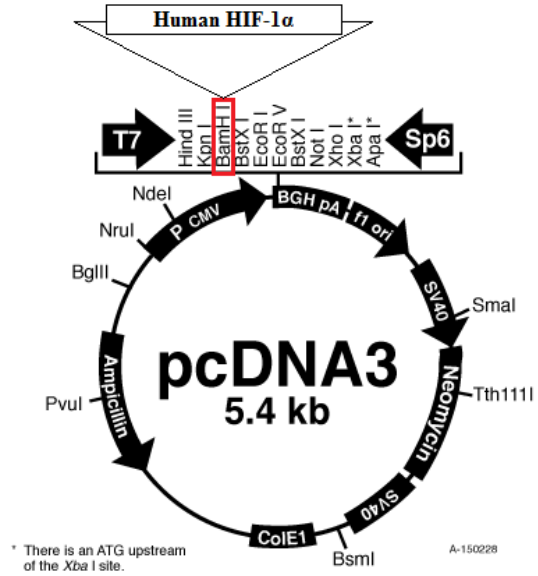

Figure A2. pcDNA3 Vector Map and insertion site (BamHI) of HIF-1α gene

APPENDIX B

B.1 CHROMATINE IMMUNOPRECIPITATION (ChIP) ASSAY

Chromatine immunoprecipitation (ChIP) is a technique that permit the selective enrichment of a chromatin fraction containing a specific antigen. Antibodies that recognize a protein or protein modification of interest can be used to determine the relative abundance of that antigen at one or more locations in the genome *in vivo*. Briefly, ChIP assay is composed by a cross-linking phase that fix the antigen of interest to its chromatin binding site, DNA sonication that renders the chromatin soluble and the immunoprecipitation of the chromatine with a specific antibody and magnetic beads. In the present study, extracts were subjected to ChIP using protein G-Sepharose beads (Protein G Mag Sepharose™, GE Healthcare, UK), according to manufacturer's instructions. The primary antibody used in the ChIP procedure was a mouse monoclonal anti-HIF-1α (ref. numb. 610959, BD Biosciences, USA) and for negative control a non-specific non-conjugated goat anti-rabbit IgG (Thermo Scientific, USA). The procedure was carried out as follows:

Cross-linking

1. Wash twice cells with 5 mL of PBS, trypsinize as appropriate (1 mL for 3 min), neutralize trypsin with 10 mL of DMEM and place cells into 15 mL conical tube
2. Centrifuge at 1200 rpm for 10 min
3. Resuspend cellular pellet in PBS 1% formaldehyde. Incubate 5 min with gently mixing
4. Quench by adding 50 µL of 2.625 M Glycine (0.125 M final) and incubate 5 min
5. Centrifuge 8 min at 500 g (4^0C)
6. Wash pellet with 10 mL ice-cold PBS and spin 8 min at 500 g (4^0C). Repeat 3 times

7. Resuspend pellet in 150 µL of FA-lysis buffer (50mM HEPES-KOH pH 7.5, 140mM NaCl, 1mM EDTA pH 8,0, 1% Triton X-100, 0,1% sodium deoxycholate, 0,1% SDS, protease inhibitor 1X). Incubate on ice for 10min

Sonication

1. Sonicate DNA by 5 cycles, amplitude 30 for 10 seconds
2. Add FA-lysis buffer to reach a final volume of 500 µL
3. Centrifuge 1 min at 8000g (4^0C). Recovery clarify supernatants
4. Quantify protein concertation by a spectrophotometer

Immunoprecipitation

1. Magnetic bead preparation:
   - Dispense 5 µL of magnetic beads (25 µL medium slurry) into a 1,5 mL eppendorf tube
   - Place the eppendorf tube in the magnetic rack and remove the storage solution
2. Equilibration
   - Add 500 µL binding buffer
   - Resuspend the medium
   - Remove the liquid
3. Binding of antibody
   - Immediately after equilibration add the antibody solution (1µg of antibody/500µL of Binding Buffer)
   - Resuspend the medium and let incubate with slow end-over-end mixing for 30 minutes
   - Remove the liquid
4. Washing
   - Add 500 µL of binding buffer
   - Remove the liquid

5. Binding of target protein
    - Add sample (25 µg/500 µL di Binding Buffer)
    - Incubate over night at 4°C with slow end-over-end mixing
    - Remove the non-bound fraction
6. Wash (perform this step 3 times totally)
    - Add 500 µL of wash buffer
    - Remove the liquid
7. Elution (perform this step 2 times totally)
    - Add 10 volumes of elution buffer compared to the magnetic bead volume (50 µL buffer to 5 µL magnetic beads)
    - Fully resuspend the medium and let incubate for 10 minutes in slow end-over-end mixing
    - Remove and collect the elution fraction

At the end of the immunoprecipitation protocol, the immunoprecipitated fraction was reverse cross linked. Briefly, 100µL of elution buffer were added and the solution was incubated at 65°C for 5h. At the end of the incubation, DNA was purified using the QIAquick PCR purification kit (Qiagen, Germany) (Appendix C).

The procedure was carried out in parallel for:

- **IP input**: cross-linked sonicated sample, not immunoprecipitated
- **Mouse IgG control**: immunoprecipitated sample using a non-specific non-conjugated goat anti-rabbit IgG (Thermo Scientific, USA)
- **Beads only control**: immunoprecipitated sample without any antibody.

B.2 BKV QUANTITATIVE Real-Time PCR (qPCR)

BKV quantitative Real-Time PCR (qPCR) was performed using the TaqMan chemistry and the 7500 Real Time PCR System (Applied Biosystems, USA). The standard curve was obtained after serial dilution of the plasmid pBKV, with 10 ng of pBKV corresponding to 10^9 copies of the viral genome (dilutions range: 10^1 to 10^4 plasmid copies/µL). The standard curve was then used to extrapolate the viral load of each sample. A negative and positive controls were included in each run. Each sample was tested in duplicate, such as the controls and the standards. Primers and probe were designed on a conserved region of the VP1 gene and their sequences and positions are shown in table B1:

PRIMERS	nt	SEQUECE
BKV Forward	2511–2531	5'-AGTGGATGGGCAGCCTATGTA-3'
BKV Reverse	2605-2586	5'-TCATATCTGGGTCCCCTGGA-3'
BKV Probe	2578-2546	5'**FAM**-AGGTAGAAGAGGTTAGGGTG TTTGATGGCACAG-3'**MGB**

Table B1. Sequence of primers and probe used in the qPCR BKV specific

The reaction mix was prepared as follows (table B2):

COMPONENT	VOLUME/ REACTION	FINAL CONCETRATION
5x Universal PCR Master Mix *	4 µL	1x
Forward Primer (80 µM)	0,05 µL	0,2 µM
Reverse Primer (80 µM)	0,1 µL	0,4 µM
BKV Probe (100 µM)	0,04 µL	0,2 µM
Viral nucleic acid	5 µL	(100 ng/µL)
DNasi-free water	10,81 µL	
Total reaction volume	**20 µL**	

Table B2. Reaction mix setup. * Solis BioDyne, Estonia

For the assay the cycling conditions were as follow (table B3):

STEP	TIME	TEMPERATURE
Holding stage	2 min	50 °C
Taq activation	15 min	95 °C
Denaturation	15 sec	95°C
Annealing/Extension	1 min	60°C
Number of cycles	**40**	

Table B3. qPCR cycler conditions

B.3 β-GLOBIN QUANTITATIVE Real-Time PCR (qPCR)

β-globin quantitative Real-Time PCR (qPCR) was performed using the TaqMan chemistry and the 7500 Real Time PCR System (Applied Biosystems, USA). The standard curve was obtained after serial dilution of the pCR2.1-βGlobin plasmid (dilutions range: 10^2 to 10^5 plasmid copies/µL) The standard curve was then used to extrapolate the load of each sample. A negative and positive controls were included in each run. Each sample was tested in duplicate, such as the controls and the standards. Primers and probe set were previously published by Lo and colleagues [Lo et al., 1998] and are shown in table B4:

PRIMERS	nt	SEQUENCE
β-globin Forward		5'-GTGCACCTGACTCCTGAGGAG-3'
β-globin Reverse		5'-CCTTGATACCAACCTGCCCAG-3'
β-globin Probe		5'**FAM**-AAGGTGAACGTGAACGTGGA TGAAGTTGGTGG-**TAMRA**3'

Table B4. Sequence of primers and probe used in the qPCR β-globin specific

The reaction mix was prepared as follows (table B5):

COMPONENT	VOLUME/ REACTION	FINAL CONCETRATION
5x Universal PCR Master Mix *	4 µL	1x
Forward Primer (80 µM)	0,1 µL	0,4 µM
Reverse Primer (80 µM)	0,1 µL	0,4 µM
β-globin Probe (100 µM)	0,04 µL	0,2 µM
Viral nucleic acid	5 µL	(100 ng/µL)
DNasi-free water	10,76 µL	
Total reaction volume	**20 µL**	

Table B5. Reaction mix setup. * Solis BioDyne, Estonia

For the assay the cycling conditions were as follow (table B6):

STEP	TIME	TEMPERATURE
Holding stage	2 min	50 °C
Taq activation	15 min	95 °C
Denaturation	15 sec	95°C
Annealing/Extension	1 min	60°C
Number of cycles	**40**	

Table B6. qPCR cycler conditions

B.4 WESTERN BLOT

Western blotting uses specific antibodies to identify proteins that have been separated based on size by gel electrophoresis. The immunoassay uses a membrane made of nitrocellulose or PVDF (polyvinylidene fluoride). The gel is placed next to the membrane and application of an electrical current induces the proteins to migrate from the gel to the membrane. The membrane can then be further processed with antibodies specific for the

target of interest, and visualized using secondary antibodies and detection reagents. The western blot assay was performed as follow:

Preparation of lysate from cell culture

- Place the cell culture flask on ice and wash the cells twice with ice-cold PBS.
- Aspirate the PBS, then add 1 mL of ice-cold RIPA Buffer (Pierce-Thermo Scientific, USA) with 2X protease inhibitor (Halt™ Protease Inhibitor Single-Use Cocktail 100x) (Pierce-Thermo Scientific, USA)
- Scrape adherent cells off the dish using a cold plastic cell scraper, then gently transfer the cell suspension into a pre-cooled microcentrifuge tube
- Maintain constant agitation for 30 min at 4°C.
- Centrifuge in a microcentrifuge at 4°C for 30 minutes at 14,000 rpm
- Gently remove the tubes from the centrifuge and place on ice, aspirate the supernatant and place in a fresh tube kept on ice, and discard the pellet.
- Read protein extract concentration with a Bradford Assay

SDS page

- Prepare SDS-PAGE gel: stacking gel (30% Acrylamide mix, 1,0 M Tris pH 6,8, 10% SDS, 10% APS, TEMED, distilled water), running gel 8% (30% Acrylamide mix, 1,5 M Tris pH 8,8, 10% SDS, 10% APS, TEMED, distilled water)
- Mix 30 µg of protein extract to 4 µL of loading dye solution 1x and RIPA buffer (final volume 24 µL) and heat at 95°C for 5 min
- Load protein into the wells of the SDS-PAGE gel, loading 12 µL of protein marker (Colorplus prestained protein marker, Broad range (7-175kDa), New England Biolabs, USA) in the first well.

- Run the gel for 30 minutes at 50 Volts until the enter of protein in the running gel then ramp to 100 V for 4 hours in 1X Running Buffer (Tris-Glycine-SDS, TGS) (Biorad, USA)

Blotting

- Assemble the transfer sandwich without forming air bubbles in the sandwich. The blot should be on the cathode and the gel on the anode
- Place the gel in 1x Transfer Buffer (Tris-Glycine, TG) (Biorad, USA) with 200 mL of ethanol (95-100%) and transfer over night in a cold room at 45 Volts

Antibody incubation

- Briefly rinse the blot in water and stain it with Ponceau solution (Sigma-Aldrich, USA) to check the transfer quality
- Rinse off the Ponceau stain with three washes with TBST (900mL H_2O milliQ + 100mL TBS 10X + 1mL Tween 20)
- Block in 5% Non Fat Dry Milk (Euroclone, Italy) in TBST at room temperature for 1 hour
- Incubate 2 hour at room temperature with the primary antibody solutions: purified Mouse Anti-Human HIF-1α (cod. 610959) (BD Biosciences, USA), diluted 1:500 in 5% Non Fat Dry Milk in TBST; α-Tubulin (DM1A) Mouse moAb (cod. 3873) (Cell Signaling Technology, USA), diluted 1:8000 in 5% Non Fat Dry Milk in TBST
- Rinse the blot 3–5 times for 5 min with TBST
- Incubate 1 hour at room temperature with the HRP-conjugated secondary antibody solution: Goat Anti-Mouse IgG Peroxidase

Conjugated (Pierce-Thermo Scientific, USA) diluted 1:5000 in in 5% Non Fat Dry Milk in TBST

- Rinse the blot 3–5 times for 5 min with TBST

Development methods

- Apply the chemiluminescent substrate WesternBright ECL HRP substrate (Advansta, USA) and incubate in a dark room for 3 minutes
- Capture the chemiluminescent signals using photographic paper (Kodac, Portugal)
- Fix the signal incubating the photographic paper in Developer and Fixer solution (Kodac, Portugal)

APPENDIX C

C.1 RNeasy FFPE KIT

The RNeasy FFPE Kit is specially designed for purification of total RNA from formalin-fixed, paraffin-embedded (FFPE) tissue sections. Firstly, all paraffin is removed from tissue sections by treating with deparaffinization solution. Next, samples are incubated in a lysis buffer, which contains proteinase K, to release RNA from the sections. A short incubation at a higher temperature partially reverses formalin crosslinking of the released nucleic acids, improving RNA yield and quality, as well as RNA performance in downstream enzymatic assays. This is followed by DNase treatment (Qiagen, Germany) that is optimized to eliminate all genomic DNA, including very small DNA fragments that are often present in paraffin-embedded samples after prolonged formalin fixation and/or long storage times. Next, the lysate is mixed with Buffer RBC. Ethanol is added to provide appropriate binding conditions for RNA, and the sample is then applied to an RNeasy MinElute spin column, where the total RNA binds to the membrane and contaminants are efficiently washed away. RNA is then eluted in a minimum of 14 µL of RNase-free water. The procedure was carried out as follows:

1. Place the sections in a 1,5 mL microcentrifuge tube
2. Add 160 µL of Deparaffinization Solution, vortex vigorously for 10 sec, and centrifuge briefly to bring the sample to the bottom of the tube
3. Incubate at 56°C for 3 min, then allow to cool at room temperature
4. Add 150 µL of Buffer PKD, and mix by vortexing
5. Centrifuge for 1 min at 11,000 x g (10,000 rpm)
6. Add 10 µL of proteinase K to the lower, clear phase. Mix gently by pipetting up and down
7. Incubate at 56°C for 15 min, then at 80°C for 15 min

8. Transfer the lower, uncolored phase into a new 2 mL microcentrifuge tube
9. Incubate on ice for 3 min. Then, centrifuge for 15 min at 20,000 x g
10. Transfer the supernatant to a new microcentrifuge tube taking care not to disturb the pellet
11. Add DNase Booster Buffer equivalent to a tenth of the total sample volume (16 µL) and 10 µL DNase I stock solution. Mix by inverting the tube. Centrifuge briefly to collect residual liquid from the sides of the tube
12. Incubate at room temperature for 15 min
13. Add 320 µL of Buffer RBC to adjust binding conditions and mix the lysate thoroughly
14. Add 720 µL of ethanol (100%) to the sample, and mix well by pipetting. Do not centrifuge
15. Transfer 700 µL of the sample, including any precipitate that may have formed, to an RNeasy MinElute spin column placed in a 2 mL collection tube. Close the lid gently, and centrifuge for 15 sec at ≥8,000 x g (≥10,000 rpm). Discard the flow-through. Repeat step until the entire sample has passed through the RNeasy MinElute spin column
16. Add 500 µL of Buffer RPE to the RNeasy MinElute spin column. Close the lid gently, and centrifuge for 15 s at ≥8,000 x g (≥10,000 rpm). Discard the flow-through
17. Add 500 µL of Buffer RPE to the RNeasy MinElute spin column. Close the lid gently, and centrifuge for 2 min at ≥8,000 x g (≥10,000 rpm) to wash the spin column membrane. Discard the collection tube with the flow-through
18. Place the RNeasy MinElute spin column in a new 2 mL collection tube. Open the lid of the spin column, and centrifuge at full speed for 5 min. Discard the collection tube with the flowthrough

19. Place the RNeasy MinElute spin column in a new 1,5 mL collection tube. Add 14 µL RNase-free water directly to the spin column membrane. Close the lid gently, and centrifuge for 1 min at full speed to elute the RNA

C.2 QIAquick PCR PURIFICATION KIT

The QIAquick system use a spin-column technology with a selective binding properties of silica membrane. Buffers provided with each kit are optimized for efficient recovery of DNA and removal of contaminants in each specific application. DNA adsorbs to the silica membrane in the presence of high concentrations of salt, while contaminants pass through the column. Impurities are washed away, and pure DNA is eluted with DNAsi free water. The procedure was carried out as follows:

1. Add 5 volumes of Buffer PB to 1 volume of the PCR sample and mix
2. Place a QIAquick spin column in a provided 2 mL collection tube
3. To bind DNA, apply the sample to the QIAquick column and centrifuge at 14,000 rpm for 30–60 s
4. Discard flow-through. Place the QIAquick column back into the same tube
5. To wash, add 0.75 mL of Buffer PE to the QIAquick column and centrifuge at 14,000 rpm for 30–60 s
6. Discard flow-through and place the QIAquick column back in the same tube. Centrifuge the column for an additional 1 min at 14,000 rpm
7. Place QIAquick column in a clean 1,5 mL microcentrifuge tube
8. To elute DNA, add 50 µL of DNAsi free water to the center of the QIAquick membrane, let the column stand for 1 min and then centrifuge the column at 14,000 rpm for 1min

C.3 NucleoSpin RNA Virus KIT

With the NucleoSpin RNA Virus method, RNA and DNA viruses are lysed by Lysis Buffer RAV1 solution and Proteinase K digestion. Lysis buffer and ethanol create appropriate conditions for binding of nucleic acids to the silica membrane of the NucleoSpin® RNA Virus Columns. Contaminations (potential PCR inhibitors) like salts, metabolites and soluble macromolecular cellular components are removed in simple washing steps with ethanolic buffers RAW and RAV3. The nucleic acids can be eluted in DNasi free water and are ready-for-use in subsequent reactions. The procedure was carried out as follows:

Lysis of viruses

- Add 600 µL of Buffer RAV1 without carrier RNA to 150 µL of the sample
- Add 20 µL Proteinase K (20 mg/mL stock solution), to the lysis mixture
- Pipette mixture up and down and vortex well. Incubate for 5 min at 70°C
- Add 600 µL ethanol (96–100%) to the clear lysis solution and mix by vortexing (10–15 s)

Bind viral RNA

- Place NucleoSpin RNA Virus Columns in collection tubes (2 mL) and load 700 µL of lysed sample. Centrifuge for 1 min at 8,000 x g
- Load the residual lysis solution onto the NucleoSpin RNA Virus Column. Centrifuge for 1 min at 8,000 x g
- Discard flow-through and place the NucleoSpin RNA Virus Column into another new collection tube (2 mL) (more than two loading steps are not recommended)

Wash and dry silica membrane

- Add 500 µL of Buffer RAW to the NucleoSpin RNA Virus Column. Centrifuge for 1 min at 8,000 x g. Discard flowthrough
- Add 600 µL of Buffer RAV3 to the NucleoSpin RNA Virus Column. Centrifuge for 1 min at 8,000 x g. Discard flowthrough
- Place the NucleoSpin RNA Virus Column in a new collection Tube (2 mL) and add 200 µL of Buffer RAV3. Centrifuge for 2–5 min at 11,000 x g to remove ethanolic Buffer RAV3 completely.

Elute viral RNA

- Place the NucleoSpin RNA Virus Column into a new, sterile 1.5 mL microcentrifuge tube
- Add 50 µL of DNase-free water (preheated to 70 °C) and incubate for 1–2 min. Centrifuge for 1 min at 11,000 x g

C.4 QIAamp DNA BLOOD MINI KIT

The QIAamp DNA purification procedure comprises four steps and is carried out using QIAamp Mini columns in a standard microcentrifuge. The lysate buffering conditions are adjusted to allow optimal binding of the DNA to the QIAamp membrane before the sample is loaded into the QIAamp Mini spin column. DNA is adsorbed onto the QIAamp silica membrane during a brief centrifugation. Salt and pH conditions in the lysate ensure that protein and other contaminants are not retained on the QIAamp membrane. DNA bound to the membrane is washed in two centrifugation using two wash buffer, Buffer AW1 and Buffer AW2 that improves the purity of the eluted DNA. Purified DNA is eluted from the QIAamp column in water, previously equilibrated at room temperature. The procedure was carried out as follows:

- Pipette 20 µL of Protease K into the bottom of a 1,5 mL microcentrifuge tube

- Add 400 µL of sample to the microcentrifuge tube
- Add 200 µL of Buffer AL to the sample. Mix by pulse-vortexing for 15 sec
- Incubate at 56°C for 10 min
- Briefly centrifuge the 1,5 mL microcentrifuge tube to remove drops from the inside of the lid
- Add 200 µL of ethanol (96-100%) to the sample and mix by pulse vortexing for 15 sec. After mixing, briefly centrifuge the 1,5 mL microcentrifuge tube to remove drops from the inside of the lid
- Apply the mixture to the QIAamp spin column without wetting the rim Close the cap and centrifuge at 6,000 x g (8000 rpm) for 1 min. Discard the filtrate and place the QIAamp spin column in a clean 2 mL collection tube
- Add 500 µL of Buffer AW1 without wetting the rim. Centrifuge at 6,000 x g (8000 rpm) for 1 min. Discard the filtrate and place the QIAamp spin column in a clean 2 mL collection tube
- Add 500 µL of Buffer AW2 without wetting the rim. Centrifuge at full speed for 3 min. Discard the filtrate and place the QIAamp spin column in a clean 2 mL collection tube
- Add 50 µL of DNAsi free water. Incubate at room temperature (15-25°C) for 1 min and centrifuge at 6,000 x g (8000 rpm) for 1 min

SCIENTIFIC PRODUCTS

1. Delbue S, Elia F, Carloni C, Tavazzi E, Marchioni E, Carluccio S, **Signorini L**, Novati S, Maserati R, Ferrante P.
   JC virus load in cerebrospinal fluid and transcriptional control region rearrangements may predict the clinical course of progressive multifocal leukoencephalopathy. *Journal of Cellular Physiology*. 2012 Oct; 227(10):3511-7. IMPACT FACTOR: 4.218

2. Delbue S, Ferraresso M, Elia F, Belingheri M, Carloni C, **Signorini L**, Carluccio S, Dallari S, Ghio L, Ferrante P.
   Investigation of polyomaviruses replication in pediatric patients with nephropathy receiving rituximab. *Journal of Medical Virology*. 2012 Sep; 84(9):1464-70. IMPACT FACTOR: 2.373

3. Delbue S, Elia F, Carloni C, Pecchenini V, Franciotta D, Gastaldi M, Colombo E, **Signorini L**, Carluccio S, Bellizzi A, Bergamaschi R, Ferrante P.
   JC Virus urinary excretion and seroprevalence in Natalizumab-treated Multiple Sclerosis patients. *Journal of Neurovirology*. 2014 Jul 23. [Epub ahead of print] IMPACT FACTOR: 3.323

4. **Signorini L**, Belingheri M, Ambrogi F, Pagani E, Binda S, Ticozzi R, Ferraresso, M, Ghio L, Giacon B, Ferrante P, Delbue S.
   High frequency of Merkel cell polyomavirus DNA in the urine of kidney transplant recipients and healthy controls. *Journal of Clinical Virology*. 2014 Dec; 61(4):565-70. IMPACT FACTOR: 3.466

5. Carluccio S, Delbue S, **Signorini L**, Setola E, Bagliani A, Valle AD, Galli A, Ferrante P, Bregni M.
   Generation of tumor-specific cytotoxic T-lymphocytes from the peripheral blood of colorectal cancer patients for adoptive T-cell transfer. *Journal of Cellular Physiology*. 2015 Jul;230(7):1457-65. IMPACT FACTOR: 3.55

6. Carluccio S, **Signorini L**, Elia F, Villani S, Delbue S and Ferrante P.
   A Potential Linkage Between the JC and BK Polyomaviruses and Brain and Urinary Tract Tumors: A Review of the Literature. *Advances in Tumor Virology.* 2014:4 17–24.

7. Delbue S, Elia F, **Signorini L**, Bella R, Villani S, Marchioni E, Ferrante P, Phan TG, Delwart E.
   Human polyomavirus 6 DNA in the cerebrospinal fluid of an HIV-positive patient with leukoencephalopathy. *Journal of Clinical Virology*. 2015 Jul;68:24-7. IMPACT FACTOR: 3.442

8. Dallari S, Franciotta D, Carluccio S, **Signorini L**, Gastaldi M, Colombo E, Bergamaschi R, Elia F, Villani S, Ferrante P, Delbue S.
   Upregulation of integrin expression on monocytes in multiple sclerosis patients treated with natalizumab. *Journal of Neuroimmunology.* 2015. IMPACT FACTOR: 2.79

9. Bella R, Dolci M, Ferraresso M, Ticozzi R, Ghio L, Rizzo J, **Signorini L**, Villani S, Elia F, Ferrante P, Delbue S.
   Human Herpes Virus-6 DNAemia in children and young adult patients after kidney transplantation. *Future Virology* (Accepted 2015, September 30). IMPACT FACTOR: 1.011

SCIENTIFIC PRODUCTS RELATED TO THIS WORK

Signorini L, Croci M, Villani S, Bella R, Elia F, Boldorini R, Ferrante P, Delbue S.
POSTER: “Interaction between the hypoxia inducible factor 1 alpha and the human Polyomavirus BK: a risk factor for the development of Polyomavirus associated nephropathy”

43° Congresso Nazionale della Società Italiana di Microbiologia, 27-30 Settembre 2015, Napoli

Signorini L, Croci M, Boldorini R, Varella R.B, Elia F, Carluccio S, Villani S, Bella R, Ferrante P, Delbue S
Interaction between Human Polyomavirus BK and Hypoxia inducible factor-1 alpha. *Journal of Cellular Physiology* [in press]. IMPACT FACTOR: 3.839

ACKNOWLEDGMENT

This project was founded by the contract grant sponsor: Italian Minister of the University Grant (PRIN 2010–2011); Contract grant number: protocol number 2010PHT9NF 003

I would like to thank professor Pasquale Ferrante and dott.ssa Serena Delbue for their scientific support, doctor Mattia Croci for his technical and scientific contribute and all my colleagues for their technical and scientific support.